

**EXPERIMENTAL STUDY ON IMPROVING  
LOCAL BUCKLING BEHAVIOR OF STEEL  
PLATES STRENGTHENED WITH GLASS FIBER  
REINFORCED POLYMERS**

**A Thesis Submitted to  
The Graduate School of Engineering and Sciences of  
İzmir Institute of Technology  
in Partial Fulfillment of the Requirements for the Degree of**

**MASTER OF SCIENCE**

**in Civil Engineering**

**by  
Can Ali GÜVEN**

**March 2009**

**İZMİR**

We approve the thesis of **Can Ali GÜVEN**

---

**Assist. Prof. Dr. O. Özgür EĞİLMEZ**  
Supervisor

---

**Assist. Prof. Dr. Cemalettin DÖNMEZ**  
Committee Member

---

**Assoc. Prof. Dr. Metin TANOĞLU**  
Committee Member

19 March 2009

---

**Prof. Dr. Gökmen TAYFUR**  
Head of the Civil Engineering Department

---

**Prof. Dr. Hasan BÖKE**  
Dean of the Graduate School of  
Engineering and Sciences

## **ACKNOWLEDGEMENTS**

I would like to thank my advisor Assist. Prof. Dr. O. Özgür Eğilmez, Assist. Prof. Dr. Cemalettin Dönmez and Assoc. Prof Dr. Metin Tanođlu. Their encouragement and guidance during my thesis period, gave me the faith to finish my study. Without their effort and patience this thesis could have never been accomplished. I would like to thank F. Erinç Sezgin for the great assistance for the laboratory work and Doruk Yormaz for the experimental stage.

Also I would like to thank my family, Deniz Alkan, Cem akırođlu, Deniz atan, Bora Gntay, H. Fırat Pulat and everyone that strengthen me with their never ending support. Thank you all.

# ABSTRACT

## EXPERIMENTAL STUDY ON IMPROVING LOCAL BUCKLING BEHAVIOR OF STEEL PLATES STRENGTHENED WITH GLASS FIBER REINFORCED POLYMERS

Glass Fiber Reinforced Polymer (GFRP) applications becoming one of the most efficient strengthening methods to improve mechanical properties of previously built steel structures. In strengthening applications FRP materials generally used in web or flange sections of steel members to provide a bracing against local buckling. By the help of their easy application and their tailorable mechanical properties, FRPs provide various options for selecting the most suitable FRP material for applications.

This study focuses on using GFRP to enhance the buckling behavior of GFRP strengthened steel plates under axial loading. For that purpose, a detailed experimental study program has been followed revealing mechanical properties of GFRP material, steel and interaction between steel-GFRP. Previous studies showed that the surface bond between GFRP and steel section as the weakest link of the structure. As a result of this, various epoxies, surface preparation primers, surface treatments are used to produce Lap-Shear specimens to provide most efficient surface interaction between GFRP and steel. Results of these experiments provided us data to decide most suitable surface treatment, surface primer and epoxy combination in the GFRP Strengthened Steel Plate Tests with the ability to in-situ application.

350x200x20 mm steel plates are strengthened with various thickness (2, 4 and 16 layers) and surface areas (80mm x 300mm, 160 x 300mm) of GFRP to compare the stabilization in buckling values with bare steel plates. Plates are strengthened with GFRP on both sides and they are tested in compression testing equipment. LVDTs are used to collect axial and lateral buckling while strain-gauges attached to both composite and steel surfaces collect strain data. Plastic buckling results of axially loaded steel plates strengthened with GFRP material showed that application of GFRP provides enhancement to the plastic buckling of steel plates.

## ÖZET

### ÇELİK PLAKALARIN MEVZİ BURKULMA DAVRANIŞLARININ CAM ELYAFLA GÜÇLENDİRİLMİŞ POLİMER İLE GELİŞTİRİLMESİ ÜZERİNE DENEYSEL ÇALIŞMA

Cam Elyafı Güçlendirilmiş Polimerlerin (CEGP) eski çelik yapıların kuvvetlendirilmesinde uygulanması günümüzün en etkin güçlendirme metotlarından bir tanesi haline gelmiştir. CEGP malzemelerin çelik yapılara uygulandığı güçlendirme uygulamalarında, polimer malzeme genel olarak gövde ve/veya başlık bölgelerine uygulanarak mevzi burkulmalara bir takviye sağlar. Uygulamalarındaki kolaylık ve değişken mekanik özellikleri, uygulamalarda en uygun CEGP malzeme seçiminde çok sayıda alternatif sağlamasına yol açar.

Bu çalışmada, CEGP uygulamasıyla güçlendirilmiş çelik plakaların aksel yük altındaki burkulma davranışlarının geliştirilmesine çalışılmıştır. Bu amaçla, CEGP malzemenin, çelik malzemenin ve CEGP-Çelik yüzey etkileşiminin mekanik özelliklerini ortaya çıkarmak için detaylı bir deneysel çalışma programı izlenmiştir. Önceki yapılmış çalışmalar, CEGP-Çelik etkileşiminin yapıdaki en zayıf bölge olduğunu göstermiştir. Bu nedenle, değişik epoksiler, yüzey hazırlama metotları ve yüzey astarlarıyla hazırlanan Yüzey-Kesme numuneleri test edilmiş olup, güçlendirme uygulamasında bize en yüksek CEGP-Çelik yüzey etkileşimini sağlayabilecek değerleri bulmak amaçlanmıştır. Elde edilen testlerin sonuçları sayesinde, saha uygulamasına olanak verecek şekilde en uygun CEGP-Çelik uygulama kombinasyonu elde edilmiş olup, CEGP ile güçlendirilmiş Çelik Plaka testlerinde bu kombinasyon kullanılmıştır.

350x200x20 mm Boyutlarında çelik plakalar değişken kalınlık (2, 4 ve 16 katman) ve yüzey alanlarında ( 80 x 300 ve 160x300 mm) CEGP ile güçlendirilmiş olup, CEGP'siz çelik plaka testleri ile burkulmanın stabilizasyonu değerleri karşılaştırılmıştır.. Çelik plakaların iki yüzü de güçlendirilmiş olup, plakalar basınç presinde test edilmiştir. Test sırasında LVDTler aksel ve yatay burkulma değerlerini ölçerken, kompozit ve çelik yüzeylere yerleştirilmiş gerinim pullarıyla gerilme değerleri toplanmıştır. CEGP ile kuvvetlendirilmiş çelik plakaların aksel yüklenmesiyle elde edilen plastik burkulma sonuçları, CEGP ile çelik plakaların plastik burkulmalarında kapasite artışı sağladığını göstermiştir.

# TABLE OF CONTENTS

LIST OF FIGURES .....	ix
LIST OF TABLES .....	xi
CHAPTER 1. INTRODUCTION .....	1
1.1. General.....	1
1.2. Research Overview .....	2
1.3. Scope of the work .....	2
CHAPTER 2. BACKGROUND .....	4
2.1. Introduction.....	4
2.2. Fiber Reinforced Polymers .....	4
2.2.1. Fibers .....	5
2.2.1.1. Glass Fibers.....	6
2.2.1.2. Carbon Fibers.....	7
2.2.1.3. Boron Fibers .....	8
2.2.1.4. Organic Fibers.....	8
2.2.2. Matrix Materials .....	8
2.2.2.1. Thermoset Polymeric Matrices.....	9
2.2.2.2. Thermoplastic Polymeric Matrices.....	9
2.2.3. Production Methods of Fiber Reinforced Polymers .....	10
2.2.3.1. Wet Lay-up Method.....	10
2.2.3.2. Prepreg Lay-Up Method .....	12
2.2.3.3. Filament Winding .....	12
2.2.3.4. Compression Molding.....	12
2.2.3.5. Pultrusion .....	13
2.2.3.6. Resin Transfer Molding .....	14
2.2.3.7. Vacuum Assisted Resin Transfer Molding.....	15
2.2.4. Previous Studies of Steel-FRP Applications .....	15
CHAPTER 3. STRENGTHENING CONCEPT.....	21
3.1. Overview.....	21

3.2. Recommended Modifications to Beam-Column Connections .....	22
3.2.1. Welded Haunch Modification.....	22
3.2.2. Reduced Beam Section Modification .....	23
3.2.3. Strengthening with Glass Fiber Reinforced Polymer Material.....	24
CHAPTER 4. MATERIALS AND TEST PROCEDURES .....	26
4.1. Introduction.....	26
4.2. Glass Fiber Material.....	26
4.3. Matrix Material .....	27
4.4. Composite Production.....	30
4.5. Test Procedures.....	31
4.5.1. Tensile Test.....	31
4.5.2. Compression Test .....	32
4.5.3. Lap Shear Test .....	34
4.5.3.1. Lap Shear Surface Treatment Methods .....	34
4.5.3.2. Parameters Examined in Lap Shear Test .....	36
4.6. V-Notch Beam Test Procedure for Determining Shear Properties of GFRP .....	36
4.6.1. Test Specimens .....	37
4.6.2. V-Notch Test Setup .....	40
CHAPTER 5. GFRP TEST RESULTS .....	47
5.1. General.....	47
5.2. Tensile Test Results of GFRP.....	47
5.3. Compression Test Results of GFRP .....	48
5.4. Lap Shear Test Results of GFRP-Steel Connection .....	50
5.5. Shear Strength (V-Notch) Test Results .....	56
CHAPTER 6. GFRP STRENGTHENED STEEL PLATE TESTS .....	58
6.1. Introduction.....	58
6.2. Steel Plate Specimens .....	58
6.3. GFRP Retrofitting Procedure.....	61
6.4. Experimental Setup.....	62
6.5. Test Procedure .....	65

6.6. Test Results.....	66
6.6.1. Introduction.....	66
6.6.2. Axially Loaded Steel Plate Test Results.....	66
6.6.3. Individual Axially Loaded Steel Plate Test Results .....	73
6.6.3.1. Axially Loaded Steel Specimen Type 1 .....	73
6.6.3.2. Axially Loaded Steel Specimen Type 2 .....	74
6.6.3.3. Axially Loaded Steel Specimen Type 3 .....	76
6.6.3.4. Axially Loaded Steel Specimen Type 4 .....	77
6.6.3.5. Axially Loaded Steel Specimen Type 5 .....	79
6.6.3.6. Axially Loaded Steel Specimen Type 6 .....	80
6.6.3.7. Axially Loaded Steel Specimen Type 7 .....	82
CHAPTER 7. CONCLUSIONS AND RECOMMENDATIONS	
FOR FUTURE STUDY .....	84
7.1. Conclusion .....	84
7.2. Recommendations.....	86
REFERENCES .....	87



# LIST OF FIGURES

<b><u>Figure</u></b>	<b><u>Page</u></b>
Figure 2.1. Tensile Stress and Strain Diagrams of Fibers .....	5
Figure 2.2. Glas Fiber Material Manufacturing Setup.....	7
Figure 2.3. Compression Molding .....	13
Figure 2.4. Pultrusion Line .....	14
Figure 2.5. Reinforced Reaction Injection Molding of Thermosets .....	15
Figure 2.6. VARTM Process .....	16
Figure 2.7. Axially Loaded T-Sections .....	19
Figure 3.1. Collapse Mechanism of a Beam.....	22
Figure 3.2. Typical Beam Span with Welded Straight Haunch .....	23
Figure 3.3. Various RBS Configurations .....	24
Figure 3.4. GFRP Application along I-Beam .....	25
Figure 4.1. Tension Test Setup .....	32
Figure 4.2. Compression Specimens.....	33
Figure 4.3. Compression Test Sample .....	33
Figure 4.4. Sample Lap-Shear Specimens .....	34
Figure 4.5. Material Coordinate System Used in V-Notch Test.....	38
Figure 4.6. V-Notch Specimen Orientations .....	38
Figure 4.7. V-Notch Specimen Orientations Shown in an Imaginary Cubic GFRP .....	39
Figure 4.8. Sample GFRP Application on I-Beam .....	40
Figure 4.9. V-Notch Beam Test Method Test Setup .....	41
Figure 4.10. V-Notch Test Apparatus.....	41
Figure 4.11. Strain-Gauge.....	42
Figure 4.12. V-Notch Beam Test Method Test Setup .....	43
Figure 4.13. Quarter Bridge Circuit Diagram.....	44
Figure 4.14. V-Notch Specimen in Test Apparatus.....	45
Figure 5.1. Sample Tension Test Specimen .....	48
Figure 5.2. Compressive Failure of GFRP Specimens .....	49
Figure 5.3. Lap Shear Results Based on No Surface Treatment.....	53
Figure 5.4. Lap Shear Results Based on Sand Papering Surface Treatment .....	54
Figure 5.5. Lap Shear Results Based on Sand Blast Surface Treatment .....	54

Figure 5.6. Lap Shear Results Based on Duratek Primer .....	55
Figure 5.7. Lap Shear Results Based on Silan Primer .....	56
Figure 6.1. Steel Plate Dimensions .....	59
Figure 6.2. GFRP Application Dimensions on Steel Plates .....	61
Figure 6.3. GFRP Strengthened Steel Plate Test Setup .....	63
Figure 6.4. Schematic of Axially Loaded Steel Plate Test Setup .....	63
Figure 6.5. LVDT Locations on Test Set-Up .....	64
Figure 6.6. Strain-Gauge Locations on Steel Plate Specimens.....	64
Figure 6.7. Strain-Gauge Identification Numbers Used in Experiments .....	65
Figure 6.8. Combined Load-Displacement Graph of 8x30 cm GFRP Strengthened Steel Plate Tests for Each Lamination Type .....	71
Figure 6.9. Combined Load-Displacement Grap of 16x30 cm GFRP Strengthened Steel Plate Tests for Each Lamination Type .....	72
Figure 6.10. Load Displacement Graph of Specimen 1 .....	73
Figure 6.11. Load-Strain Graph of Specimen 1 .....	74
Figure 6.12. Load-Strain Graph of Specimen 1 (Yield) .....	74
Figure 6.13. Load Displacement Graph of Specimen 2.....	75
Figure 6.14. Load-Strain Graph of Specimen 2.....	75
Figure 6.15. Load-Strain Graph of Specimen 2 (Yield) .....	76
Figure 6.16. Load Displacement Graph of Specimen 3.....	76
Figure 6.17. Load-Strain Graph of Specimen 3.....	77
Figure 6.18. Load-Strain Graph of Specimen 3 (Yield) .....	77
Figure 6.19. Load Displacement Graph of Specimen 4.....	78
Figure 6.20. Load-Strain Graph of Specimen 4.....	78
Figure 6.21. Load-Strain Graph of Specimen 4 (Yield) .....	79
Figure 6.22. Load Displacement of Specimen 5.....	79
Figure 6.23. Load-Strain Graph of Specimen 5.....	80
Figure 6.24. Load-Strain Graph of Specimen 5 (Yield) .....	80
Figure 6.25. Load Displacement Graph of Specimen 6.....	81
Figure 6.26. Load-Strain Graph of Specimen 6.....	81
Figure 6.27. Load-Strain Graph of Specimen 6 (Yield) .....	82
Figure 6.28. Load Displacement Graph of Specimen 7.....	82
Figure 6.29. Load-Strain Graph of Specimen 7.....	83
Figure 6.30. Load-Strain Graph of Specimen 7 (Yield) .....	83

## LIST OF TABLES

<b><u>Table</u></b>	<b><u>Page</u></b>
Table 2.1. Classification of Carbon Fibers.....	8
Table 4.1. Physical Properties of Duratek Epoxy .....	28
Table 4.2. Physical Properties of Resoltech Epoxy .....	28
Table 4.3. Mechanical Properties of Duratek Epoxy .....	29
Table 4.4. Mechanical Properties of Resoltech Epoxy .....	30
Table 4.5. Parameters used in Lap Shear Tests.....	36
Table 5.1. Tension Test Results of GFRP Material .....	48
Table 5.2. Compression Test Results of GFRP Material .....	49
Table 5.3. Lap Shear Test Results of Steel GFRP Interface .....	52
Table 5.4. V-Notch Test Results of GFRP Material .....	57
Table 6.1. Tensile Test Results of Coupons Taken from Steel Plates .....	59
Table 6.2. GFRP Strengthened Steel Plate Test Specimen Types .....	60
Table 6.3. Control and GFRP Strengthened Steel Plate's Maximum Load and GFRP Failure Modes.....	68
Table 6.4. Control and GFRP Strengthened Steel Plate's Maximum Lateral, Axial Displacement Values .....	68
Table 6.5. Maximum Strain-Gauge Readings From GFRP Strengthened Steel Plate Tests .....	69
Table 6.6. Lateral and Axial Displacement Readings from LVDTs at 775kN .....	69

# CHAPTER 1

## INTRODUCTION

### 1.1. Introduction

Various aging steel structures around the world increase the demand of different strength improvement studies. Nowadays composite materials, such as fiber reinforced polymers, have become one of the widely preferred strengthening material with advanced mechanical properties. Composite term is commonly used for a material having two or more components including a matrix material and a reinforcing material. Consequently, composite materials can achieve great improvements, which can not be obtained from the separate components. Thanks to their unique properties, it is commonly used in aircraft, aerospace, automotive, marine, sporting goods, electrical, chemical and construction applications.

Freedom of shape, great weight savings, corrosion resistance, good physical properties, thermal or electric conductivity are the primary advantages of composite materials. Continuous advancements on manufacturing techniques keep improving their capabilities of composite polymers and reduce their cost. Different material choices for reinforcing and matrix components can ensure various application areas of composite polymers. Glass, carbon, aramid, high-strength polyolefin, boron, and silicon carbide for reinforcing fibers and thermoset and thermoplastic resins for matrix materials are the main alternative components that form fiber reinforced polymers. Each material has different advantages/disadvantages, allowing engineers to design variable fiber reinforced polymers for specific requirements.

The unique properties of composite polymer materials have made them popular in structural engineering studies, mostly in strengthening of previously built reinforced concrete and steel structures. Studies related with strengthening steel sections using FRP materials revealed the abilities of polymer composites in strengthening applications. The ease of application and high strength to weight ratio of composite polymer materials make them an effective solution in strengthening and rehabilitation of structural concrete and steel members.

## **1.2. Research Overview**

Fiber reinforced polymers can be applied to steel members for mainly two purposes: a) strengthening applications; b) improvement of behavior. For strengthening applications materials with high modulus of elasticity, like carbon fiber reinforced materials, are preferred to provide high stiffness in order to increase the load capacity of the sections. On the other hand, to provide flexural enhancement without any strength increase in the section, materials with low modulus of elasticity, like glass fiber reinforced polymers, are preferred. The objective of this study is to experimentally investigate the behavior of axially loaded steel plates strengthened with GFRP materials. Specifically the improvement of ductility by postponing local buckling in steel plates is investigated.

## **1.3. Scope of the Work**

The high strength and stiffness of steel complicates the application of FRP materials. FRPs are often attached to steel by the use of different epoxies. However, the low shear strength of the steel-FRP connections limits the critical load transfer to polymer. In addition, the interlaminar shear capacity of composite materials can also be exceeded during the load transfer. In order to reveal these cases, this experimental study has been divided into two phases.

In the first phase the mechanical properties of GFRP material and GFRP-steel interaction in steel plates is investigated. At first hand, composition of composite material is defined considering the requirements of the GFRP application to steel. The production and experiments are done confirming to appropriate ASTM Standards. Tension, compression, and shear tests are done to determine the mechanical properties of GFRP materials. These tests are followed by lap-shear tests, which reveal the surface bonding relationship between steel surface and fiber reinforced composite materials. Lap shear tests include different surface treatments and primers in order to find the most effective interaction between steel and composite. Lastly, the v-notch beam test is applied to composite polymer to reveal interlaminar shear properties of the material.

The second phase of the experimental program comprises from steel plate tests with and without GFRP. Steel plates are loaded under axial compression and the

behavior of bare steel plates with plates strengthened with different GFRP thicknesses and GFRP dimensions are compared. In steel-GFRP systems the best surface treatment, primer and epoxy combinations obtained from standard tests are utilized. GFRPs are applied to steel plates in various thicknesses and dimensions to provide a comparison between different thickness and local buckling behavior.

# CHAPTER 2

## BACKGROUND

### 2.1. Introduction

The use of fiber reinforced polymers (FRP) in steel strengthening and rehabilitation applications is increasing as the cost of FRPs is dropping and their mechanical properties are improving through new advanced manufacturing processes. The unique material properties of FRP materials, makes them one of the most attractive material of engineers, interested in strengthening and rehabilitation applications. In that manner, studies related with concrete-FRP and steel-FRP applications are not few. This chapter presents information on fiber reinforced polymer materials and provides background information on steel-FRP hybrid systems.

### 2.2. Fiber Reinforced Polymers

Fiber composite materials can be categorized as polymer matrix composites (PMCs), metal matrix composites (MMCs), ceramic matrix composites (CMCs), carbon composites (CCCs), and inter-metallic composites (IMCs) (Shalin 1995). PMCs, including fiber reinforced polymers, are one of the most advanced composite types in composite classes. PMC polymers are widely used in different industry applications. The primary contents of PMCs are reinforcing fibers and a matrix material that allows uniform load distribution to the reinforcements. There are different constituent materials available to design a composite material that satisfies the required field of work. Combining high strength and high modulus fibers with a low modulus matrix material provides stress transfers from matrix to fibers which results in a high modulus , high strength composite. For instance, higher interface between reinforcement and matrix considerably increases the fracture toughness of the material. As a result of PMCs materials' various different properties, design of composite materials can be challenging.

However, this anisotropic structure of composite materials inhibits a unique property in itself to reinforce a structure in the direction of major stresses and increase the stiffness in the required direction (Hull and Clyne 1995).

### 2.2.1. Fibers

Fibers are the main constituents in a fiber reinforced composite material. They are available in various orientations such as woven, mat, knits, and braid. Their choice affects the specific gravity, tensile strength and modulus, compressive strength and modulus, fatigue strength and failure mechanism, electric and thermal conductivities and cost of the composite material (Shalin 1995). Fibers can be categorized into 5 main groups as Glass, Carbon, Boron, Aramid, and Organic. The stress-strain behaviors of these fibers are presented in Figure 2.1.

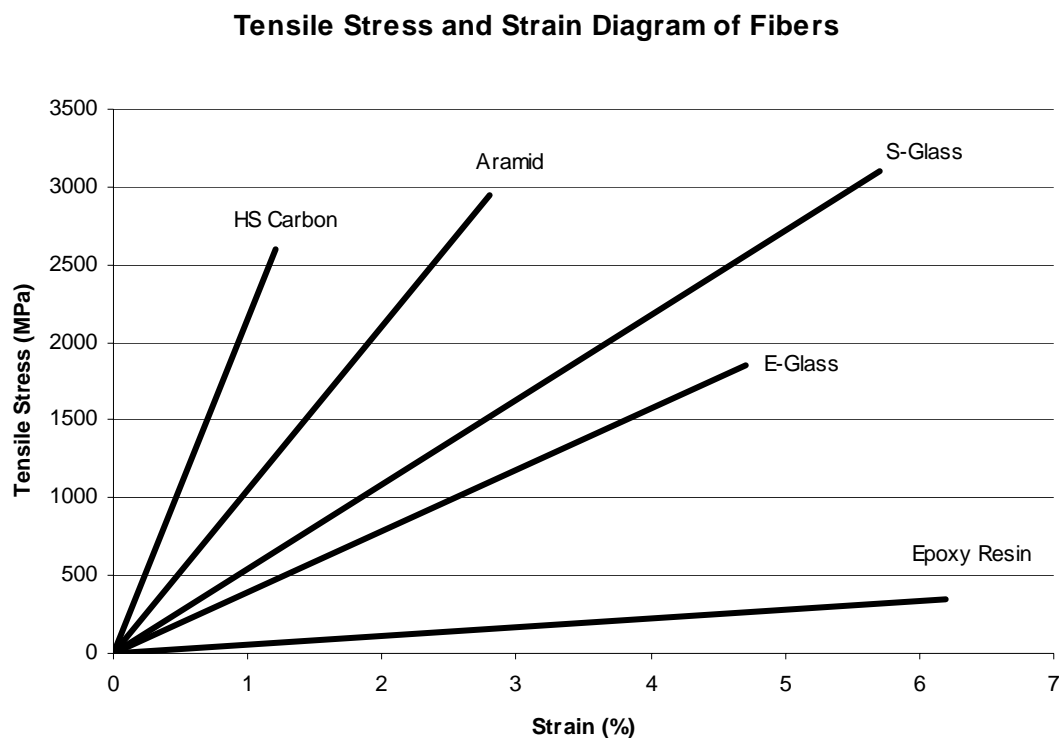


Figure 2.1. Tensile Stress and Strain Diagram of Fibers  
(Source: Gutowski 1997)



### **2.2.1.1. Glass Fibers**

Glass fibers are the most common reinforcement material in polymer matrix composites. High tensile and impact strengths, high chemical resistance, relatively low modulus of elasticity is their major properties. There are four widely manufactured Glass Fibers types, which are E-Glass, S-glass, C-Glass and quartz. E-glass fibers have a calcium aluminoborosilicate composition with maximum alkali content of 2%. They are preferred when high strength and electrical resistance is required. S-Glass is approximately 40% higher in strength than E-Glass and it has better retention properties at elevated temperatures. C Glass has a soda-lime borosilicate composition and because of its chemical stability, it is preferred in corrosive environments. Quartz is used when low dielectric material is needed (Jang 1994).

The main contents of fiber glass are silica sand, limestone, boric acid and small amounts of clay, coal, and fluorospar. Two manufacturing methods are used to obtain glass fibers from molten glass mixture. First method is called Marble Melt. In this method small glass marbles are produced from molten glass. These are then sorted and graded and then fed into a re-melting furnace. After melting they are fed into the filament formation bushing. In the second method the molten glass can be introduced directly from the manufacturing furnace into the filament formation bushing. Using marbles gave better results in controlling the quality of the fiber, however continuing improvements on direct-melt method, made this method the main manufacturing method for glass fibers (Jang 1994)

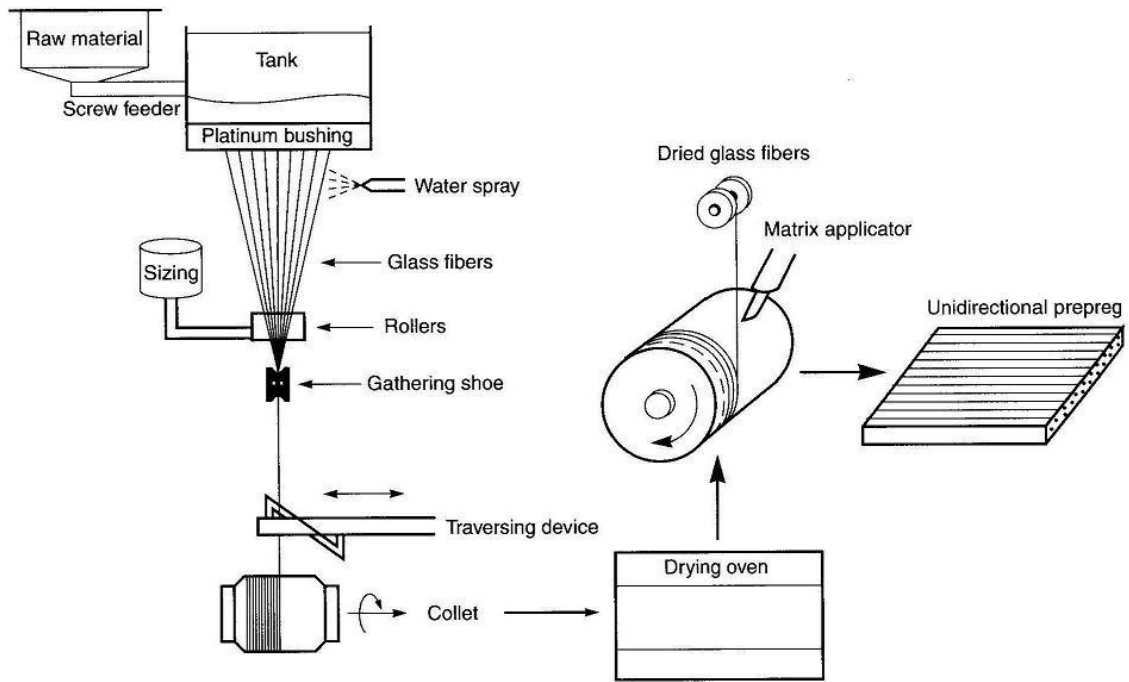


Figure 2.2. Glass Fiber Manufacturing Setup  
(Source: Hyer 1998)

### 2.2.1.2. Carbon Fibers

Carbon fibers are mostly used in cloth forms in composite materials. They are mostly known by their high tensile strength-to-weight and tensile modulus-to-weight ratios. Thus, they are widely used in structural engineering applications. Carbon fibers have 2 major groups: high-Strength with high tensile strength and moderate modulus of elasticity and high-modulus fibers with high stiffness and moderate tensile strength.

In the manufacture process of carbon fibers 2 major materials are used. First is textile and the other is pitch. Polyacrylonitrile (PAN) is most preferred textile precursor. Pitch is a product of petroleum refining or coal coking. Table 2.1 presents the mechanical properties of carbon fibers.

Tale 2.1 Classification of carbon fibers  
(Source: Shalin 1995)

<b>Fiber classification</b>	<b>Young Modulus (GPa)</b>	<b>Tensile Strength (MPa)</b>	<b>Precursor</b>
Low modulus	35-70	350-1000	pitch
Intermediate modulus	200-300	2700-5500	PAN
High modulus	350-420	2000-2750	PAN, pitch
Very high modulus	450-800	1700-2600	PAN, pitch

### **2.2.1.3. Boron Fibers**

The Boron fibers provide higher stiffness values with the help of its high modulus of elasticity. They offer high strength and stiffness in tension, compression and bending. However, they are sensitive to stress concentrations. Boron Filament is manufactured by chemical vapor decomposition CVD. The main substrate that is used in the manufacturing of boron fibers is tungsten wire, which is an expensive and dense substrate. For this reason, presently boron fibers are mainly used in aerospace applications.

### **2.2.1.4. Organic Fibers**

Aramids are known as the most common organic fibers that are used for reinforcement applications. The aramid fibers have a tendency to form fibrils. So they have higher energy absorption capacity than brittle fibers. However, they have a highly anisotropic structure that causes poor transverse properties and lower axial compressive strengths. They are mainly used as reinforcements for tires, belts, and bulletproof vests.

### **2.2.2. Matrix Materials**

Reinforcing fibers are bound together by a matrix material, which provides the integrity of the composite material. They transfer stresses between the fibers and provide protection from privative environments. Matrix materials do not have much

effect on tensile strength of composite materials. On the other hand they have a major effect on the shear properties of composite. Matrix materials can be categorized into two groups: thermoset and thermoplastic polymeric matrices.

### **2.2.2.1. Thermoset Polymeric Matrices**

Thermoset polymeric matrices are manufactured from resin and a curing agent. If required, a solvent material can be used to lower the viscosity of the matrix. The Chemical resistance, thermal resistance, thermal stability, and glass transition temperatures of the matrix are controlled by curing agents (Jang 1994). In the first stage of production, the matrix is a viscous liquid. In the next stage, matrix material enters the curing process that can be at room or elevated temperatures. This second curing stage provides three dimensional linked polymer chains in the polymer material. Most common thermoset polymeric matrices are known as epoxy, phenolic, polyester, and vinyl ester resins.

Epoxy resins are the most advanced thermoset polymeric matrix material in present. They can be produced from a wide range of starting components, which provide a large spectrum of properties. They have high mechanical and adhesive properties and good productivity. They can stay in uncured stage in long durations that supplies sufficient time for the manufacturing process of FRPs.

### **2.2.2.2. Thermoplastic Polymeric Matrices**

Thermoplastic Polymeric matrices can be melted at high temperatures and can solidify with cooling. Recycle ability of thermoplastic matrices provides an unlimited lifetime for them. They do not require curing stage and this reduces the cost of for the manufacturing process of thermoplastic matrices. Thermoplastic polymeric matrices require high pressure followed by a cooling process to form them. As a result, fiber usage in thermoplastic polymeric matrices is limited due to the fiber damages in high pressures while forming the material. Therefore combining thermoplastic matrix with fibers requires the use of special fibers and treatment.

### **2.2.3. Production Methods of Fiber Reinforced Polymers**

Since there are several methods to manufacture polymer composites, it is important to decide which one of these methods will be an effective solution to reduce time, cost and improve the quality of the product for the required application. The production methods of FRPs that contain both thermoset and thermoplastic matrices will be described here. Focus will be given to thermoset composite manufacturing methods considering the aim of this study. Composite material production methods can be divided into 7 parts:

1. Open Mould Processes;

Wet-Lay Up/Spray-Up

Prepreg Lay Up

Filament Winding

2. Closed Mould Processes;

Compression Molding

Pultrusion Method

Resin Transfer Molding

Vacuum Assisted Resin Transfer Molding

#### **2.2.3.1. Wet Lay-up Method**

Wet lay-up is the most common manufacturing method of composite materials. Wet lay-up method is based on laying reinforcement material into the mold and applying the catalyzed resin afterwards. First, a parting agent is applied to the mold in order to prevent the composite to stick to the mold. Then the dry reinforcement is placed into the mold and the resin material is applied. While applying resin into the reinforcement in the mold, it is rolled continuously to ensure the matrix is distributed to the reinforcement and clear the air pockets inside. When reinforcement is saturated with the resin, another reinforcement layer is applied on top of first layer. This loop of process is continued until the target thickness is reached. Applying pressure by hand rolling or vacuum bagging will clear the entrapped air in the FRP material, which will

prevent small cavities inside the composite. When the composite laying process is completed, the composite is allowed to cure.

Advantages/Disadvantages of wet lay up technique (Jang 1994):

- Tooling can consist of any material that will hold its shape under minimal pressure,
- Tooling can be changed easily during experimental phases or to accommodate engineering redesign,
- Investment in pressure devices such as a press autoclave or vacuum pump is not required, although a vacuum pump is often used with epoxy parts and some polyester parts,
- Curing ovens are not needed,
- Semiskilled workers can be readily trained.

Limitations of wet- lay-up technique:

- Only addition-type cross-linking resins can be used because condensation types require some form of pressure to avoid porous, poorly laminated structures
- Production uniformity, both within a single part and from part to part is difficult to maintain,
- Because of the inability to compact laminate with any pressure, the resin content is often quite high,
- Voids are common,
- Mechanical properties are low in comparison with other composite manufacturing methods,
- Tight-weave fabrics are difficult to saturate with high viscosity resins, resulting in low strength,
- Draining from vertical walls can be a problem. Puddles near the base and resin-poor area in the wall can develop, although most resins have an appropriate viscosity to prevent this,
- There is shrinkage in resin rich areas.

### **2.2.3.2. Prepreg Lay-up Method**

Prepreg is a ready-to-mold material in sheet form which may be cloth, mat, or paper pre-impregnated with resin and stored for use. The resin is partially cured and supplied to the fabricator who lays up the finished shape and completes the cure with heat and pressure. This method allows better control of resin/fiber ratio. However prepreg lay-up method usually requires vacuum bagging. The prepregs used for lay-ups should have a slight roughness to ensure the layers will not slide over one during lay-up. The accord of prepregs to mold is also important.

### **2.2.3.3. Filament Winding**

This method can be thought as a type of the lay down methods done by an automated machine, which incorporates the impregnation of the fiber tows as part of the filament winding process. Filament winding method is a method in which a continuous tape of resin is impregnated to the fibers wrapped over a mandrel to form the part. Layers are added continuously in same or different angles until required thickness is reached. The main point of the successful filament winding is the relative speed of the mandrel and the head. These two motions define wrapping angles and overlap.

### **2.2.3.4. Compression Molding**

In compression molding method the molding material, generally preheated, is placed in an open, heated mold cavity. After that the mold is closed with a top force. Pressure is applied to force the material into contact with all mold areas. Following this, heat and pressure is applied until the molding material has cured enough. The process employs thermosetting resins in a partially cured stage. Compression molding is a high-volume, high-pressure method suitable for molding complex and high-strength fiberglass reinforcements. Advanced composite thermoplastics can also be compression molded with unidirectional tapes, woven fabrics, randomly orientated fiber mat, or chopped strand. The advantage of compression molding is its ability to mold large, fairly intricate parts. Figure 2.2 shows the important parts of the compression molding process.

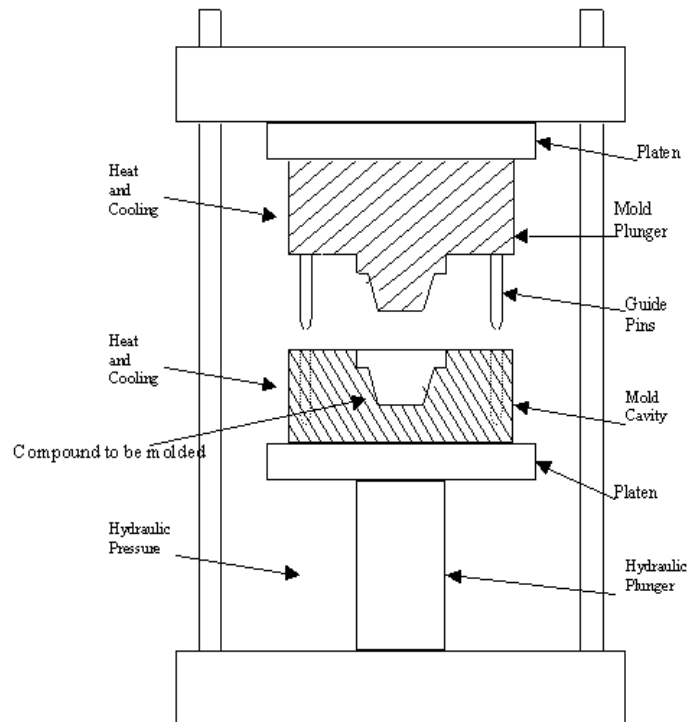


Figure 2.3. Compression Molding  
(Source: Louisiana State University 2009)

### 2.2.3.5. Pultrusion

Pultrusion is a continuous process of manufacturing with continuous reinforcement fibers. The process starts with pulling resin impregnated fiber reinforcement through a perforator followed by a heated die to cure the resin. Because of the continuous production, resin that will be used in composite material must cure quickly. Its major limitation is the constant cross section of composite because of the extrusion process. Figure 2.3 shows the important parts of the pultrusion process.



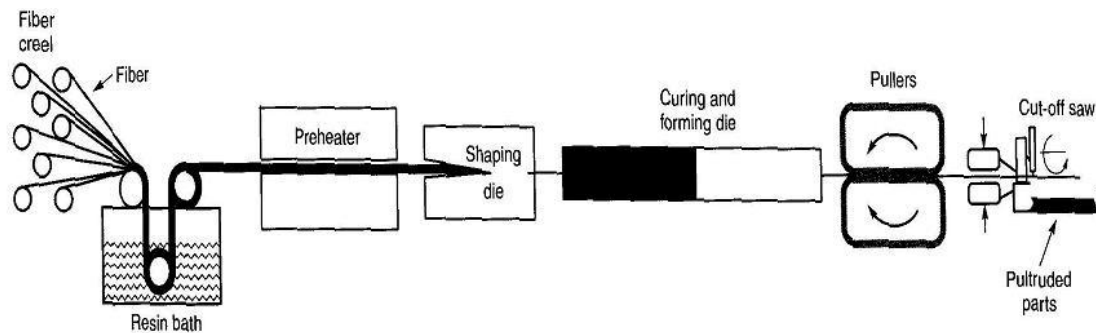


Figure 2.4. Pultrusion Line  
(Source: Hyer 1998)

### 2.2.3.6. Resin Transfer Molding

Resin transfer molding (RTM) is also known as resin injection molding (RIM). In this process a closed mold, loaded with reinforcement, is injected with resin. The mold is generally put under vacuum in order to remove entrapped air from reinforcement and quicken the RTM process. In the RTM method there are plenty of important points that will directly affect the quality of the composite material. The mold design is one of the most important parts of the RTM process. Mold must be designed to provide resin access to all areas with same concentrations throughout. Another point is the resin injection pressure. If resin is not injected through mold with an appropriate pressure, it might cause the movement of the reinforcement. On the other hand vents pulling air out of mold is quite important for the uniformity of the composite material. Figure 2.4 shows the important parts of the resin transfer molding process.

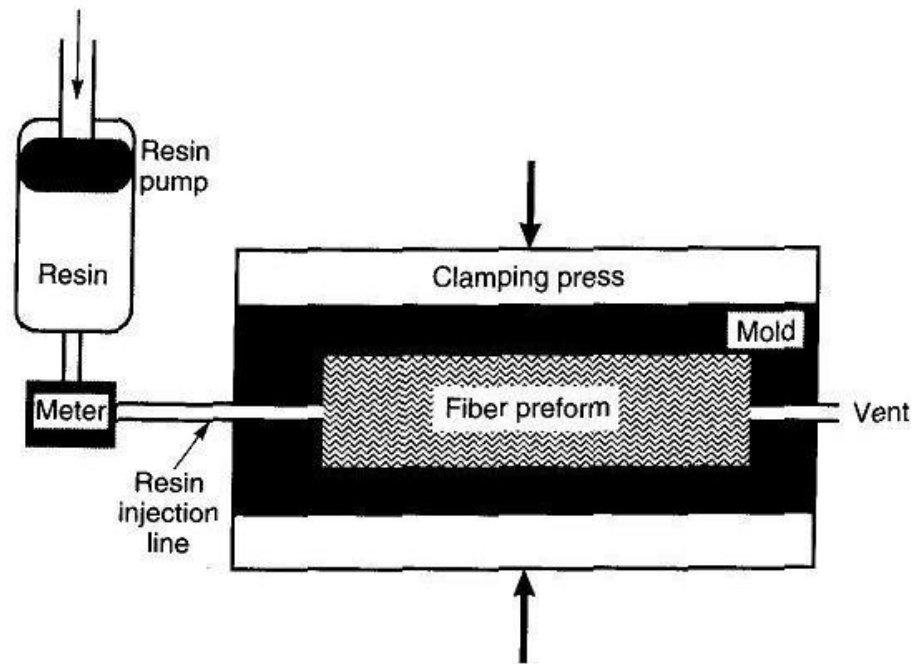


Figure 2.5. Reinforced Reaction Injection Molding of Thermosets  
(Source: Hyer 1998)

### 2.2.3.7. Vacuum Assisted Resin Transfer Molding

Vacuum Assisted Resin Transfer Molding (VARTM) is a derivative manufacturing method of resin transfer molding. This method has some improved modifications over traditional RTM method. For example matched metal tool in RTM is replaced in the VARTM process by a formable vacuum bag material and the vacuum provides the dual advantage of the pressing the layers together by simultaneously withdrawing the excess. Figure 2.6 shows the important parts of the vacuum assisted resin transfer molding process.

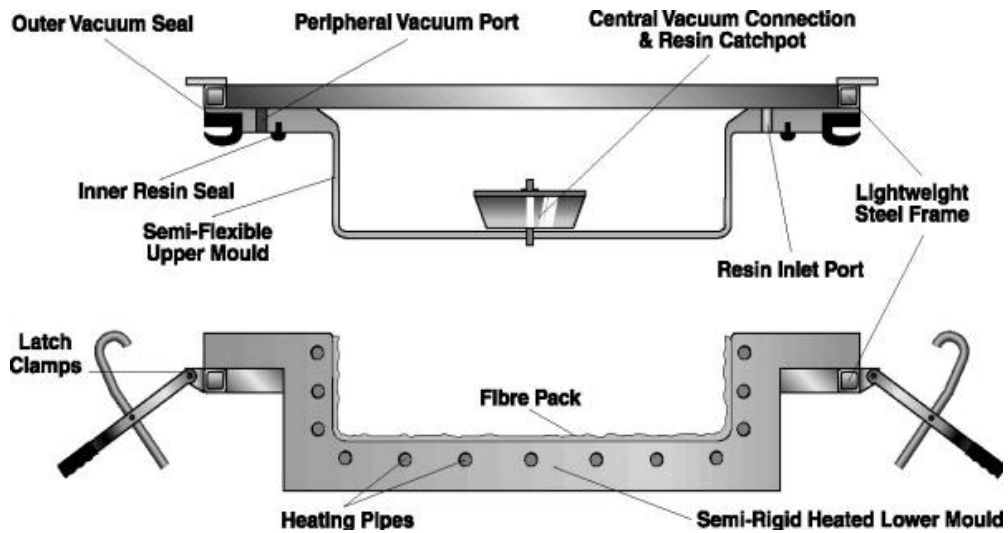


Figure 2.6. VARTM Process  
(Source: Resin Infusion 2009)

## 2.4. Previous Studies of Steel-FRP Applications

Some general reviews about the application of polymer composites in civil constructions were written by (Pendhari, et al. 2007) and (Bakis, et al. 2002). As seen in these reports, a large number of studies are available on rehabilitation and strengthening of steel members by the use of FRP materials. There are various studies aimed to increase the ductility and strength of steel members by glass FRP (GFRP) or carbon FRP (CFRP).

(Accord, et al. 2005) studied the enhancement of structural steel beam members ductility by using GFRP materials. This finite element based study investigates the effects of GFRP strips placed in compression flange of beam plastic hinge regions on providing bracing to local buckling in flanges. This reinforcing strategy increased the flexural strength of the beams by 25% and significantly improved the ductility of the beams when compared with bare steel members. The location and length of the GFRP strips were also investigated. The study revealed that using GFRP strips on half the beam length had the same effect as using the strips on the full beam length. The study also showed that the most effective location to place the strips was adjacent to the flange tips since local buckling is more severe at flange tips rather than closer to the web.

(Photiou, et al. 2006) used externally bonded CFRP and GFRP hybrid laminates to increase the flexural capacity of steel beams by placing composite materials to an artificially degraded rectangular cross sectional steel beam. A total of four beams were strengthened. Two of the beams were strengthened by U-shaped prepregs which continue to the mid-point of the rectangular beams in vertical axis. The remaining two beams are strengthened by a flat prepreg. FRP prepregs in strengthening applications are generally in situ manufactured and they bonded to the steel surface by an adhesive film. Rehabilitated beams was loaded under a 4 point loading test setup and specimens reached even higher ultimate loads and deflections without any adhesive failure as compared to the full capacity of the beams with no degradation.

(Sen, et al. 2001) studied strengthening steel bridge sections using CFRP laminates. 6 steel beams acting compositely with a reinforced concrete slab, were loaded until they past the yield strength of the tension flange. Damaged beams were strengthened by 3.65m length and 2 or 5 mm thick CFRP laminates bonded to the tension flange. Experiments were continued until failure. Results showed significant ultimate strength gains with an improvement in elastic response.

Generally, CFRP and GFRP materials are used in steel strengthening or rehabilitation applications. In order to make sure the best performance is achieved from the steel-FRP hybrid systems, the right FRP should be chosen for specific applications. Therefore, the advantages and disadvantage of each material should be known. Some of the basic facts and properties are stated below ( El Damatty, et al. 2005):

- 1- Due to the superior properties of the CFRP sheets, failure of the retrofitted steel member generally occurs in the adhesive and thus the capacity of the CFRP sheets is not fully utilized.
- 2- Galvanization can occur when steel and carbon surfaces are in direct contact.
- 3- CFRP cost is much higher than that of GFRP.

As (El Damatty, et al. 2005) mentioned studies with CFRP and GFRP revealed the common major failure mode in FRP strengthened steel members: debonding. It is important to find out factors affecting the bond between FRP and steel surface. Studies related with the interaction of steel and FRP material in strengthening and rehabilitation applications are also of interest.

Some studies, which aimed to increase the surface shear strength between steel and GFRP, focused on steel surface treatment methods. Due to the fact that chemical surface treatment is expensive and inconvenient, mechanical abrasion is a very good alternative to consider. Grit-Blasting is the most effective type of mechanical surface treatment of steel members (Hollaway and Cadei 2002). (Harris and Beevers 1998) studied the effects of grit blasting on surface properties for adhesion. He found that grit blasting resulted in higher adhesive joint strengths compared to those of as-rolled surfaces. However, results showed no difference in strength between fine and coarse grits. Another traditional well known surface treatment is mechanical abrasion with sand brushing. (Possart, et al. 2002) showed that as the roughness of the surface is increased, the effective surface area for the bond also increases. In addition, in these studies surface cleaning after mechanical treatment was also investigated. (Hollaway and Cadei 2002) stated that the dust cleaning with solvent redistributes remaining dust on whole surface and it will result in poor surface bonding. They suggest removing the dust by dry wipe or vacuum head with brushes. However, there are also tests that show good performance of bonding with solvent cleaning after grit blasting (El Damatty et al. 2003, Photiou, et al. 2004). Hence, it is important to pay attention to surface cleaning with solvents.

(Schnerch, et al. 2005) investigated the bond behavior of CFRP strengthened steel bridges and structures. Surface preparation methods and preventing galvanic corrosion is discussed followed by the results of an experimental test, which consists of an FRP strengthened I-beam with CFRP strips in the tension flange with various development lengths and adhesives. Different failure types observed for different adhesives under same conditions revealed the significant effect of adhesives on strengthening applications.

(Chiew, et al. 2005) studied debonding failure model for FRP retrofitted steel beams. The study included finite element and experimental tests of same adhesive and epoxy for different loading conditions to obtain the bond strength of joints. Double-lap joint, single-lap joint, T-peel joint and tubular joint specimens were prepared with same surface treatment. A bond failure model for FRP strengthened structures was developed from the results of FE and experimental analysis.

(Buyukozturk, et al. 2004) did a general review on debonding problem of FRP strengthened steel and reinforced concrete members. The study stated debonding

problems were a limiting barrier against FRP usage in steel and concrete strengthening applications.

(El Damatty, et al. 2003) investigated various adhesives that can be used in GFRP-steel bonding. Results obtained from a previous research were followed by a further study, where they used GFRP sheets to strengthen steel bridge deck. Both experimental and finite element analytical results showed that major failure mode of the connection was debonding of FRP material from steel surface.

These mentioned studies lead researchers to investigate the improvement of bonding between steel and FRP materials. (Melogranna and Grenstedt 2002) studied on improving joint performance between composites and steel using perforations. Study included perforated stainless steel strips with circular or triangular holes. Results showed perforations increased the interaction between steel and FRP material.

Additional studies with surface treatment and cleaning were also studied experimentally in order to increase the shear transfer between steel and FRP material. (Molitor, et al. 2000) claimed bond strengths could be significantly improved by surface treating the adherents prior to bonding. In that manner different mechanical and chemical surface preparation methods were tested in various studies.

(Peck 2007) conducted a study on stabilization of plastic buckling behavior of slender steel sections with FRP. WT 6x7 (inch) steel sections were strengthened with both GFRP and CFRP plates with various thickness and width values.

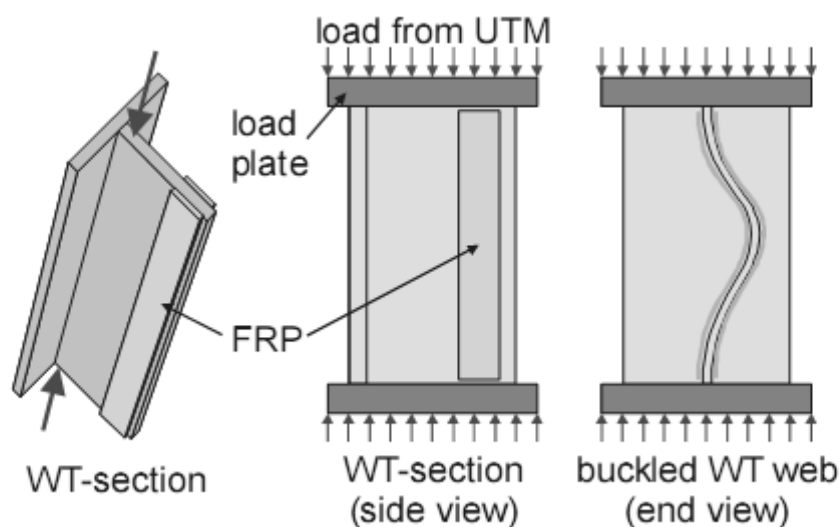


Figure 2.7. Axially Loaded T sections  
(Source: Peck 2007)

His study revealed:

The FRP retrofit measures did not provide a substantial increase in the axial compression load carrying capacity of the WT steel section members. The GFRP specimens exhibited an increase in axial capacity of 9%. The stem was supported by the FRP until the debonding of the FRP material from steel surface and the failure behavior may be described as end-peel debonding.

## **CHAPTER 3**

### **STRENGTHENING CONCEPT**

#### **3.1. Overview**

In recent years, aging of existing steel structures increased the demand of effective strengthening or rehabilitation methods. In addition, observations in steel moment frame buildings in the aftermath of 1994 Northridge and 1995 Kobe earthquakes revealed some faults in design methodologies and lead the steel industry to conduct extensive research programs (Nakashima, et al. 1998) to overcome the brittle fractures in connection points of steel moment frames. Major recommendations of these research programs were to shift the plastic hinge zone of the beams away from the column face in beam-column connections. As a design rule, moment frames are built within the aim of energy absorption at highest levels possible. The design of beam-column connections in welded steel moment frames is generally based on the strong column – weak beam concept, where the majority of the energy dissipation is expected to occur at beam plastic hinges near the column face. Figure 3.1 shows the favorable collapse mode of a beam in a steel moment frame building. The research results showed that the stress concentrations at the beam-column groove welds were a threat to the ductility of the structure; and could be mitigated by shifting the plastic hinge region at the beam away from the column face.



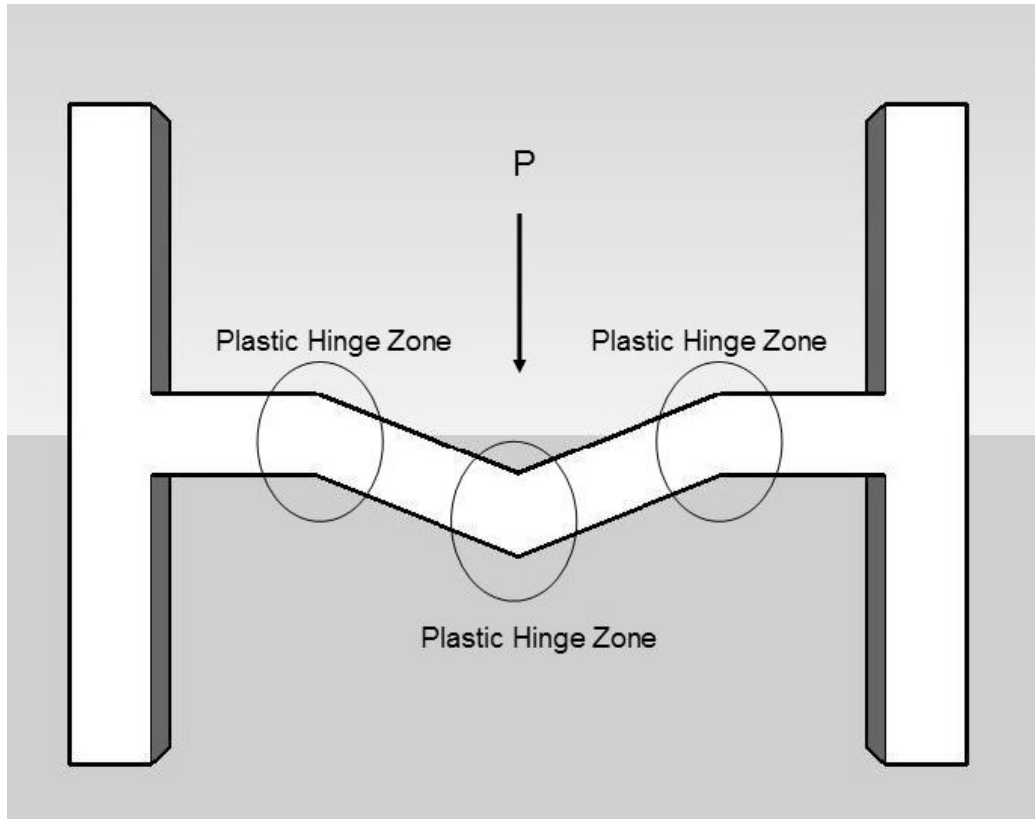


Figure 3.1. Collapse Mechanism of a Beam

### 3.2. Recommended Modifications to Beam-Column Connections

The major recommendations of the post-Northridge and Kobe research were: a) to use a weld metal with a higher Charpy V-Notch toughness in beam-column groove welds; b) providing a welded haunch, bolted bracket, or reduced beam section modification to shift the beam plastic hinge region away from the column face. Two of these modifications will be briefly presented in this section.

#### 3.2.1. Welded Haunch Modification

Additional haunch welding method is based on strengthening the beam-column connection zone to provide enough stiffness to the beam in order to shift the beam plastic hinge zone away from the connection. (Lee 2003) studied this type of straight haunch connections with I beams and results showed satisfactory levels of connection ductility without fracture. Figure 3.2 shows a sketch of a steel frame story, where the

beams are modified by a straight haunch. Other haunch types can also be utilized (AISC 1999).

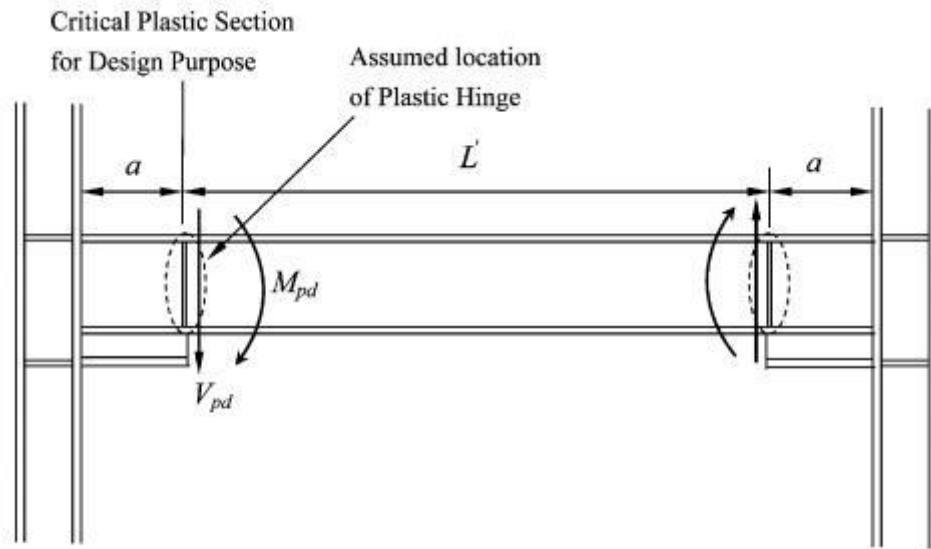


Figure 3.2. Typical Beam Span with Welded Straight Haunch  
(Source: Lee 2003)

### 3.2.2. Reduced Beam Section Modification

Another preferred modification method is trimming the steel beam section in the plastic hinge zone with pre-defined shapes. This type of a modification is often referred as a reduced beam section modification and is often more practical and economical compared to the additional haunch modification strategy. A large number of studies were conducted based on this concept. (Lee 2006, Jin 2004) This method of modification is mostly known as reduced beam section. Different trimming methods are investigated in these researches (Figure 3.3); however circular trimming is widely used.

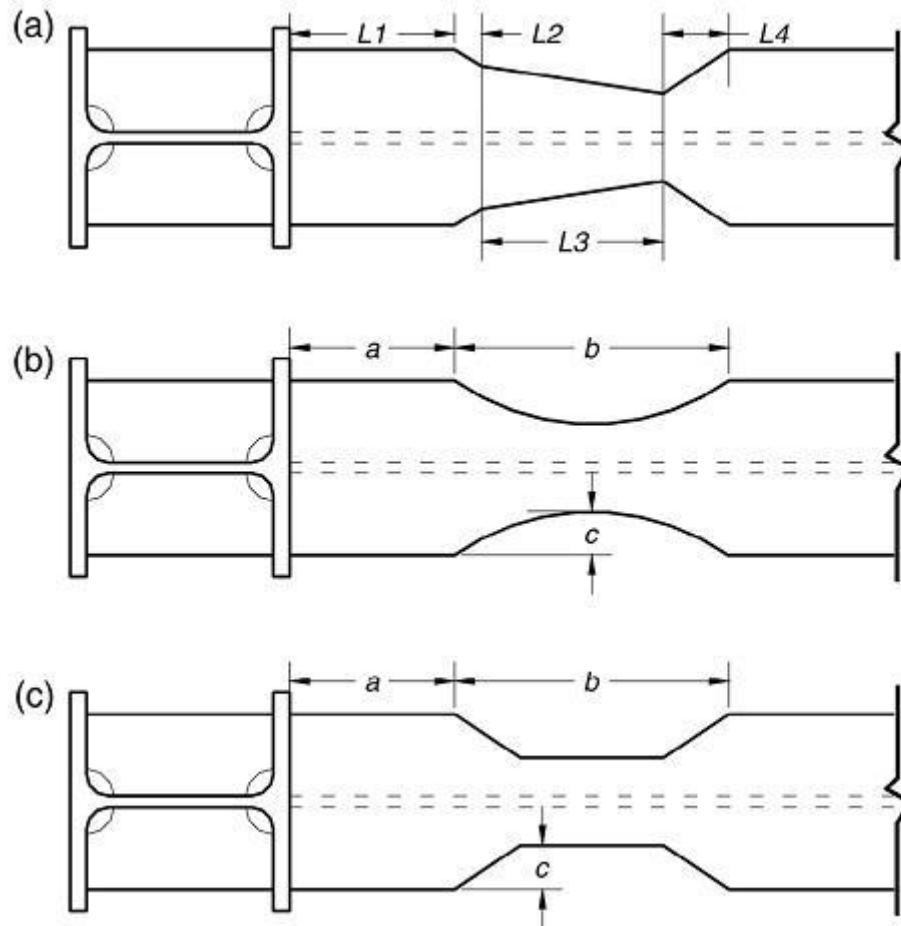


Figure 3.3. Various RBS configurations: (a) tapered cut, (b) radius cut, (c) straight cut  
(Source: Jin 2004)

(Lee 2006) has investigated RBS with I beams in cyclic loading and observed an increase in plastic rotation developed and significant improvement in cyclic rotations capacity without fracture.

### 3.2.3. Strengthening with Glass Fiber Reinforced Polymer Material

In contrast to other fiber reinforced polymers, GFRP has a much lower modulus of elasticity as compared to steel, which prevents significant strength increase in steel members. With this unique property, GFRP has become one of the most suitable composite polymer to prevent local buckling of steel sections. Application of GFRP material to top/bottom flange and web surfaces can provide sufficient bracing to

buckling, which in turn will improve the ductility of steel sections. This experimental study investigates the local buckling behavior of steel plates reinforced with GFRP.

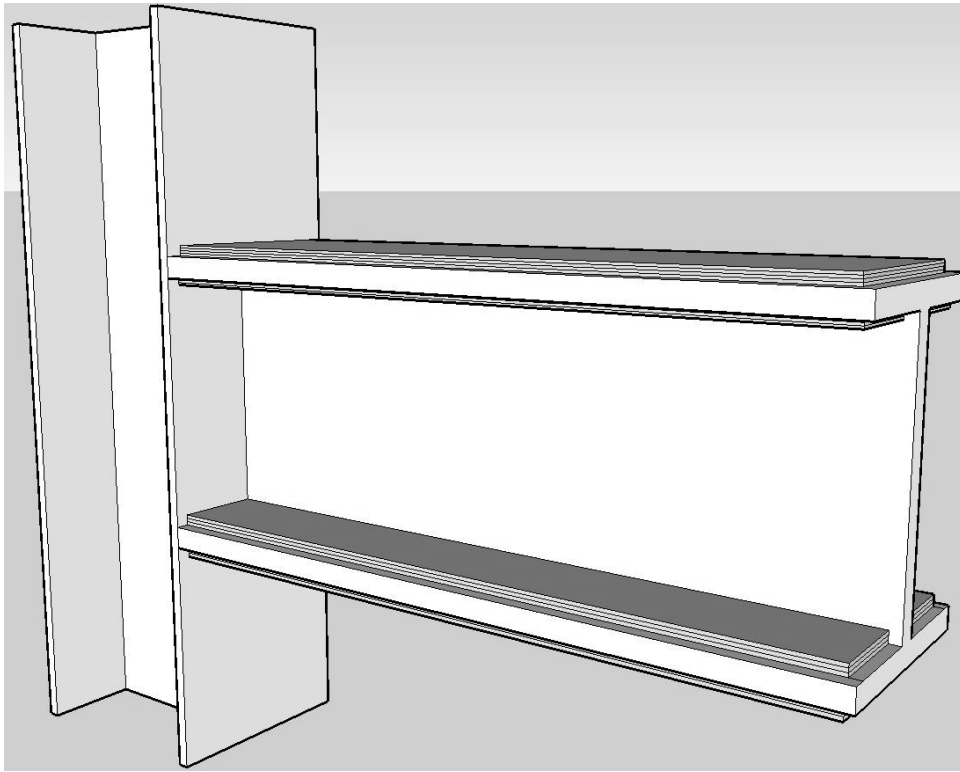


Figure 3.4. GFRP application along I-Beam

## CHAPTER 4

### MATERIALS AND TEST PROCEDURES

#### 4.1. Introduction

In order to effectively study the behavior of steel-GFRP systems the mechanical properties of the GFRP material, polymer matrix, and the interface between steel and GFRP need to be identified. This section consists of description of the standard test procedures utilized to define the tensile, compressive, and shear properties of GFRP laminates, and shear properties of the interface between steel plates and GFRP. Materials used in the study, as well as the production method of GFRP materials are also presented.

#### 4.2. Glass Fiber Material

In this study E-glass fibers with  $0^\circ/90^\circ$  and  $0^\circ/+45^\circ/90^\circ/-45^\circ$  fiber orientations were used as the reinforcement material for GFRP productions. The E-glass fibers were produced by Telateks Textile Products Company. For the  $0^\circ/90^\circ$  fiber orientation, fibers with specific weights of  $1250 \text{ gr/m}^2$  were used. For the  $0^\circ/+45^\circ/90^\circ/-45^\circ$  fiber orientation, fibers with specific weight of only  $1250 \text{ gr/m}^2$  were used. The tensile strength of the fibers given by the manufacturer was 2500 MPa.

### 4.3. Matrix Materials

As discussed in the previous chapter the two main constituents of GFRP materials are glass fibers and epoxy resin. Epoxy resins have good bonding capabilities to metal surfaces and they are generally the preferred matrix element of FRP materials produced by wet lay-up process (Cadei, et al. 2004). In this study, since GFRPs were produced by wet lay-up process and applied on steel surfaces, epoxy resin was chosen as the polymer matrix material. Two different epoxies were used. These epoxies were purchased from Duratek and Resoltech companies. Resoltech epoxy was specified as Resoltech 1040 resin and Resoltech 1048 curing component. Duratek epoxy was specified as Duratek lamination resin Duratek 1000/1100/A and Duratek 1000/1100/B with Duratek 1000/1105/B curing components. In addition, primer materials were used to increase the bond between the steel surface and GFRP. Two primer types were utilized: Duratek and Silan. Duratek Primer was purchased from Duratek Company and Silan was prepared in the Material Science of Engineering Laboratory of Izmir Institute of Technology.

The epoxy polymer had two fields of implementation in this steel-GFRP application study. The epoxy resin was used in the production of GFRP materials, as the polymer matrix, and also was used in attaching GFRP strips to steel surfaces, as the bond material. In the first application the elastic modulus of the resin becomes the important mechanical property, as the elastic modulus of the finished composite product depends on both the volume fraction of the resin and its elastic modulus. In the second field of application the primary mechanical property is the shear behavior of the bonded steel-GFRP interface.

The Duratek DTE 1000+ resin was used with both DTS 1100 and DTS 1105 curing agents. These 2 curing agents have similar properties but they differ in gel duration, which provides sufficient time to complete the production of GFRP in larger scales. In other words the curing agents determine the curing time of epoxy resins. Curing compound Duratek DTS 1100 has 30 minutes gel duration (@23°C, 100ml DIN 1994). Curing compound DTS 1105 has a gel duration of 450 minutes (@23°C, 100ml DIN 1994). They can be used in any mixture ratio in order to obtain the desired gel

duration. Resoltech 1040 epoxy resin was used with curing component Resoltech 1048, which had a gel duration of 40 minutes.

Material properties of Duratek and Resoltech epoxies given by the manufacturers are categorized as physical and mechanical and are presented in Table 4.1. Table 4.2 Table 4.3. Table 4.4.

Table 4.1. Physical Properties of Duratek Epoxy

Property	DTE 1000+	
	DTE 1100	DTE 1105
Mixture Ratio by Weight	100+35	100+35
Density (kg/l) DIN 2001	1.1 ±0.05	1.10 ±0.05
Viscosity (MPas) ASTM 2007	900 ±50	920 ±50
Gel Time(min)		
@23°C,100ml DIN 1989	30	450

Table 4.2. Physical Properties of Resoltech Epoxy

Epoxy	1040
Curing Component	1048
Mixture Ratio by Weight	100+22
Density (gr/cm <sup>3</sup> )	1.1
Viscosity (MPas)	400
Gel Time(min)	40

Table 4.3. Mechanical Properties of Duratek Epoxy

<b>Epoxy</b>	<b>DTE 1000+</b>	
	<b>DTE 1100</b>	<b>DTE 1105</b>
<b>Curing Component</b>		
Tensile Strength (MPa)		
Cure @ 23°C 7 Days ;DIN 1994	70±5	63±5
Tensile Strength (Mpa)		
Cure @ 23°C 1 Day + @ 50°C 19 hours ;DIN 1994	80±5	80±5
Modulus of Elasticity (Mpa)		
Cure @ 23°C 7 Days ;DIN 1994	2600±100	2350±100
Modulus of Elasticity (Mpa)		
Cure @ 23°C 1 Day + @ 50°C 19 hours ;DIN 1994	2800±100	2500±100
Elongation (%)		
Cure @ 23°C 7 Days ;DIN 1994	2.15±0.10	2.15±0.10
Elongation (%)		
Cure @ 23°C 1 Day + @ 50°C 19 hours ;DIN 1994	2.00±0.1	2.1±0.1



Table 4.4. Mechanical Properties of Resoltech Epoxy

Property	1040 Epoxy 1048 Curing Component
Tensile Strength (MPa)	65
Tensile Modulus (MPa)	3600
Flexural Strength (MPa)	100
Flexural Modulus (MPa)	3300
TG (°C)	90

#### 4.4. Composite Production

Composite productions were carried out by hand lay up method as explained in Chapter 2. Hand lay up is a simple manufacturing method with an opportunity of in-situ application. If desired, GFRP can be manufactured directly in strengthening areas of steel members (direct wet lay-up, DWL) or it can be manufactured outside of construction site and then GFRP can be plastered onto steel sections externally (preformed wet lay-up, PWL). Curing agents providing longer gel times can be preferred to supply enough production time for in-situ applications during larger GFRP manufacturing processes. In the manufacturing process utilized in this study, composites were also cured in room temperature to reveal in-situ production quality. All GFRP materials were produced by great care in a clean laboratory environment. Manufacturing method and curing conditions are the primary factor affecting the properties of GFRP materials. During the manufacturing process with hand lay-up method, it is important to saturate reinforcing glass fibers with resin. Furthermore, during the process all glass fiber layers need to be rolled with iron roller to help remove the trapped air inside the composite.

## **4.5. Test Procedures**

The following test procedures were used on determining the mechanical properties of GFRP and epoxy resin: 1- Tensile Test, 2- Compression Test, 3- Lap shear Test, 4- V-Notch beam test, 5- Steel Plate Compression Test.

### **4.5.1. Tension Tests**

Tension tests were performed for each glass fiber orientation of  $0^\circ/90^\circ$  and  $0^\circ/+45^\circ/90^\circ/-45^\circ$ . Tensile test were conducted according to (ASTM 2008). As stated in (ASTM 2008). These specimens were taken from a GFRP plate, which was prepared by hand lay up method. GFRP was cured for 7 days at room temperature. Test specimens were cut with composite saw with water spray. Tests were conducted in a Shimadzu universal test machine. During the tests, both force and strain data were collected. Strain data were collected by video-extensometers that followed stick markers placed to the tension specimens. For each fiber orientation, seven specimens were tested. After each test, maximum force, specimen section area and strain values were used to determine the maximum stress and modulus of elasticity of the specimens. Figure 4.1 shows a photograph of a tension specimen in the test machine.



Figure 4.1. Tension Test Set Up

#### 4.5.2. Compression Tests

The compressive mechanical properties of GFRP materials were determined following the (ASTM 2002) standard. There are 2 main compression directions for GFRP laminars as shown in Figure 4.2: a- Laminar direction, b- In-plane direction. However, compression tests were done in the in-plane direction, which was expected to give the lowest compression results. Both  $0^\circ/90^\circ$  and  $0^\circ/+45^\circ/90^\circ/-45^\circ$  oriented glass fibers were used to produce compression specimens. Two productions were done for  $0^\circ/+45^\circ/90^\circ/-45^\circ$  fiber orientation and one production was done for  $0^\circ/90^\circ$  fiber orientation. Specimens were prepared by hand lay up method and cured for 7 days at room temperature. They were cut by composite saw with water spray. Loading, stroke and cross section area values were collected to determine the compression modulus of elasticity and maximum compression strength values for each specimen. Figure 4.3 shows a photograph of a compression specimen in the test machine.

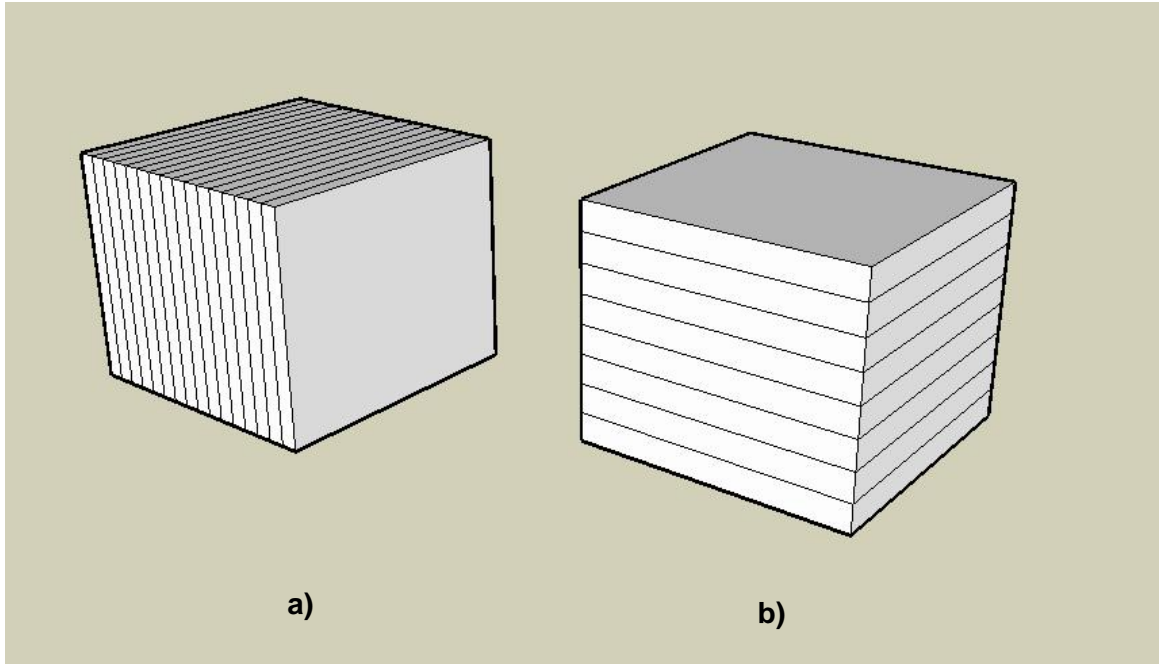


Figure 4.2. Compression Specimens: a- In Plane Direction b- Laminar Direction

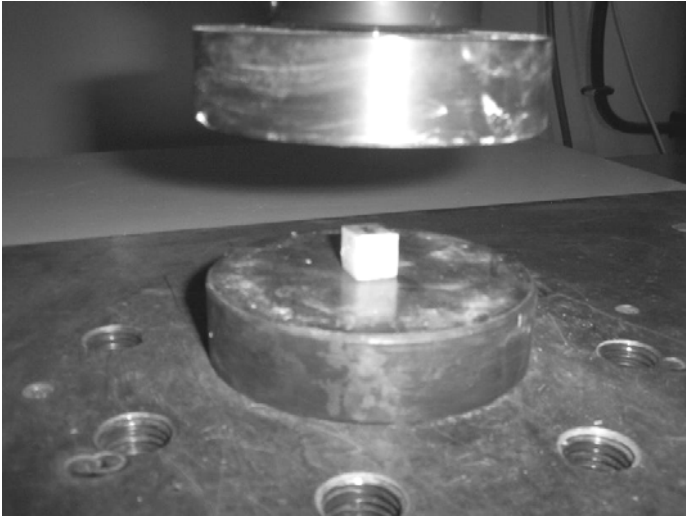


Figure 4.3. Compression Test Specimen in Test Setup

### 4.5.3. Lap Shear Tests

In this study lap shear test method defined by (ASTM 2001) was used to determine the shear transfer capacity between steel and GFRP material. The bond between steel and FRP is maintained by epoxy material, which is generally the weakest point in such connections. In order to achieve the most efficient shear transfer between steel and GFRP, different surface treatments and surface primers have been tried. In this test the (ASTM 2001) standard requires two 25.4 by 76.2 mm plates (for this study, one steel and one GFRP plate was used) be attached to each other at plate ends with an attachment length of 25.4 mm. Figure 4.4 shows 3 steel-GFRP lap shear test specimens oriented in different directions.

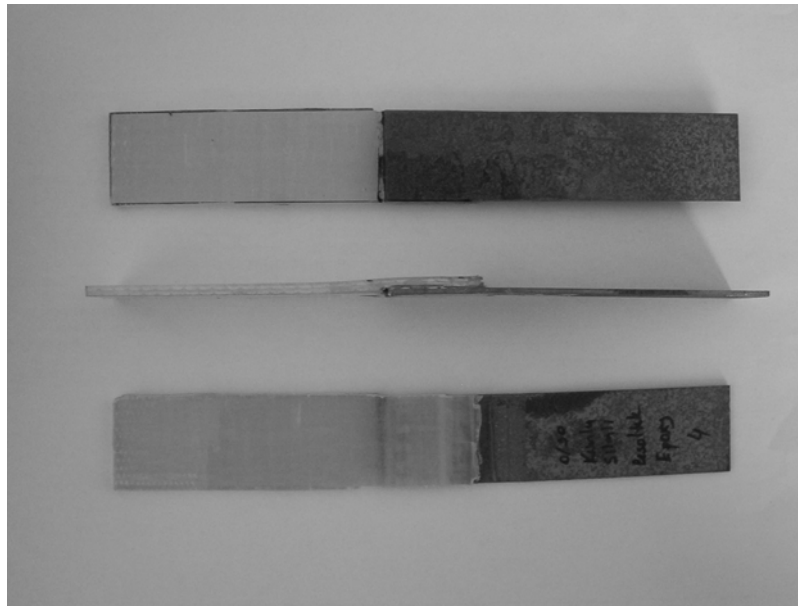


Figure 4.4. Lap Shear Test Specimens

#### 4.5.3.1. Lap Shear Surface Treatment Methods

Surface condition is an important factor affecting the shear between steel and GFRP. Smooth steel surface is not an appropriate surface condition to transfer adequate

shear stresses from steel to GFRP. For this purpose two different surface treatments were applied to the metal surface of the test specimens. Surface conditions tested in lap shear tests consisted of:

- 1- Metal surface without any process,
- 2- Sand papered metal surface
- 3- Sand blasted metal surface

Metal surface without any process is a smooth surface with no corrosion on the surface of the metal specimen. The steel surface was just cleaned with acetone to remove grease and dust on the surface. Sand papered metal surfaces were rubbed with sand paper (number 60) perpendicular to the shear force applied to the surface of the specimen. All sand papered specimens were sand papered for 10 minutes to create similar conditions. The other surface condition tested in this study was sand blasting in which solid particles were blown to the surface at high speeds. Different blasting particle sizes can be used through this application.

In addition to surface treatments mentioned above, some surface preparation primers were also used to increase the shear interaction between steel and GFRP. These surface primers were Duratek GR4480 and Silan. Duratek surface preparation primer consisted of two compounds. After mixing the two compounds, the primer was applied to surface with a brush. Thin primer layer was cured for 7 days in room temperature. On the other hand Silan is a chemical compound, which is prepared in laboratory conditions. Silan is prepared as follows:

- 1- 20% ethanol and 80% deionized water is filled in a container as needed,
- 2- Acid drops are added to the mixture until the Ph value reaches 4,
- 3- 1% Gglycidoxypropyltrimethoxysilane is added to the mixture,

After application, this primer must be cured for 3 hours in 80°C. After curing, the surface is ready for polymer application to bond the GFRP. Due to the curing time and temperature Silan primer is unsuitable for in-situ application. However, in order to see the limits of surface primers, Silan was also applied to the test specimens.

### 4.5.3.2. Parameters Examined in Lap Shear Tests

A total of 7 specimens for each combination of surface treatment and surface preparation primer were tested. Table 4.5 lists the parameters used in lap shear tests.

Table 4.5: Parameters used in Lap-Shear Tests

Surface Type	Primer Type	Curing	GFRP Fiber Orientation	GFRP Production
No Treatment	None	None	0°/+45°/90°/-45°	DWL*
No Treatment	Duratek	Room Temp.	0°/+45°/90°/-45°	DWL*
No Treatment	Silan	Oven 80°C	0°/+45°/90°/-45°	DWL*
Sand Papered	Duratek	Room Temp.	0°/+45°/90°/-45°	DWL*
Sand Papered	Silan	Oven 80°C	0°/+45°/90°/-45°	DWL*
Sand Blasted	Duratek	Room Temp.	0°/+45°/90°/-45°	DWL*
Sand Blasted	Silan	Oven 80°C	0°/+45°/90°/-45°	DWL*
Sand Blasted	Duratek	Room Temp.	0°/90°	DWL*
Sand Blasted	Silan	Oven 80°C	0°/90°	DWL*
Sand Blasted	Silan	Oven 80°C	0°/+45°/90°/-45°	PWL**
Sand Blasted	Silan	Oven 80°C	0°/90°	PWL**

\* DWL direct wet lay up

\*\* PWL pre-produced wet lay up

## 4.6. V-Notch Beam Test Procedure for Determining Shear Properties of GFRP

Interlaminar or in-plane shear strength of GFRP materials is also a limiting value for the design of strengthening steel beams. Beam plastic hinge regions in beam-column connections of welded steel moment frames are the main energy dissipating locations. GFRP attached to the flanges will be subjected to high shear forces with the formation of the plastic hinge in the beam near the column face. In determining the shear strength of GFRP laminates (ASTM 2005) V-Notch Beam method was followed.

### 4.6.1. Test Specimens

Test specimens were prepared using DURATEK DTS 1000/1100 epoxy and glass fiber with a weight of 1250 gr/m<sup>2</sup> and a fiber orientation of 0°/45°/90°/-45°. Specimens were cured for 7 days in room temperature. Specimen dimensions were taken as specified in (ASTM 2005). Cutting process of V-Notch specimens were done with water-jet process in Izmir. Cutting with water does not have any effect on the composite material. Meanwhile, water jet has an accurate cutting ability in small dimensions like notch parts of V-notch specimens. As a result, water-jet is the most suitable method to shape out composite materials.

In Figure the material coordinate system used to identify the directions of shear forces is presented. As seen in Figure GFRP material has 3 different shear directions because of its anisotropic structure. In Figure X-axis shows 0° fiber orientation, Y-axis shows 90° fiber orientation, and finally Z-axis is the lamination direction.  $\tau_{xz}$  ( $\tau_{zx}$ ) and  $\tau_{yz}$  ( $\tau_{zy}$ ) are interlaminar shear stresses and  $\tau_{xy}$  ( $\tau_{yx}$ ) is the in-plane shear stress. The aim of the V-Notch beam tests was specifically to determine the shear strength in the XZ (YZ) and ZX (ZY) and shear modulus in the XZ (YZ) and ZX (ZY). While the shear modulus in the XZ (YZ) and ZX (ZY) directions should be the same, the shear strengths in these directions would be different. The reason for the difference is due to the fact that in the XZ (YZ) direction the shear force is perpendicular to the fiber direction and in the ZX (ZY) direction the shear force is parallel to the fiber direction.

Figure 4.5 shows the 3 dimensional specimens tested in the V-Notch tests. . Although shown in the figure specimens in the XY and YX directions were not produced. In Figure 4.6 the specimens are located in an imaginary cubic GFRP in order to give a better idea on shear planes.



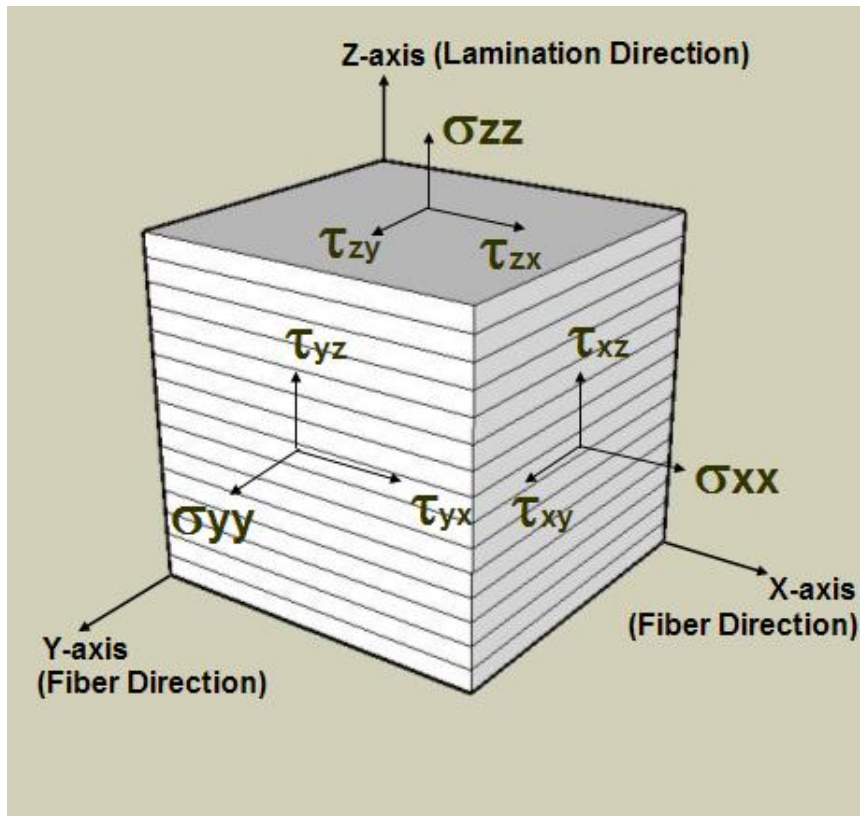


Figure 4.6. Material Coordinate System used in V-Notch Tests

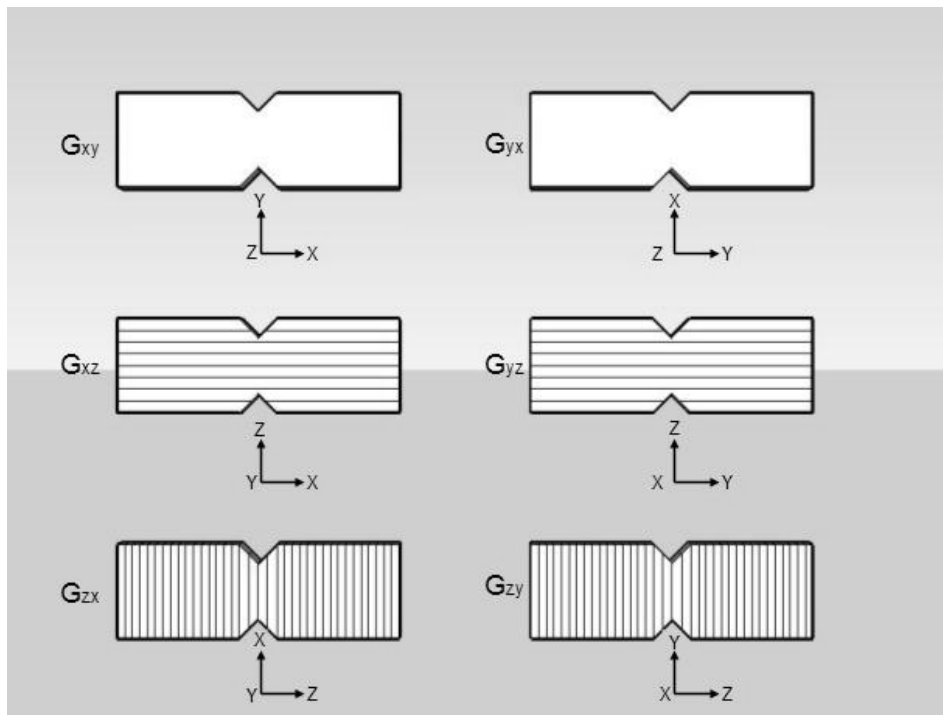


Figure 4.5. V-Notch Specimen Orientations

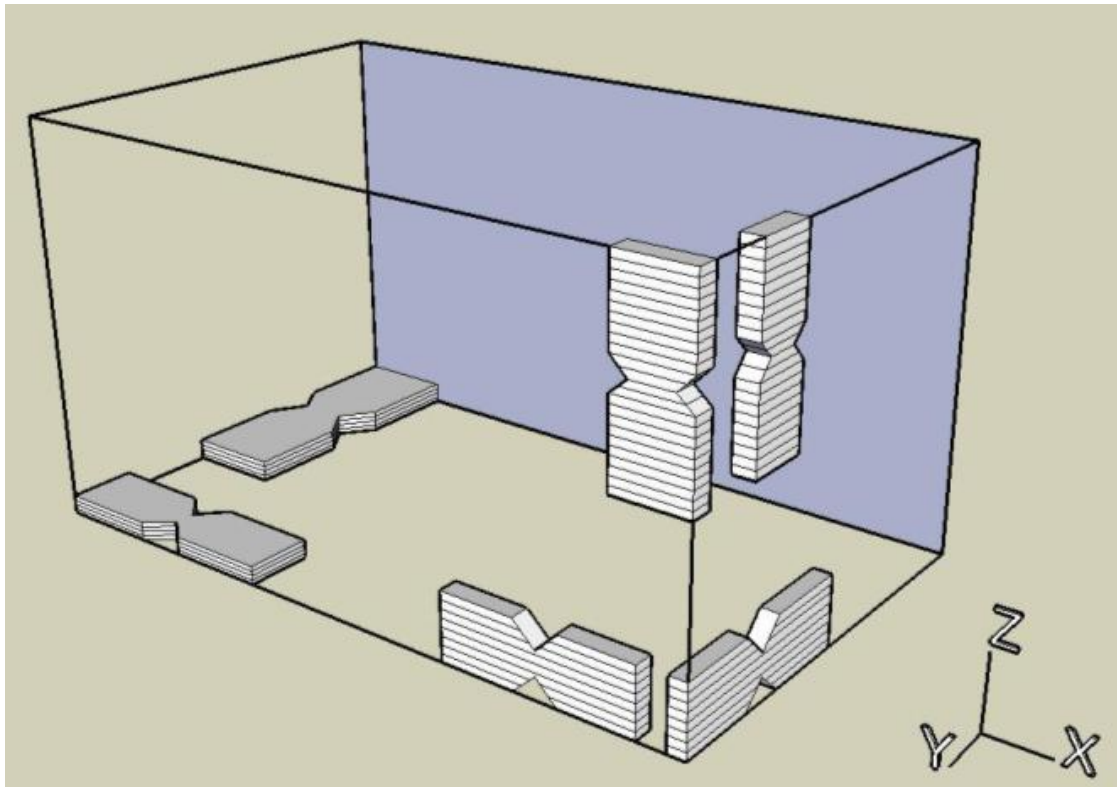


Figure 4.6. V-Notch Specimen Orientations Shown in an Imaginary Cubic GFRP

Figure 4.7 shows the beam-column connection with GFRP applied to the top and bottom flanges of the beam. This figure also reveals that the connection has no shear stress in plane XY (YX). For this reason interlaminar shear stress for plane XY (YX) was not tested. The weakest interlaminar shear strength is expected to be the ZX (ZY) planes, which do not have any reinforcing fibers perpendicular to the shear direction.

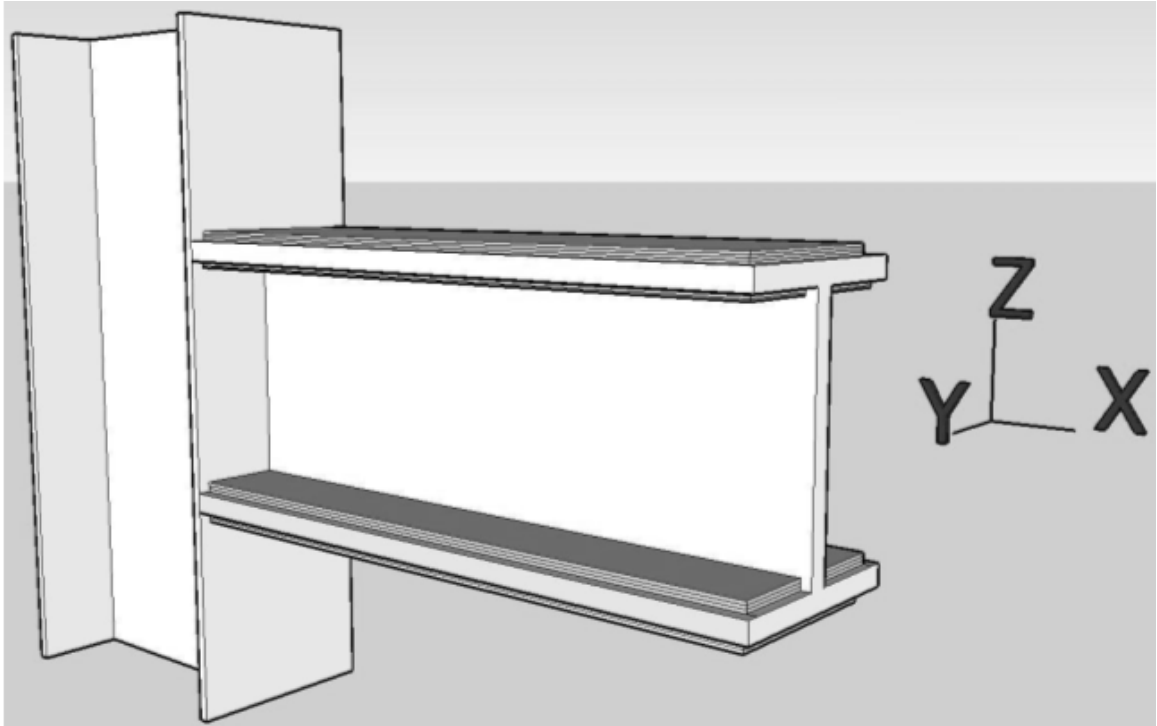


Figure 4.7. Sample GFRP application on Steel I-Beam

#### **4.6.2. V-Notch Test Setup**

V-notch beam shear test setup consisted of test apparatus, Shimadzu universal mechanical test machine, Data Acquisition Device, and strain gauge attached to V-notch specimens. Data Acquisition (DAQ) device has the ability to measure electrical, physical, mechanical or acoustic signals. In this study National Instruments DAQ device was used as the data measurement system. All test measurement set-up was designed and run in Labview Software (2007). The test apparatus shown in Figure 4.10. was built in Izmir Industry confirming to ASTM Adjunct ADID 5379 to V-Notch Test Standard.

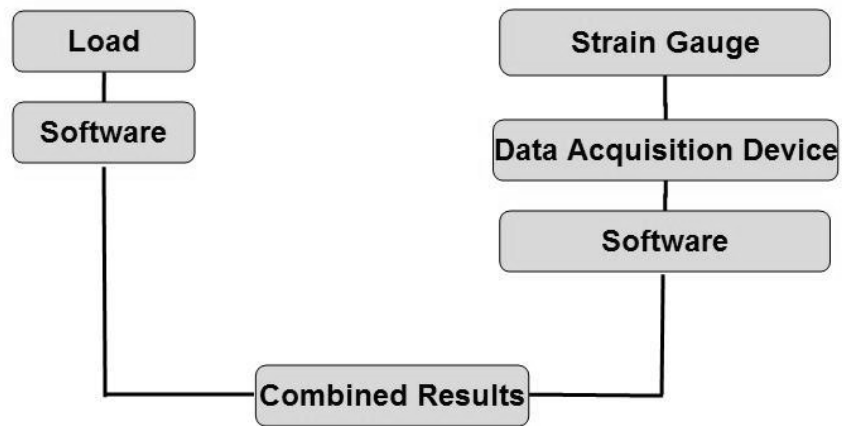


Figure 4.9. V-Notch Beam Test Method Test Set-up



Figure 4.10. V-Notch Test Apparatus

Major mechanical property differences of metal and composite materials can cause a significant strain difference in experimental analysis. Lower modulus of elasticity values of GFRP materials can significantly affect measured strains if compared with metal materials with higher modulus of elasticity. Rapid increase of strain values of composite materials is a typical example to this difference. In addition, high elongation requirements with different bonding procedures of composite materials, forces manufacturers to develop strain gauges with ability to satisfy composite material

demands. For these reasons a composite material strain gauge series of TML strain gauges were used in GFRP tests in this study.

If strain gauge type is the first decision on a test set-up, gauge length is the next decision to be made. Gauge length can be seen in Figure 4.11. This length determines the grid area covered by the strain gage. Covering greater area improves strain averaging on inhomogeneous materials such as fiber-reinforced composites. However, the specimen sizes used in this study limited this length. In this study a strain gauge with 5 mm active gauge length was used confirming to (ASTM 2005).

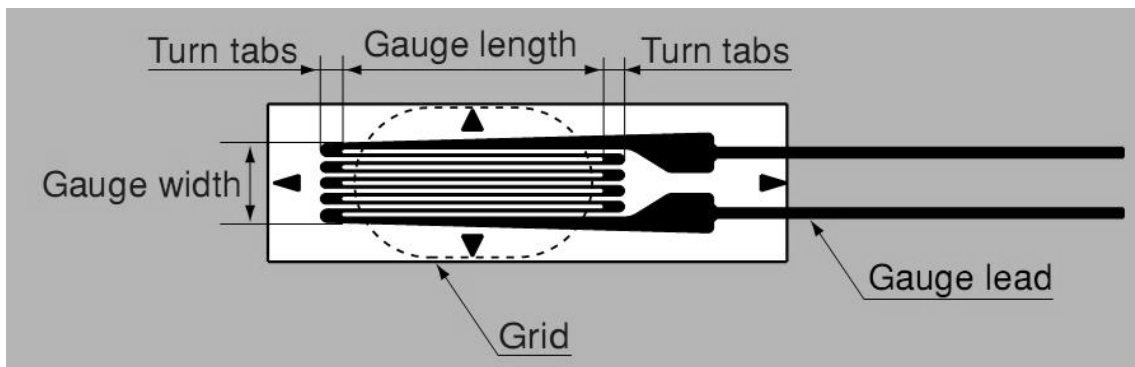


Figure 4.11. Strain Gauge

(Source : TML Catalog)

Surface cleaning and surface preparation of composite materials tend to be highly material specific. Furthermore, the aim of application can even limit the surface preparation applications of composite materials. For example, in V-Notch tests the physical surface treatments before placing strain gauges on specimen could damage the epoxy covering the reinforcing fibers, which will result scattered strain measurement while testing. This means that, deciding the right treatment has great importance on the performance of composite materials. Generally, surface preparation of composite materials consists of 2 steps. First step is physical treatment with a coated abrasive (ex. sand paper) with a fine grit to prevent deep epoxy abrasion. Second step is the cleaning of the surface with a solvent to remove oil and grease from surface of composite. Type of solvent depends on the type of the composite to make sure there will not be a

chemical reaction between solvent and composite. For this purpose acetone was used to clear the surface of composite before applying the strain gauges in this study.

Even the right surface preparation with the right strain gauge can give improper test result without a proper adhesive which bonds the strain gauge directly to the material surface. In this situation strain gauge manufacturer recommendations have great importance. Most of the strain gauge manufacturers produce suitable adhesives for their strain gauges considering surface type and gauge properties. In this study CN series adhesives recommended by TML Company was used to provide best surface bonding between strain gauge and composite.

Bonding process has a risk to damage the strain gauge while splitting the wires or applying the pressure. Therefore a voltmeter was used to check every single strain gauge attached to the composite material after the bonding process was completed. Figure 4.12 shows two V-notch specimens with and without strain gauge.

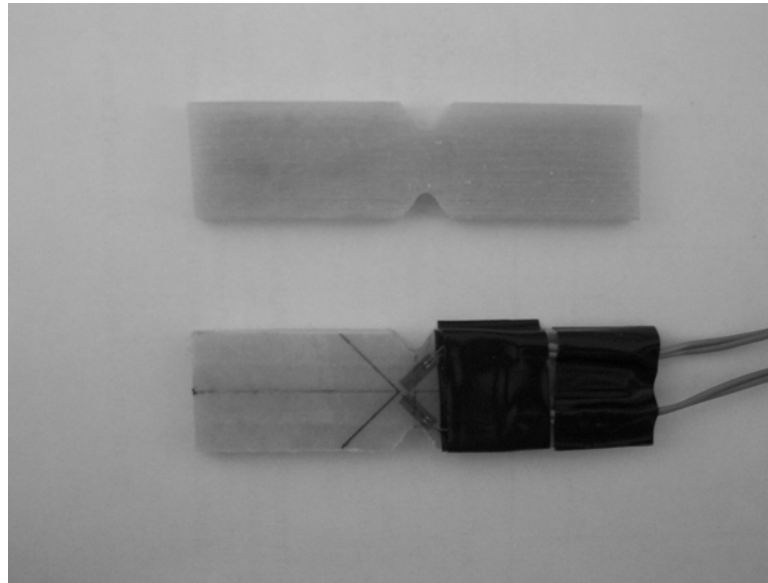


Figure 4.12. V-Notch Specimens with and without Strain Gauges Attached

DAQ device measures the strain values from the variation of the electrical resistance on the strain gauge by increase or decrease on its active gauge length. This variation refers to the exact strain value as stated below:

$$\varepsilon = \frac{\Delta L}{L} = \frac{\Delta R / R}{K} \quad (4.1)$$

where:

- $\varepsilon$  : Strain measured
- $R$  : Gauge resistance
- $\Delta R$  : Resistance change due to strain
- $K$  : Resistance factor as given from the manufacturer

Because of the set-up in the DAQ device a wheatstone bridge circuit to change the obtained data into a voltage output was required. For this situation a quarter bridge set up was designed in DAQ device software Labview (2007). This setup is shown below in Figure 3.

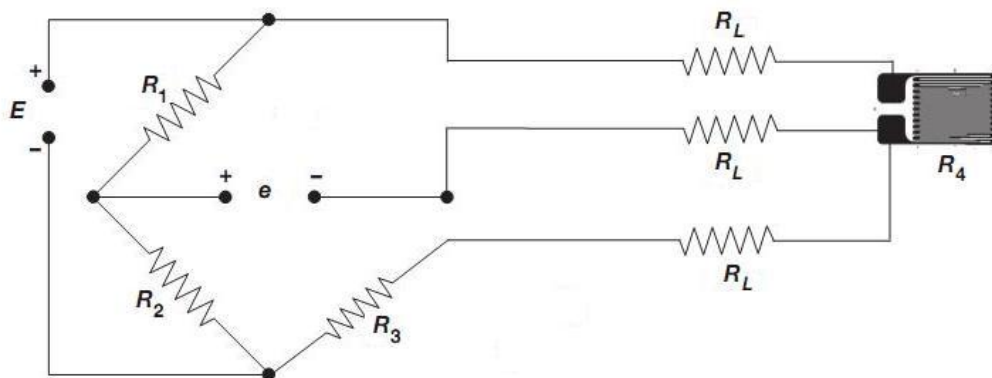


Figure 4.13. Quarter-Bridge Circuit Diagram

where:

- $R_1$  = half- bridge completion resistor.
- $R_2$  = half- bridge completion resistor.
- $R_3$  = quarter – bridge completion resistor, known as a dummy resistor.
- $R_4$  = active strain gage element measuring tensile strain ( $+\varepsilon$ ).

$E$  = excitation voltage.

$R_L$  = lead resistance.

$e$  = measured voltage.

During experiments data was collected simultaneously from two sources: universal mechanical test machine and DAQ device. Shimadzu Mechanical Test Machine was run displacement controlled at a rate of 2 mm/min as specified in (ASTM 2005) standard and load values were collected with the help of its software. DAQ device collected values from 2 strain gauges separately from 2 quarter bridges. Later on, these quarter bridge data were collected to form a strain data for each composite material. Each set of specimens had 7 specimens and results were averaged from these specimens. Figure 4.14. shows a photograph of a V-notch specimen placed in the V-notch test apparatus.

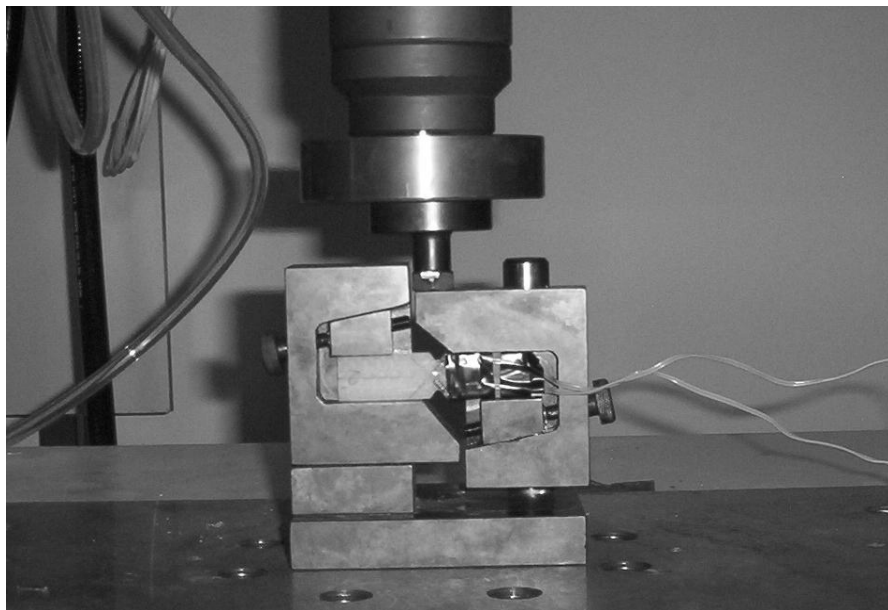


Figure 4.14. V-Notch Test Specimen in Test Apparatus



The strain gauge properties used in V-Notch tests were as follows:

Active length	5 mm
Gauge Resistance	119.8
Gauge Factor	2.1
Transverse Sensitivity	% 0.4

# CHAPTER 5

## GFRP TEST RESULTS

### 5.1. General

This chapter presents results of the tests described in Chapter 4. In summary GFRP tension test, GFRP compression test, lap shear test, and V-Notch beam shear test results will be presented briefly. The GFRP productions in all of the tests were done with wet lay up (Direct wet lay up or Pre-produced wet lay up) method that was detailed in Chapter 2. ASTM standard specification procedures were applied to all tests as explained in Chapter 4. Production methods, materials used in manufacturing, and their properties were also presented in Chapter 4. Almost all of the GFRPs were produced using Duratek epoxy, with a volume ratio of approximately 60% epoxy and 40% fiber.

### 5.2. Tension Test Results of GFRP

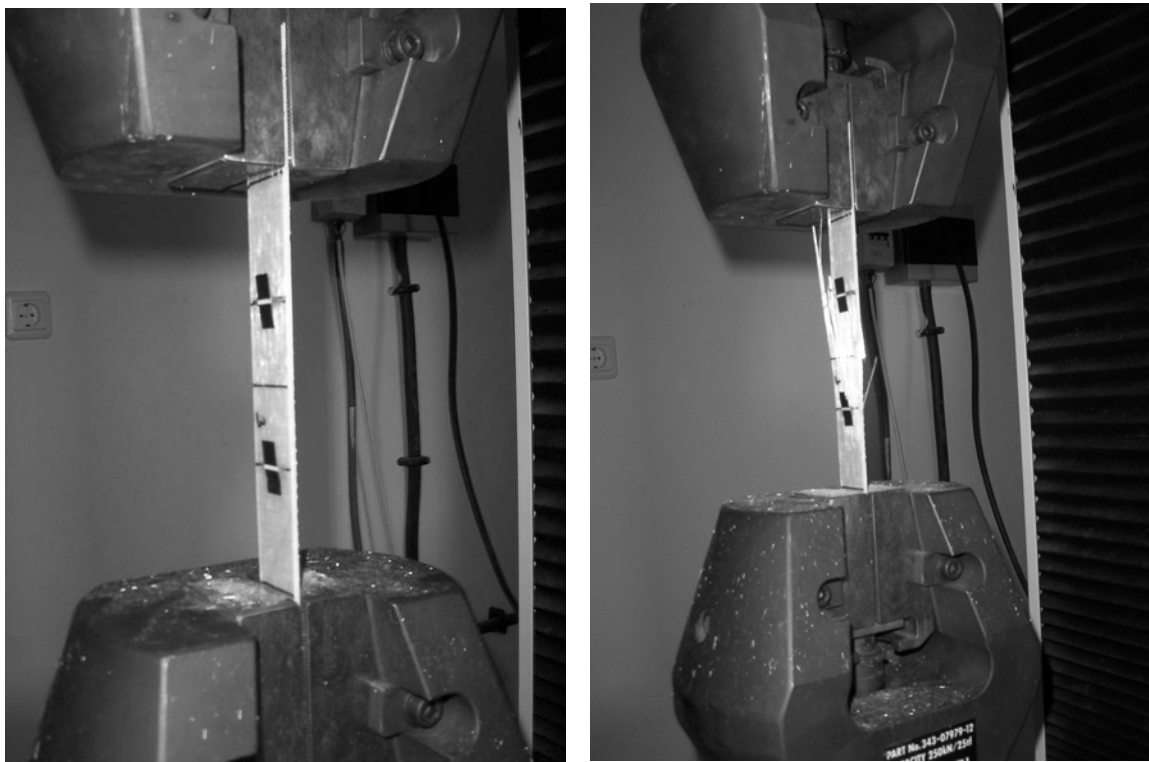
Tensile strength of GFRP materials was measured to determine their tensile capacity. Tests were conducted according to (ASTM 2008) standard. Table 5.1 presents results for GFRPs produced by fibers with  $0^\circ/90^\circ$  and  $0^\circ/+45^\circ/90^\circ/-45^\circ$  orientation with unit weight of  $1250 \text{ gr/m}^2$ . Results presented are mean values obtained from 7 tension coupons. Both materials had a unit weight of  $1250 \text{ gr/m}^2$ . Duratek epoxy was used in the production. Since both fiber compositions had the same specific weight, it was expected that GFRP with  $0^\circ/90^\circ$  fiber orientation would have a higher tension capacity in  $0^\circ$  direction, than that of GFRP with  $0^\circ/+45^\circ/90^\circ/-45^\circ$  fiber orientation. That means GFRP with  $0^\circ/90^\circ$  fiber orientation had more fiber density in the direction of applied tension ( $0^\circ$  direction), than that of GFRP with  $0^\circ/+45^\circ/90^\circ/-45^\circ$  fiber orientation. It can be seen from Table 5.1 that the tensile capacity of GFRP with  $0^\circ/90^\circ$  fiber orientation was 65 % greater than that of GFRP with  $0^\circ/+45^\circ/90^\circ/-45^\circ$  fiber orientation.

Table 5.1. Tension Test Results of GFRP Material

Fiber Orientation	Tensile Strength (Mpa)
0°/45°/90°/-45°	228.8 (9.95)*
0°/90°	376.5 (20.58)*

\*Standard Deviation values

Figure 5.1 shows photographs of a tension GFRP specimen during loading and a failed specimen after loading, respectively.



a)

b)

Figure 5.1. : Sample Tension Test Specimen (a) and Failure (b)

### 5.3. Compression Test Results of GFRP

Compressive test results of GFRP materials with 1250 gr/m<sup>2</sup> unit weight per area for 0°/90° and 0°/+45°/90°/-45° fiber orientations is presented in Table 5.2. Results presented are mean values obtained from 5 specimens. The compressive tests were conducted according to (ASTM 2002) standard. Compressive strengths of GFRPs with

a fiber orientation of  $0^\circ/45^\circ/90^\circ/-45^\circ$  and  $0^\circ/90^\circ$  were essentially the same (about 224 MPa). The compression elastic modulus of GFRPs with a fiber orientation of  $0^\circ/45^\circ/90^\circ/-45^\circ$  was about 10000MPa.

Table 5.2. Compression Test Results of GFRP Material

<b>Fiber Orientation</b>	<b>Compressive Strength (Mpa)</b>	<b>Modulus of Elasticity (MPa)</b>
$0^\circ/45^\circ/90^\circ/-45^\circ$	224.9 (11.95)*	10029 (435)*
$0^\circ/90^\circ$	224.4 (27.83)*	-

\*Standart Deviation Value

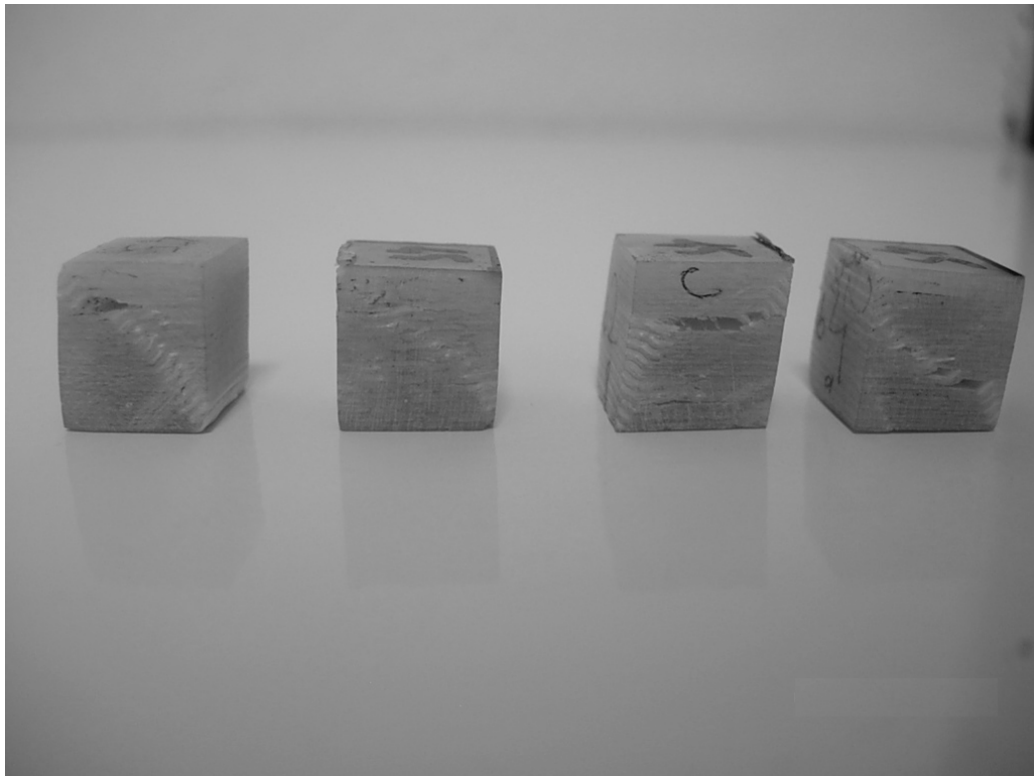


Figure 5.2. Compressive Failure of GFRP Specimens

The main purpose of using GFRPs in beam plastic hinge locations is to mitigate flange and web local. Since local buckling occurs under compressive forces, the compressive mechanical properties of GFRPs become more important than their tensile mechanical properties. In other words, in choosing which GFRP to use throughout the

study the compressive strength and modulus become the determining property. From the compressive properties of GFRPs it is seen that using either fiber orientation is acceptable. GFRPs with a fiber orientation of  $0^\circ/45^\circ/90^\circ/-45^\circ$  and a fiber unit weight of  $1250 \text{ gr/m}^2$  were used throughout the rest of the study. Using GFRPs with  $0^\circ/+45^\circ/90^\circ/-45^\circ$  fiber orientation will be more effective in controlling local buckling with respect to using GFRPs with  $0^\circ/90^\circ$  fiber orientation.

#### **5.4. Lap-Shear Test Results of GFRP-Steel Connection**

The main purpose of lap-shear experiments was to reveal the shear strength of steel-GFRP connection. This process is directly related with the material properties and surface conditions. Three different surface types of lap shear specimens: 1- no treatment, 2- sand papered, 3- sand blasted were tested with 2 different surface primers: 1- Silan, 2- Duratek. All productions were done by wet lay up method and all productions were cured at room temperature. The test procedure was explained in Chapter 4. In most of the lap shear tests GFRPs were produced from fibers with fiber orientations of  $0^\circ/45^\circ/90^\circ/-45^\circ$  as reasoned in the previous section. However some specimens were produced using fibers with  $0^\circ/90^\circ$  orientation in order to examine the effect of fiber orientation on the shear behavior of the interface surface between steel and GFRP. Table 5.3. Presents results from lap shear tests. 7 specimens were tested for each set of experiment and values presented in, are the average values of these experiment results. Standard deviation values are presented in parenthesis. The first and second columns in Table 5.3. identify the surface treatment and primer type used, respectively. Column three indicates whether the primer was cured at room temperatures or at elevated temperatures. Column four gives the fiber orientation and column 5 indicates whether the GFRP was produced using direct wet lay-up or pre-prepared wet lay-up technique. Finally columns six and seven present the shear strength values of the interface surface between steel and GFRP for Duratek and Resoltech epoxies, respectively.

The following conclusions can be drawn from the results presented in Table 5.3.

- 1- The least shear strength was obtained from the connection where no surface treatment and primer were used.
- 2- Comparing rows 2 and 3 reveals that using Duratek or Silan primer does not make a difference when there is no surface treatment.
- 3- Comparing rows 4 and 5 reveals that using Silan primer results in about 100% higher shear strength with respect to using Duratek primer for sand papered connections. On the other hand, using Duratek or Resoltech epoxy does not have a considerable effect.
- 4- Comparing rows 6 and 7 reveals that using Silan primer results in about 100% higher shear strength with respect to using Duratek primer for sand blasted connections. On the other hand, using Duratek or Resoltech epoxy does not have a considerable effect.
- 5- Comparing rows 5 and 7 reveals that sand papering is better with Duratek epoxy. However, sand papering or sand blasting resulted in almost the same shear strengths for Resoltech epoxy.
- 6- Comparing rows 6 and 8, and 7 and 9 reveals that using  $0^{\circ}/45^{\circ}/90^{\circ}/-45^{\circ}$  or  $0/90^{\circ}$  fibers does not change the shear strength much as expected.
- 7- Comparing rows 7 and 10 reveals that using DWL or PWL does not change the behavior for applications with Resoltech epoxy, but increases the strength by about 40% for applications with Duratek epoxy.

Table 5.3. Lap Shear Test Results of Steel-GFRP Interface Surface

	1	2	3	4	5	6	7
Surface Treatment	Primer Type	Primer Cured @	Fiber Orientation	GFRP Production		Shear Strength (MPa)	
				Type	Resoltech Epoxy	Duratek Epoxy	Resoltech Epoxy
1	None	-	0°/45°/90°/-45°	DWL*	1.71 (0.14)	-	-
2	None	Room Temp.	0°/45°/90°/-45°	DWL*	4.45 (0.59)	3.56 (0.29)	
3	None	80°C	0°/45°/90°/-45°	DWL*	4.50 (1.57)	-	
4	Sand Papered	Room Temp.	0°/45°/90°/-45°	DWL*	5.40 (0.51)	5.79 (0.62)	
5	Sand Papered	80°C	0°/45°/90°/-45°	DWL*	10.42 (0.64)	10.88 (1.10)	
6	Sand Blasted	Room Temp.	0°/45°/90°/-45°	DWL*	5.25 (0.64)	4.64 (0.50)	
7	Sand Blasted	80°C	0°/45°/90°/-45°	DWL*	8.42 (0.38)	11.09 (0.42)	
8	Sand Blasted	Room Temp.	0°/90°	DWL*	6.05 (0.47)	5.17 (0.34)	
9	Sand Blasted	80°C	0°/90°	DWL*	8.08 (0.40)	7.94 (0.53)	
10	Sand Blasted	80°C	0°/45°/90°/-45°	PWL**	11.85 (1.15)	10.44(0.50)	

\* DWL: Direct Wet Lay-up

\*\* PWL: Pre-prepared Wet Lay-up

Lap-shear test results are also presented graphically. In all figures the results are from GFRPs produced by DWL technique and using fibers with fiber orientation of  $0^{\circ}/45^{\circ}/90^{\circ}/-45^{\circ}$ .

Figure 5.3 presents results for specimens with no surface treatment. As seen in Figure 5.3, GFRP materials' bonding capability to steel surfaces are limited without any treatment to the surface. This directly shows the surface treatment's significant effect on shear transfer between GFRP and steel. The figure also reveals the necessity of using a primer. Using a primer increases the bonding of GFRP to steel nearly 2.6 times.

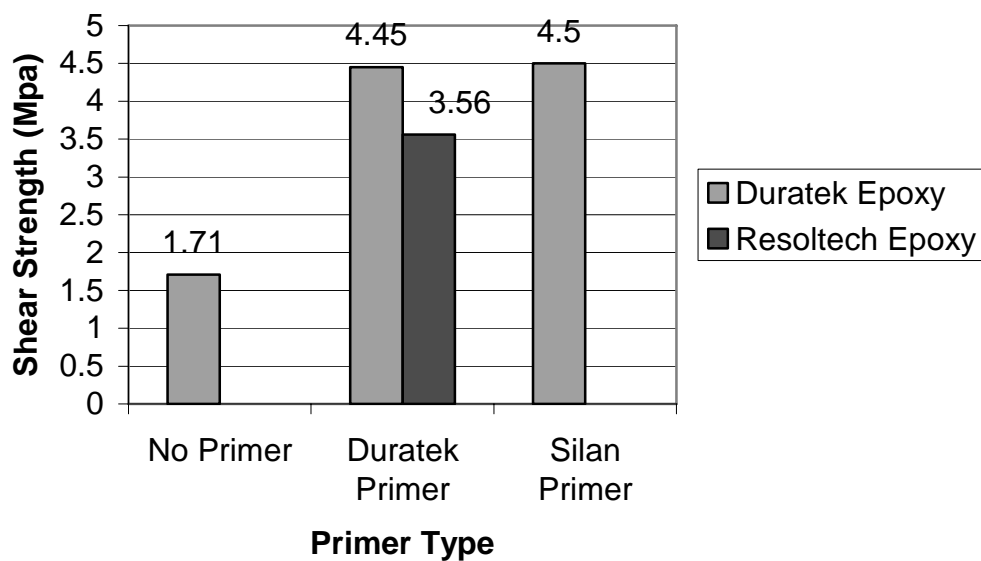


Figure 5.3. Lap-Shear Results for Connections with no Surface Treatment

Figure 5.4. shows results obtained from steel-GFRP lap shear tests for sand papered surfaces. Here, it can be clearly seen that the type of epoxy has a negligible effect on strength. However, using silan primer greatly improves the shear strength.



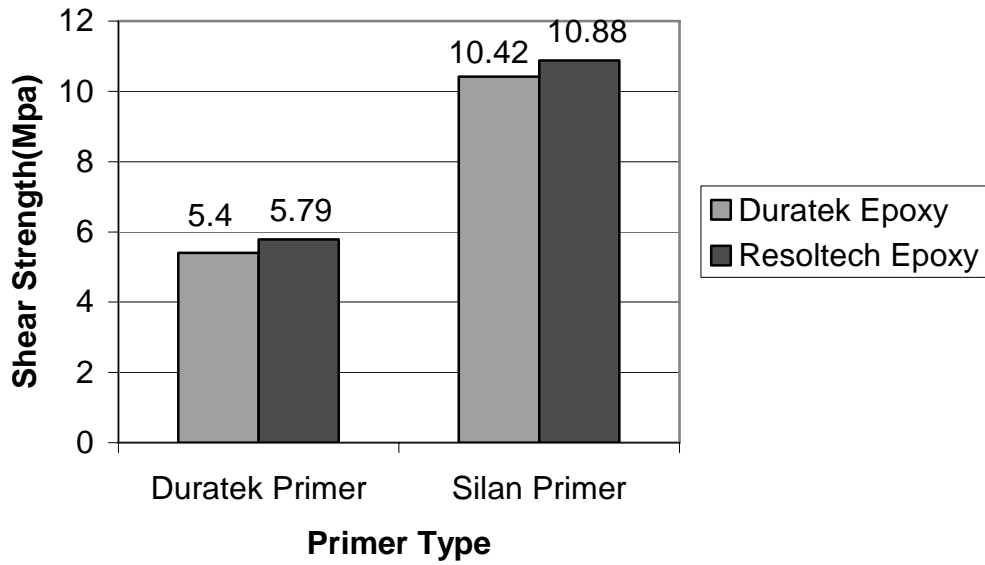


Figure 5.4. Lap Shear Test Results for Sand Papered Connections

Figure 5.5. shows results for sand blasted steel surfaces. It can be seen that sand blasting does not have any effect on specimens prepared with Duratek primer. For specimens prepared with Silan primer, using Resoltech epoxy resulted in better shear strengths.

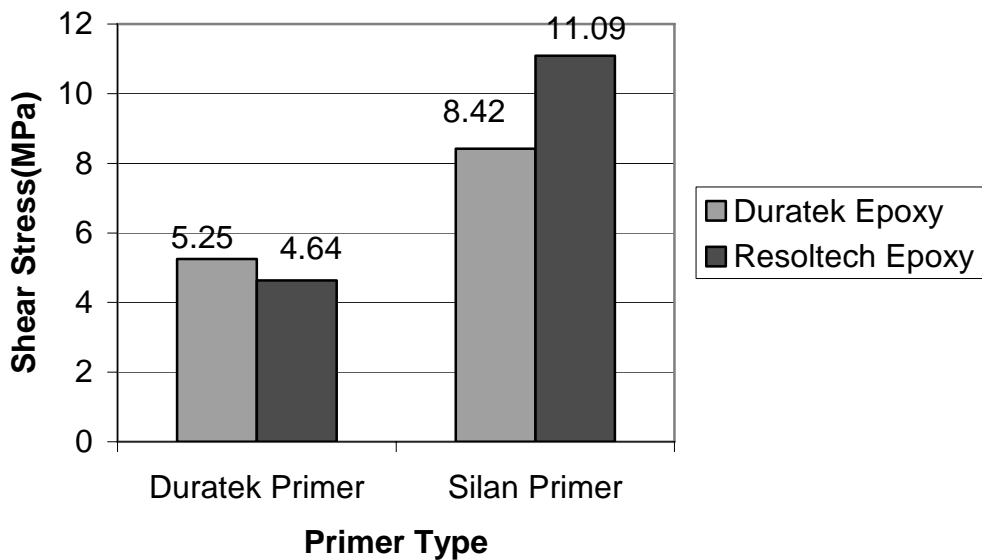


Figure 5.5. Lap Shear Test Results for Sand Blasted Connections

Figure 5.6. presents results for connections using Duratek surface primer. As can be seen from the figure sand papered surfaces resulted in highest strength values for both Duratek and Resoltech epoxy applications.

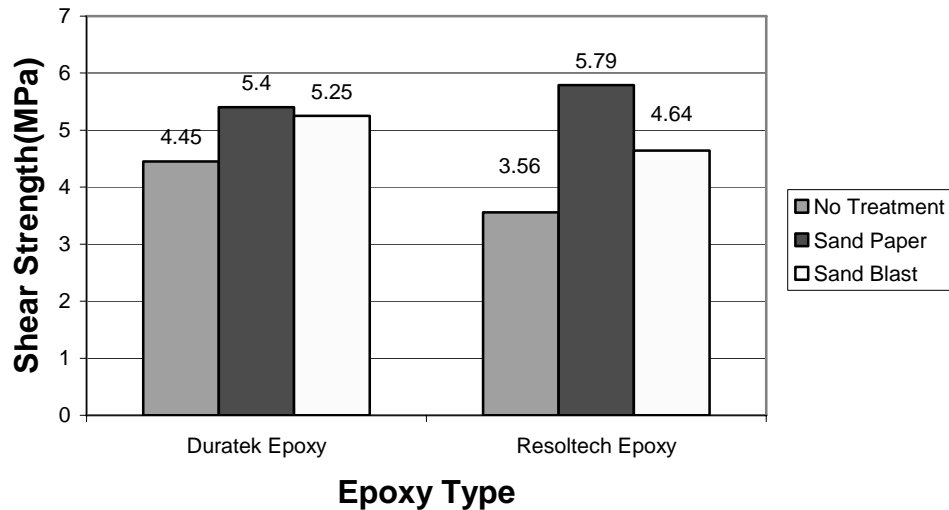


Figure 5.6. Lap Shear Test Results for Connections with Duratek Surface Primer

Figure 5.7. Presents results for connections produced using Silan surface primer. As can be seen from the figure sand papered surfaces resulted in highest strength values for Duratek epoxy applications. For Resoltech epoxy applications applying sand papering or sand blasting to the steel surface did not change the shear strength of the interfacial surface between steel and GFRP much. In addition, the shear strengths of sand blasted connections with either Duratek or Resoltech epoxy were very close to each other. Using Duratek or Resoltech epoxy did not change the shear strength much.

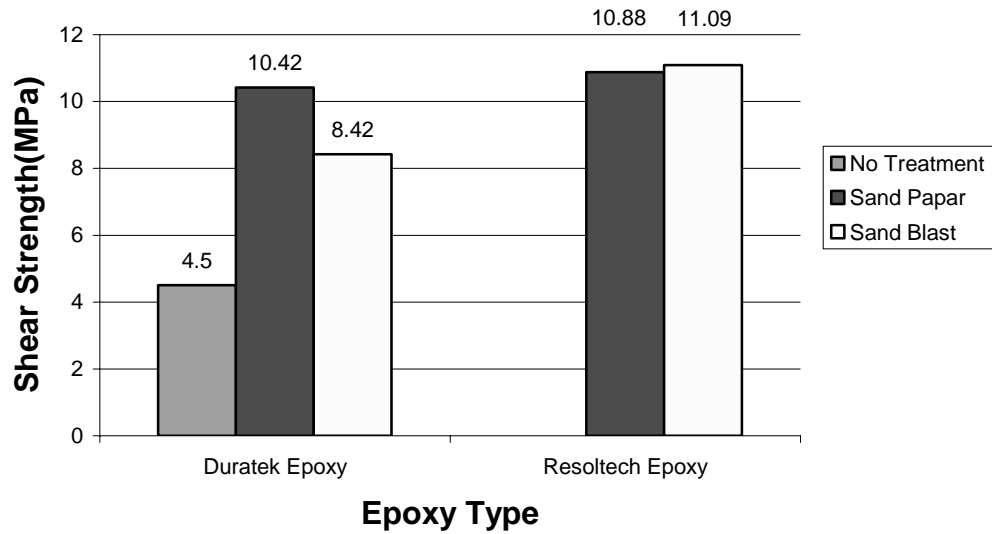


Figure 5.7. Results Based on Silan Surface Preparation Primer

The following conclusions can be drawn after examining the results:

- 1- A surface treatment is necessary. Use either sand papering or sand blasting.
- 2- A surface primer is essential. Silan primer resulted in much greater shear strengths than Duratek primer.
- 3- Epoxy type was not very important. Duratek epoxy was used in the rest of the study.
- 4- Fiber orientation was not important. GFRP produced from fibers with fiber orientations of  $0^{\circ}/45^{\circ}/90^{\circ}/-45^{\circ}$  were used for the rest of the study due to reasons stated for compression tests.
- 5- Production method (DWL or PWL) did not affect the shear results much. Either production method can be used. However, DWL is chosen over PWL in the rest of the study due to the ease of application in the field.

### 5.5. Shear Strength (V-Notch) Test Results

This test examines the shear strength capacity of GFRP materials. For this test (ASTM 2005) V-Notch beam test method procedures had been followed. All GFRP

productions were done by wet lay up method and all of the specimens were cured in room conditions for 7 days. In the production of the specimens Duratek epoxy and  $0^\circ/45^\circ/90^\circ/-45^\circ$  fiber orientation was used. Shaping of GFRP specimens were done by water-jet cutting system.

Table 5.4. presents results from the V-Notch beam tests. Results are the mean values from 7 tests and values in parenthesis the standard deviations. Shear strength of the GFRP materials in the XZ and YZ directions are the same as expected and greater than the shear strength of the GFRP material, in the ZX and ZY directions. In the ZX directions the shear plane is parallel to the direction of the fibers. In the XZ and YZ directions the shear plane is perpendicular to the direction of the fibers. The shear modulus of elasticity in all three directions should be the same. However, the results show that the shear modulus in the ZY direction was 2110 MPa, whereas the shear modulus in the XZ and YZ directions were about 2700 MPa. The difference in these values is believed to lie in the production process. The fiber/epoxy volume ratios could be different for the two directions.

Table 5.4. V-Notch Test Results of GFRP Material  
( $0^\circ/45^\circ/90^\circ/-45^\circ$  Fiber Orientation)

<b>Fiber</b>	<b>Shear Strength</b>	<b>Shear Modulus of Elasticity</b>
<b>Orientation</b>	<b>(MPa)</b>	<b>(Mpa)</b>
XZ(1 <sup>st</sup> )	43.61 (1.82)*	2655 (143.62)*
XZ(2 <sup>nd</sup> )	44.90 (0.80)*	2715 (247.97)*
YZ(1 <sup>st</sup> )	42.95 (0.20)*	2752 (162.02)*
YZ(2 <sup>nd</sup> )	43.89 (0.96)*	2733 (186.20)*
ZX	13.11 (3.07)*	2110 (223.35)*
ZY	13.00 (2.67)*	2440 (299.76)*

\*Standard Deviation Value

## CHAPTER 6

### GFRP STRENGTHENED STEEL PLATE TESTS

#### 6.1. Introduction

This chapter presents results from compression tests of steel plates reinforced with GFRP. This chapter includes information about specimen properties, instrumentation, test procedure, and behavior of GFRP strengthened steel plates under axial compression.

#### 6.2 Steel Plate Specimens

Steel section dimension were determined to ensure plastic local buckling would govern the failure mode of the steel plates; while the capacity of the compression-testing machine was not exceeded (2000 kN). Since very short plates were considered it was safe to assume the plates would plastically yield. The plastic yield strength of a plate can be calculated by the following formula:

$$P_u = C_{pr} \times F_y \times A_{section} \quad (6.1)$$

Where,

$F_y$  = yield strength of steel,

$C_{pr}$  = coefficient to account for strain hardening (can be taken as 1.2, AISC2005a),

$A_{section}$  = area of the plate.

The plate dimensions were chosen as 350×200×20 mm and 8 such plates were purchased from a single batch. The yield strength of the batch was determined through standard tensile coupon tests conducted according to ASTM (2003b). Test results are presented in Table 6.1. The mean yield strength was 186.3 MPa as seen in Table 6.1.

Table 6.1 Tensile Test Results of Coupons Taken from Steel Plates

Specimen No	F <sub>y</sub> yield (MPa)	F <sub>r</sub> rupture (MPa)
1	180	407
2	186	404
3	200	447
4	170	396
5	187	402
6	195	416
Average	186.3	412
Std. Dev.	10.6	18.3

The ultimate strength of the plates can be calculated by using Eq. (6.1) as: This ultimate load corresponded to about 45% of the capacity of the compression-testing machine. Being below the capacity by about 45% was desirable because the addition of the GFRP laminates would increase the ultimate strength of the plates. Figure 6.1. shows a sketch of the plates used in the tests.

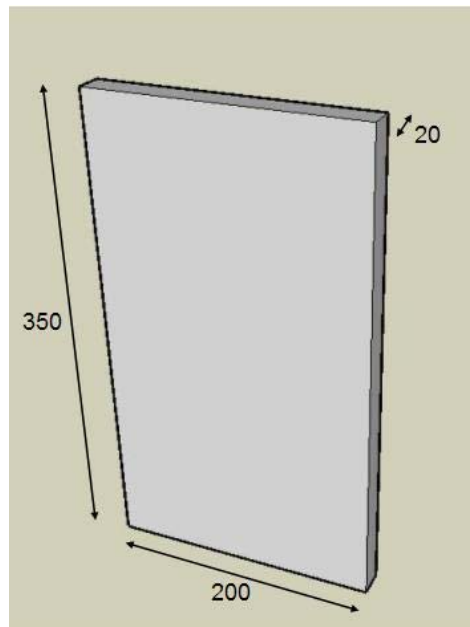


Figure 6.1. Steel Plate Dimensions ( mm.)

GFRP laminates were attached to both faces of the steel plates. Two different GFRP dimensions (300×80 mm and 300×160 mm, 300 mm being the depth and 80/160

mm being the width) and 3 different layer numbers (2, 4 and 16 layers) were tested. Specimen designations and properties are presented in Table 6.2. One specimen was tested for each designation, except bare steel plates where 2 specimens were tested. The presented result value for the Bare (Control) Plates is the average value of the 2 results obtained from experiments. Figure 6.2. Shows a sketch of steel plates with GFRP and the parameters A and B are specified in Table 6.2.

Table 6.2 GFRP Strengthened Steel Plate Test Specimen Types

Specimen No	GFRP Layer	GFRP Dimensions ( mm)	
		A*	B*
BP(Control)	none	-	-
P-GFRP-2-8-30	2	80	300
P-GFRP-4-8-30	4	80	300
P-GFRP-16-8-30	16	80	300
P-GFRP-2-16-30	2	160	300
P-GFRP-4-16-30	4	160	300
P-GFRP-16-16-30	16	160	300

A\*, B\* dimensions are specified in Figure 6.2

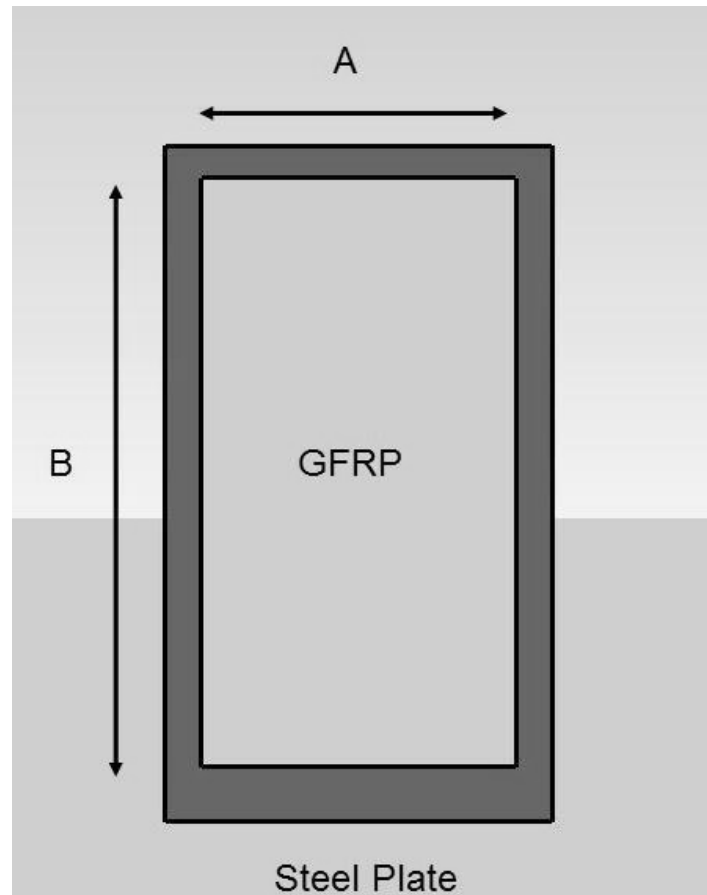


Figure 6.2. GFRP Application Dimensions on Steel Plates

### 6.3. GFRP Retrofitting Procedure

Previous tests defining the mechanical properties of GFRP material and their interaction with steel surfaces showed that the surface bonding was the weakest link in the connection. In order to achieve maximum interaction between GFRP material and steel surface, the most effective and in-situ applicable combination of epoxy – primer and surface treatment was chosen based on the lap-shear test results presented in Chapter 4. GFRPs were produced from fibers with  $0^{\circ}/45^{\circ}/90^{\circ}/-45^{\circ}$  fiber orientation and Duratek epoxy. The steel surface was sand blasted and Duratek primer was used. The shear strength of the interfacial surface obtained from lap shear tests was 5.25 MPa for a connection with the mentioned materials and surface treatment.

The sand blasting of the steel specimens were done by a commercial company without any major degradation in steel sections. It was shown in Chapter 4 that rougher surfaces achieved with sand blasting provided higher surface interaction values between



steel and GFRP material. Duratek Primer was applied to sand blasted surface to provide a better surface interaction between steel and GFRP material as proved in lap-shear test results. After the Duratek epoxy surface preparation primer was applied to the steel plates, the plates were cured in room conditions for 1 week to achieve maximum strength as suggested by Duratek. Curing stage was followed by the application of GFRP material to the steel specimens by direct wet lay-up method. GFRP materials were cured for 1 week in room conditions before the experiments. Detailed material properties of epoxy, curing component, glass fiber and manufacturing procedures were specified in Chapter 3.

## **6.4. Experimental Setup**

All specimens including control specimens (Steel plates without any GFRP Stabilization) and GFRP strengthened steel plates were tested under axial compressive load by a load-controlled compressive testing machine with a capacity of 2000kN. The lateral movement of the plates at top and bottom were prevented. The boundary condition at top and bottom were close to fixed supports. Specimens were loaded with a rate of approximately 3000 N/sec. A photograph of a specimen in the compression-testing machine is given in Figure 6.3.

During tests, 3 different data were collected from two sources and combined to understand the behavior of the steel plates. One load, two displacement and 6 strain gauge readings were collected. Figure 6.4. shows the schematic representation of the data acquisition. Applied load data was recorded by the computer software of the compressive-testing machine and the displacement and strain gauge measurements were taken by the National Instrument DAQ. The sample data reading times of the DAQ and compression-testing machine were equal to each other (3 data per second), to provide data overlap between load and displacement.



Figure 6.3. GFRP Strengthened Steel Plate Test Set-up

Two LVDTs were used during the experiments. First LVDT was located in the middle of GFRP strengthened steel plate, measuring the horizontal displacement values of the specimens. The other LVDT was placed to the uplifting part of the compressive-testing machine to record the axial deformation of the steel plate specimens. Figure 6.5 shows the LVDT locations on the test setup.

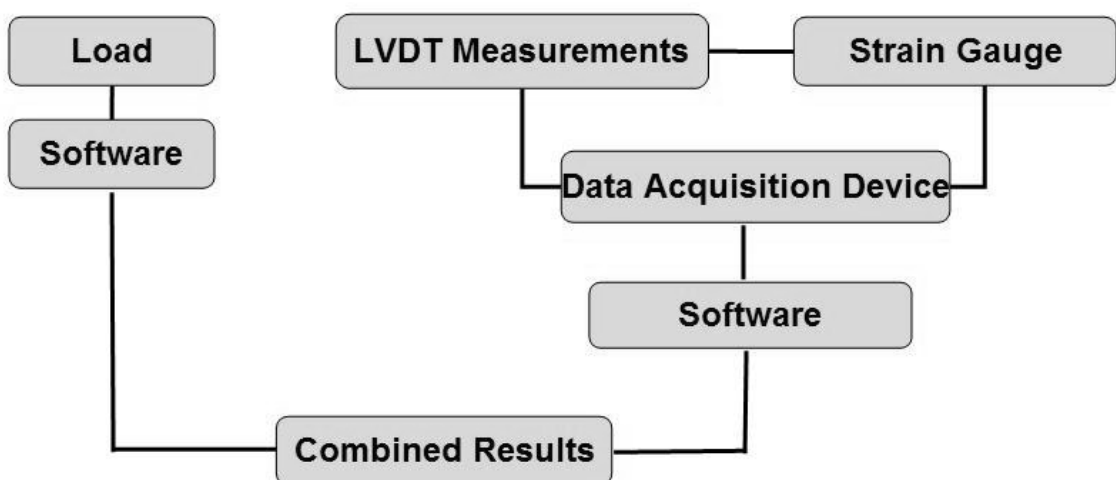


Figure 6.4. Schematic of Axially Loaded Steel Plate Test Setup

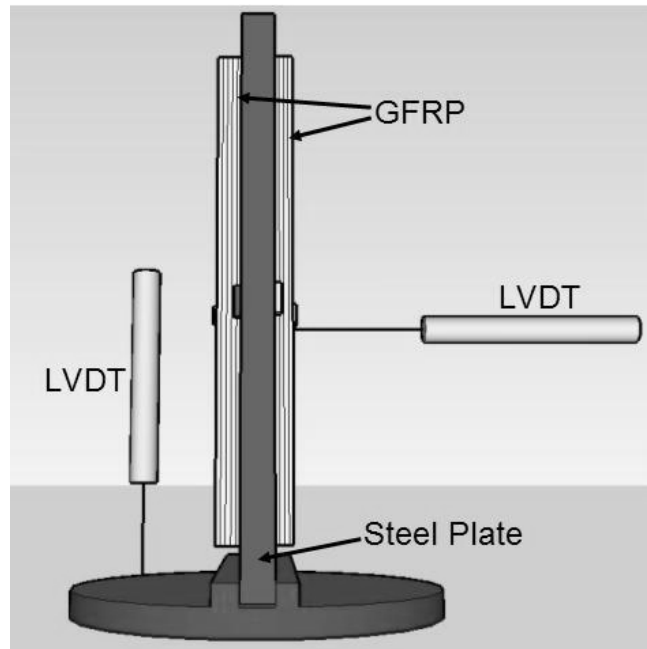


Figure 6.5. LVDT Locations on Test Setup

Two different strain gauges were used: one for steel and one for GFRP. The strain gauges for steel were capable of withstanding large plastic strains. The post-yielding metal surface strain-gauges (Type-1) were attached 7.5 mm away from middle tip of steel specimens. Composite strain gauges (Type-2) were attached on the GFRP at the center point of the steel plate specimens. Strain-gauge attachment locations are shown in Figure 6.6.

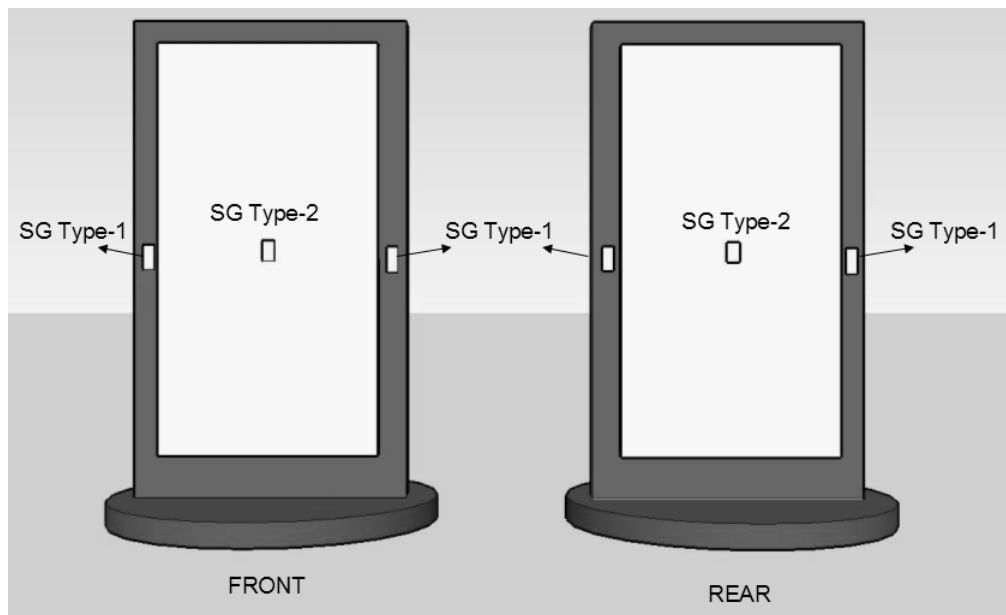


Figure 6.6. Strain-Gauge Locations on Steel Plate Specimens

## 6.5. Test Procedure

For this experimental program, a total of 8 specimens were prepared including 2 non-GFRP control specimens and 6 GFRP strengthened steel plate specimens as specified in Table 6.2. These specimens were loaded beyond their peak load and loading was stopped when the load dropped to 50% of the peak load. All collected data including applied load, LVDT measurements and strain-gauge values were combined and stabilization effect of GFRP material for steel plates were investigated.

Strain-gauge numbers were identified according to their position on steel plate specimens. 4 strain gauges attached to the metal surface were numbered anti-clockwise starting from front side (1<sup>st</sup>, 2<sup>nd</sup>) to rear side (3<sup>rd</sup>, 4<sup>th</sup>). 2 composite strain-gauges were numbered following the same procedure, as 5<sup>th</sup> composite strain gauge was attached to the front side between 1<sup>st</sup> and 2<sup>nd</sup> metal surface strain gauges and 6<sup>th</sup> composite strain gauge was attached to the rear side between 3<sup>rd</sup> and 4<sup>th</sup> strain gauges. Identification numbers of the strain gauges are shown in Figure 6.7..

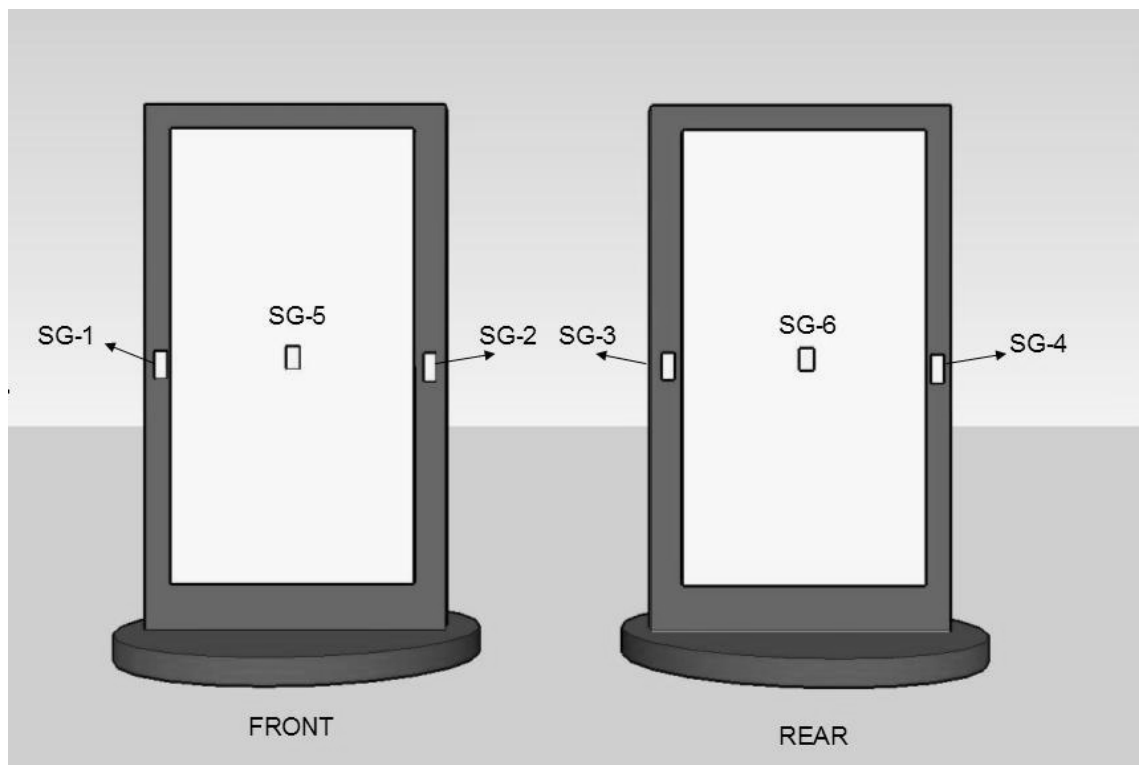


Figure 6.7. Strain-Gauge Identification Numbers Used in Experimental Test

## **6.6. Test Results**

This section includes the results of GFRP strengthened axially loaded steel plate tests.

### **6.6.1. Introduction**

Test results section is categorized into two main parts. First part will be representing the axially loaded steel specimens test results with a comparison of entire test program, including Load-Displacement Graphs of GFRP strengthened steel plates sorted by their GFRP application dimension (80x300mm ,160x300mm) and tables specifying the maximum lateral and axial displacement values, maximum strain values. Second part of the Test Results section is consists of the test results of the axially loaded GFRP strengthened steel plate test results individually, including Load-Displacement (Axial and lateral) and Load-Strain graph of steel plate specimens.

### **6.6.2. Axially Loaded Steel Plate Test Results**

This section presents experimental results and investigates the behavior of GFRP strengthened steel plates (350×200×20mm) under axial loading. All specimens, including the 2 bare control plates and 6 GFRP strengthened steel plates were designed to fail by domination of plastic buckling.

Peak load the specimens have reached and the failure modes are presented in Table 6.3. It is seen from the table that the addition of GFRPs increases the maximum loads achieved by the specimens. It can also be seen that the failure mode of GFRPs changes as the number of layers of GFRP increases. The 2-layered GFRPs failed by rupture of the GFRP laminates. The 4 and 16-layered GFRPs failed from the interface between the steel and GFRP.

The stabilization effect of GFRP materials can be investigated by LVDT measurements at a fixed load for every specimen. For that reason a fixed load was chosen to provide a baseline for investigation of lateral buckling behavior of the steel plates while GFRPs were still attached to the steel surface and at the same time the interfacial shear limit was close to failure. LVDT measurements at 775 kN load for each specimen is presented in Table 6.6. As expected the axial deformation of the plates

decreases with the increase in GFRP layer number. The lateral deformation of steel plates without any GFRP application has an average value of 7.5 mm, whereas the lateral deformation of specimen P-GFRP 2-8-30 and P-GFRP 16-8-30 are 5.24 mm and 2.38 mm, respectively. The effect of the GFRP layers on mitigating local buckling can be observed by looking at the lateral displacement values. It can be observed from the table that increasing the number of GFRP laminates decreases the lateral deformation. For 2-layered with 80 mm wide GFRP specimen the decrease in the lateral displacement was not very significant. However, going to 4 layers from 2 layers decreases the lateral displacements significantly. The decrease is more when the GFRP width is increased to 16 mm. Going to 16 layers did not have a great effect as compared to the specimens with 4 layers of GFRP. As a conclusion it can be said that 4 layers of GFRP with a width of 16 mm improves the behavior significantly. The ratio of the areas of GFRP to steel for specimen P-GFRP 4-16-30 is 0.32. However, it should be noted that the yield strength of steel used in the tests were very low. Although an enhancement in the local buckling behavior was observed in these tests at a load close to the peak load, the same might not be valid for steel plates with a yield strength of 345 MPa. In such a steel-GFRP system, the shear strength of the interface between steel and GFRP might well be exceeded before yielding the plate; prior to plastic local buckling.

The effects of the GFRP reinforcement in the local buckling behavior of steel plates can also be observed from load-lateral displacement graphs. The load-lateral displacement graphs of 80x300mm GFRP plates and 160x300 mm GFRP plates are presented in Figure 6.28 and Figure 6.29 respectively. In both of the figures the graph of the bare steel plate is the mean values obtained from the two bare steel tests. It can be observed from Figure 6.28 and 6.29 that the lateral displacements of all GFRP strengthened plates are smaller than that of the bare steel plates especially after the bare steel plate enters the post-yield region beyond an axial load of 700 kN. The difference in failure modes can also be seen from Table 6.3. The 2-layered steel GFRP plate behaves almost identical to the bare steel plate as the GFRP rupture in the steel-GFRP system. However, for the steel-GFRP system with 16 layers of GFRP the load increases until the interface gives up. There is an identifiable load drop in the steel-GFRP system with 16 layers of GFRP when the interface fails due to high shear transfer. The same behaviors can be observed for steel-GFRP systems for GFRPs with a width of 160 mm.

Table 6.3. Control and GFRP Strengthened Steel Plate's  
Maximum Load and GFRP Failure Modes

<b>Specimen Type*</b>	<b>Max Load (kN)</b>	<b>Failure Mode of GFRP</b>
BP(Control)	781.44	-
P-GFRP-2-8-30	776.89	Rupture of GFRP
P-GFRP-4-8-30	804.73	Interfacial Bond Failure
P-GFRP-16-8-30	847.67	Interfacial Bond Failure
P-GFRP-2-16-30	811.4	Rupture of GFRP
P-GFRP-4-16-30	855.41	Interfacial Bond Failure
P-GFRP-16-16-30	811.88	Interfacial Bond Failure

\*Specimens Type Details are given in Table 6.2

Table 6.4 Control and GFRP Strengthened Steel Plate's  
Maximum Axial and Lateral Displacement Values

<b>Specimen Type</b>	<b>Max Axial Displ.(mm.)</b>	<b>Max Lateral Displ.(mm.)</b>
BP(Control)	11.21	38.7
P-GFRP-2-8-30	12.46	28.93
P-GFRP-4-8-30	9.04	32.95
P-GFRP-16-8-30	10.37	35.2
P-GFRP-2-16-30	11.88	37.50
P-GFRP-4-16-30	8.9	32.23
P-GFRP-16-16-30	10.1	35.70

\*Specimens Type Details are given in Table 6.2

Table 6.5. Maximum Strain-Gauge Readings from GFRP Strengthened Steel Plate Tests

Specimen Type*	Maximum Strain Gauge Measurements***					
	SG-1	SG-2	SG-3	SG-4	SG-5	SG-6
1	-0.0690	-0.0627	0.0546	0.0558	-	-
2	0.0490	0.0358	-0.0568	-0.0616	0.0232	-0.0044
3	-0.0569	-0.0589	0.0418	0.0401	-0.0092	0.0068
4	-0.0664	-0.0598	0.0457	0.0432	-0.0032	0.0040
5	0.0453	0.0475	-0.2611**	-0.0621	0.0291	-0.0108
6	-0.0560	-0.0532	0.0383	0.0363	-0.0068	0.0091
7	-0.2618**	-0.0446	0.0422	0.0446	-0.0022	0.0004

\*Specimens Type Details are given in Table 6.2

\*\*Failure (Before Exact End of Loading)

\*\*\*Strain Gauge locations identifications are specified in Figure 6.7

Table 6.6 Lateral and Axial Displacement Measurements from LVDTs at 775kN

Specimen Type*	Lateral Displacement	Axial Displacement
	(mm)	(mm)
1	7.51	3.41
2	5.24	3.74
3	2.93	2.66
4	2.38	2.51
5	5.00	3.82
6	2.04	2.82
7	2.1	3.24

\*Specimens Type Details are given in Table 6.2

In previous sections, Load-Displacement graphs for each axially loaded GFRP strengthened steel plate are presented. These graphs include experimental data from the beginning of the axial loading until each specimen has reached to 50% of their axial peak value. By combining these graphs, the comparison of results for each GFRP strengthening dimension (8x30cm, 16x30 cm) can be presented. On this account, Figure 6.21 and 6.22 include the Load-Displacement Graphs for different GFRP lamination types for 2 GFRP strengthening dimensions; 8x30cm and 16x30cm. Also



these graphs can provide a visual comparison of buckling values presented in Table 6.6. which supplies the axial and lateral buckling values for each specimen type at 775 kN.

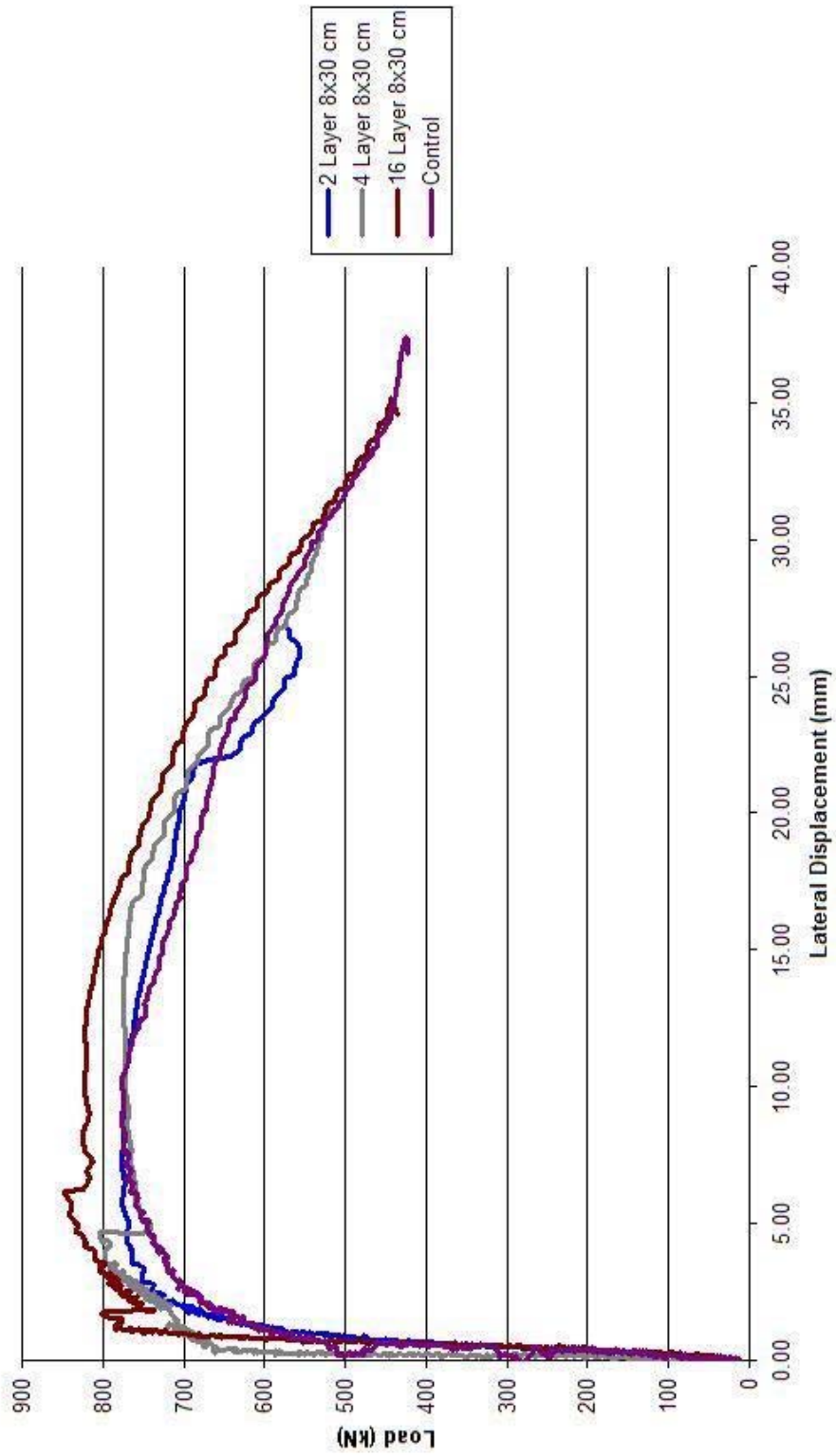


Figure 6.8. Combined Load-Displacement Graph of 8x30 cm GFRP Strengthened Steel Plate Tests for Each Lamination

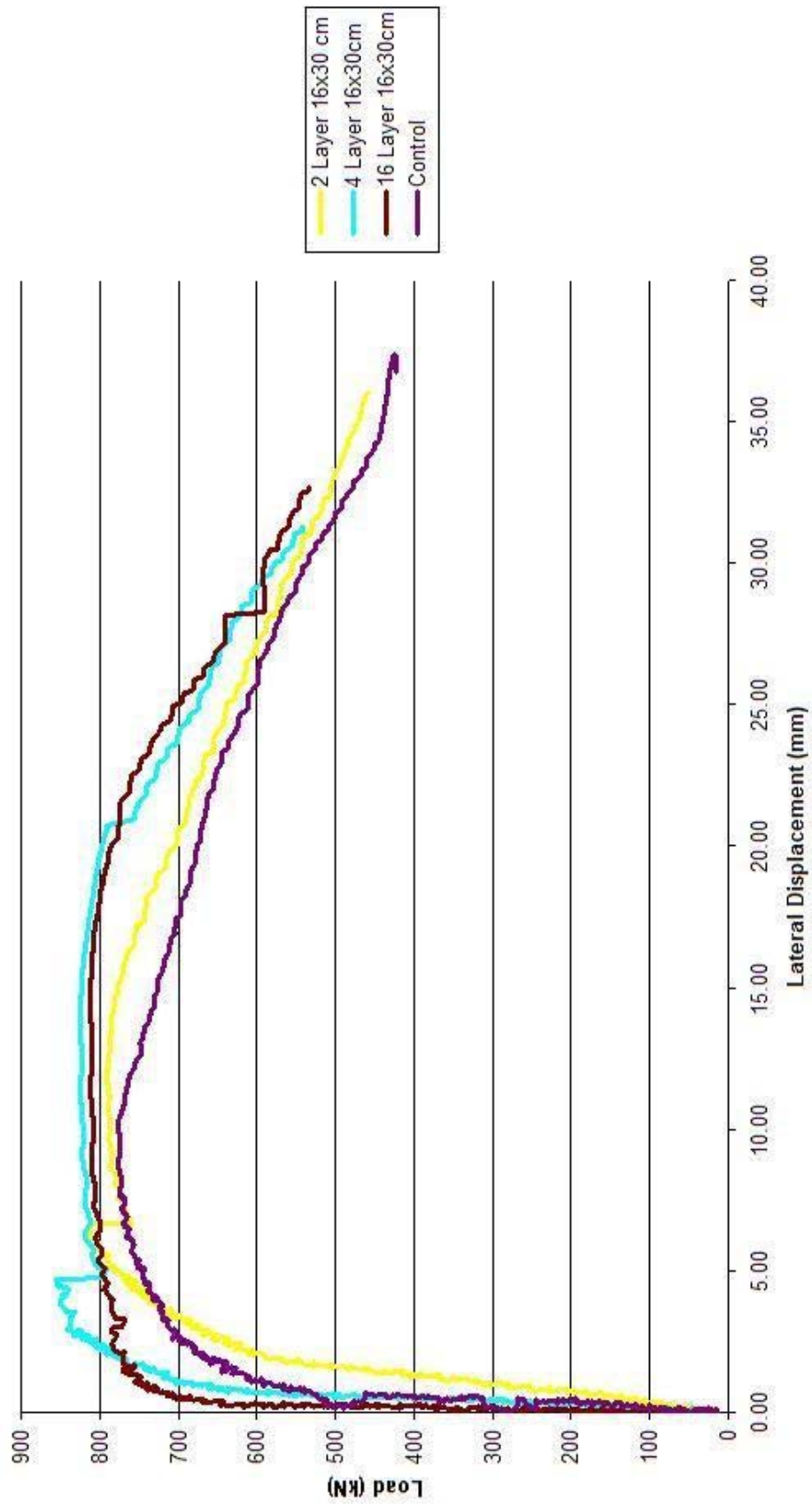


Figure 6.9. Combined Load-Displacement Graph of 16x30 cm GFRP Strengthened Steel Plate Tests for Each Lamination

### 6.6.3. Individual Axially Loaded Steel Plate Test Results

This section presents individual test results for entire axially loaded steel plate test results. 3 graphs for each specimen including Load-Lateral, Axial Displacement and 2 Load-Strain measurements, collected from steel plate surface. For Load-Strain graph, average value of 2 strain-gauges attached to tension and compression side of the steel plate are used and 1 Load-Strain graph is focused on the yield strain of the axially loaded plate.

#### 6.6.3.1. Axially Loaded Steel Specimen Type 1

This experiment involves non GFRP stabilized control specimens. 2 Control specimens' results are averaged for the graphs. Load-Displacement and Load-Strain Graphs are shown below.

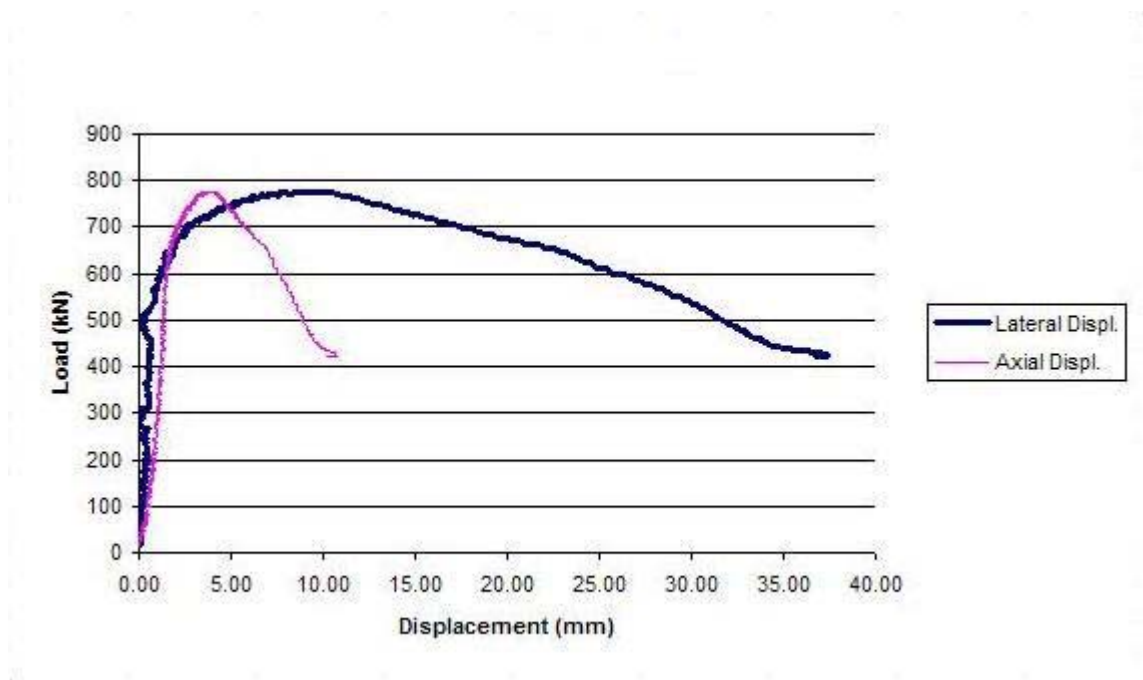


Figure 6.10. Load-Displacement Graph of Specimen Type 1

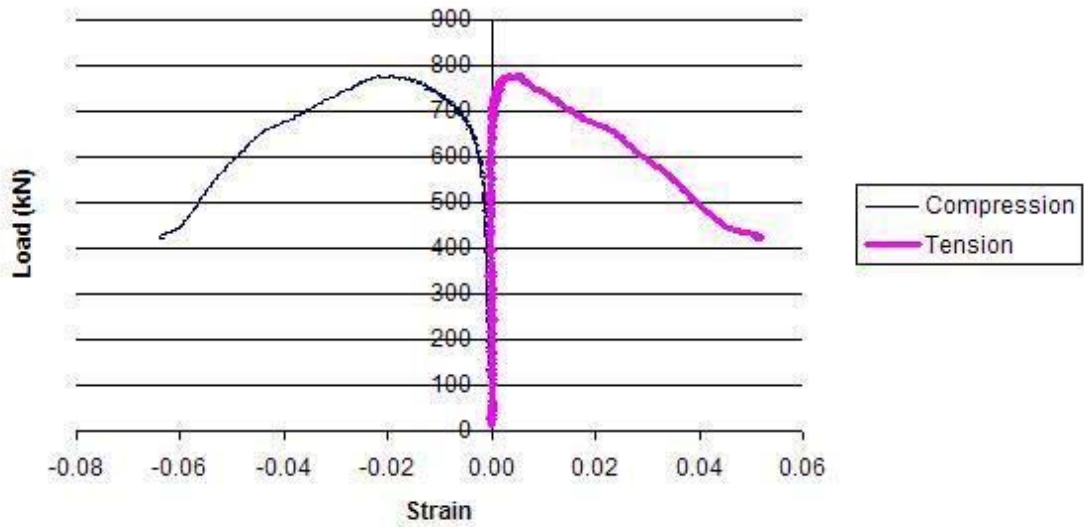


Figure 6.11. Load-Strain Graph of Specimen Type 1

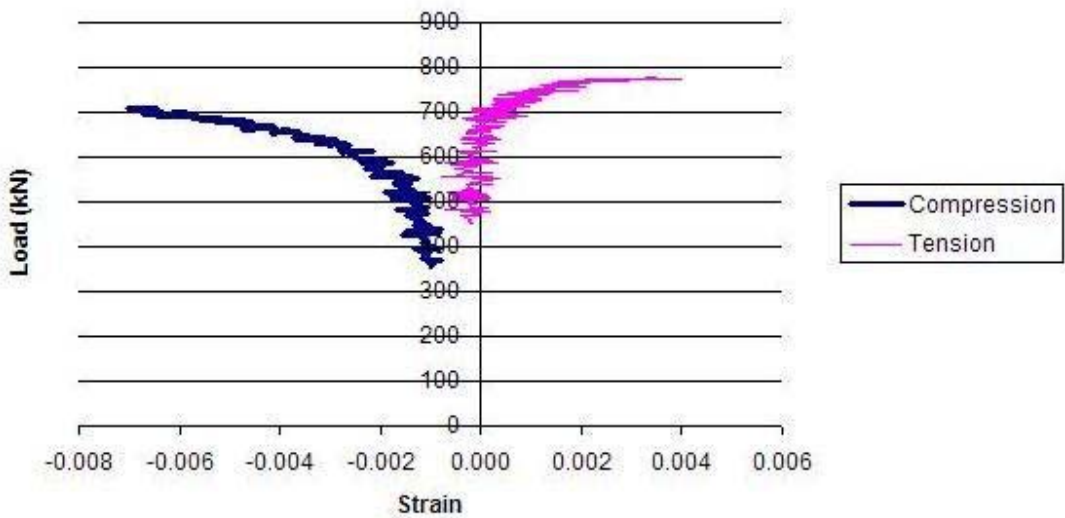


Figure 6.12. Load-Strain Graph of Specimen Type 1 (Yield Strain)

### 6.6.3.2. Axially Loaded Steel Specimen Type 2

This experiment consists of GFRP strengthened steel plate specimen. This specimen has 2 layers of GFRP with 8x30 cm dimensions. Experimental results of

axially loaded GFRP strengthened steel plate including Load-Displacement and Load-Strain Graphs are shown below.

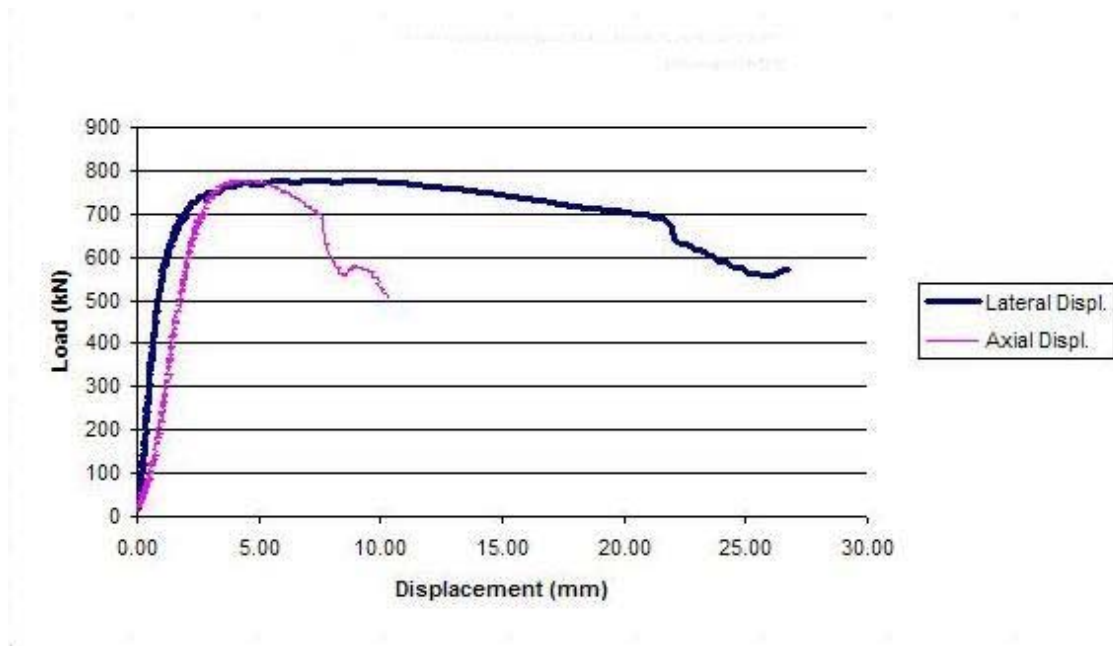


Figure 6.13. Load-Displacement Graph of Specimen Type 2

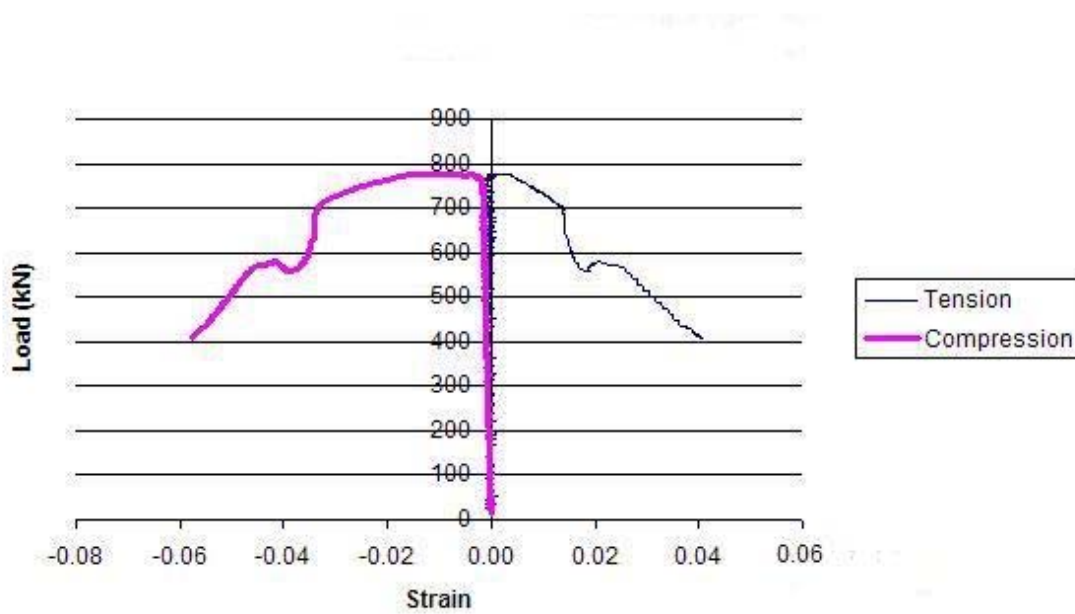


Figure 6.14. Load-Strain Graph of Specimen Type 2

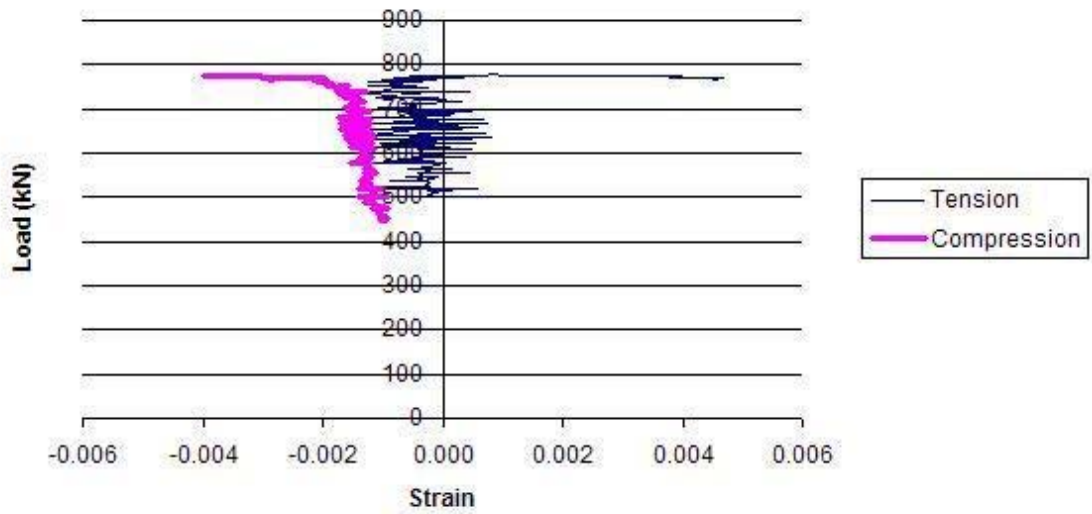


Figure 6.15. Load-Strain Graph of Specimen Type 2 (Yield Strain)

### 6.6.3.3. Axially Loaded Steel Specimen Type 3

This experiment consists of GFRP strengthened steel plate specimen. This specimen has 4 layers of GFRP with 8x30 cm dimensions. Experimental results of axially loaded GFRP strengthened steel plate including Load-Displacement and Load-Strain Graphs are shown below.

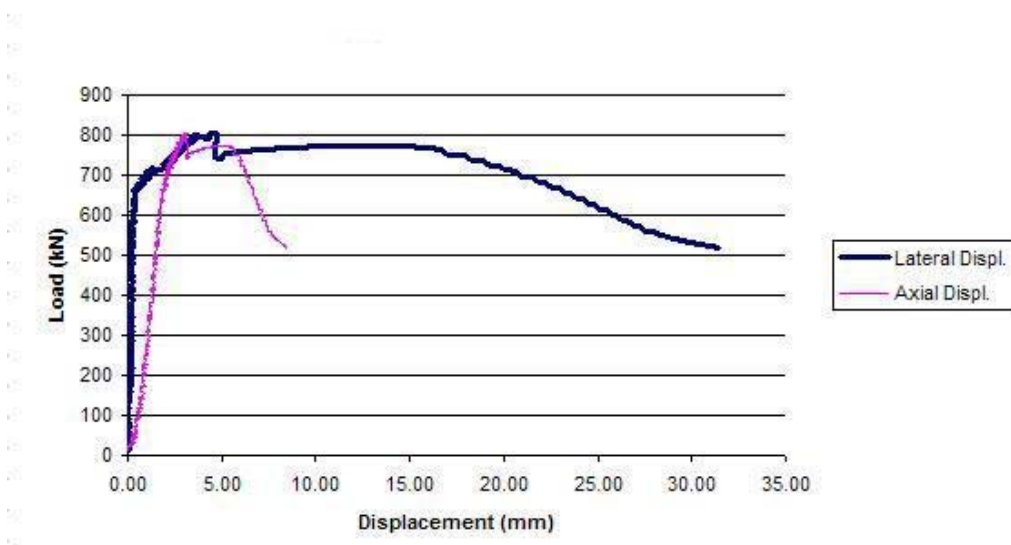


Figure 6.16. Load-Displacement Graph of Specimen Type 3

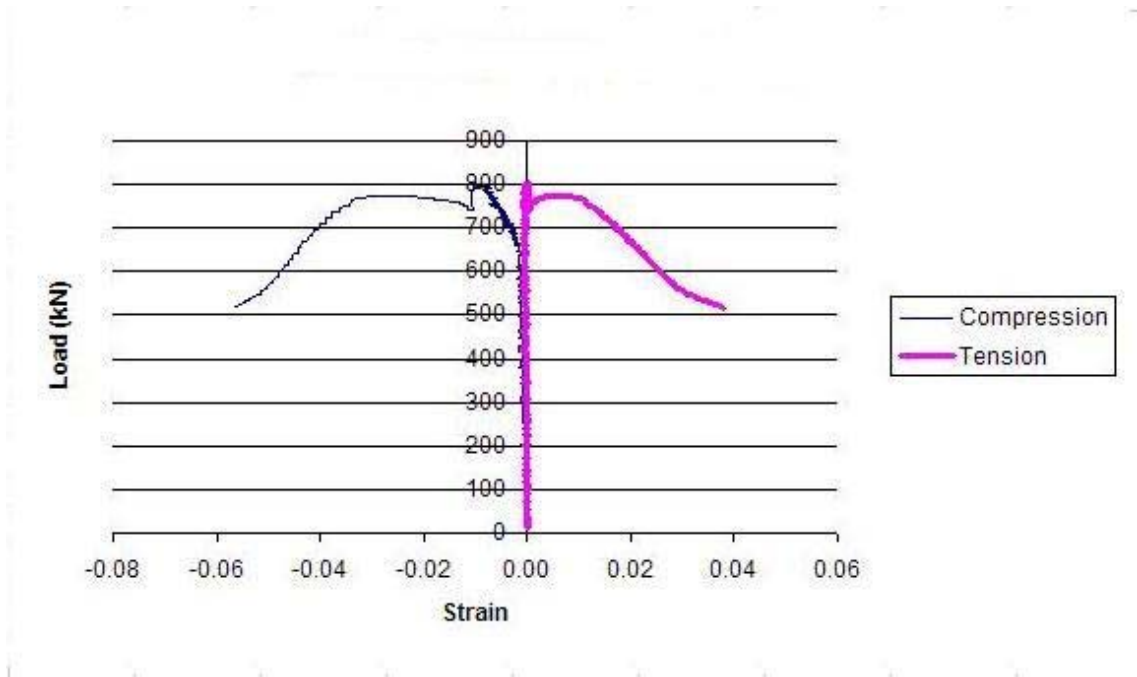


Figure 6.17. Load-Strain Graph of Specimen Type 3

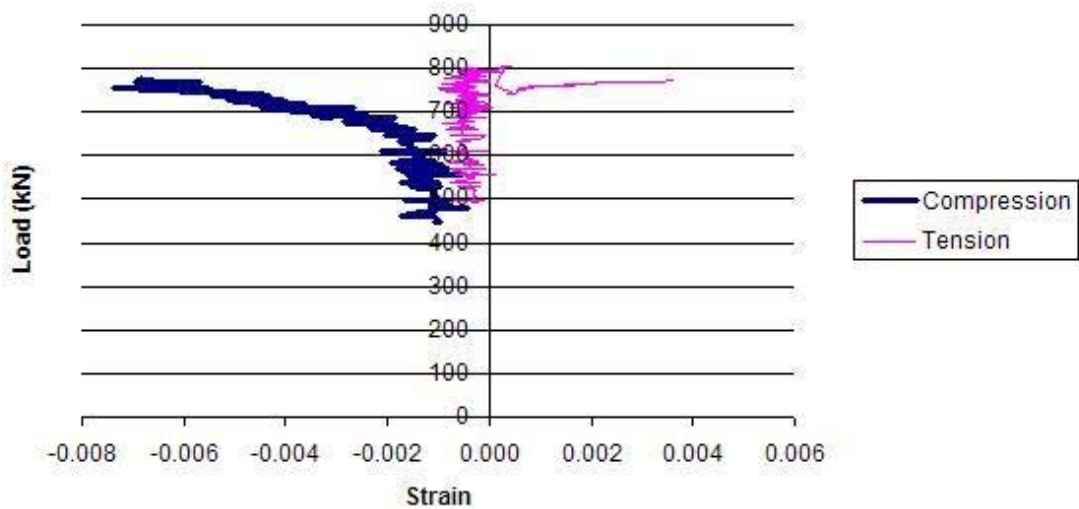


Figure 6.18. Load-Displacement Graph of Specimen Type 3 (Yield Strain)

#### 6.6.3.4. Axially Loaded Steel Specimen Type 4

This experiment consists of GFRP strengthened steel plate specimen. This specimen has 16 layers of GFRP with 8x30 cm dimensions. Experimental results



of axially loaded GFRP strengthened steel plate including Load-Displacement and Load-Strain Graphs are shown below.

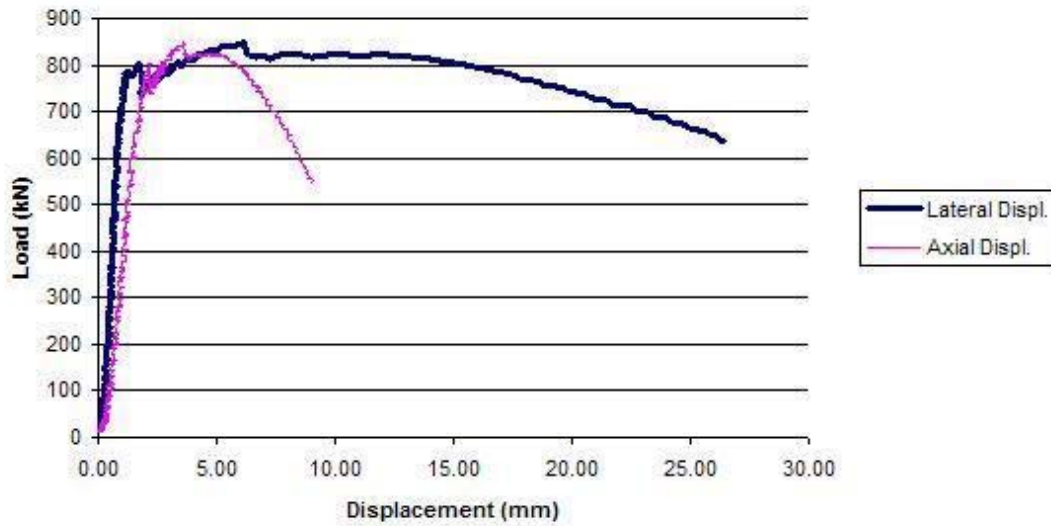


Figure 6.19. Load-Displacement Graph of Specimen Type 4

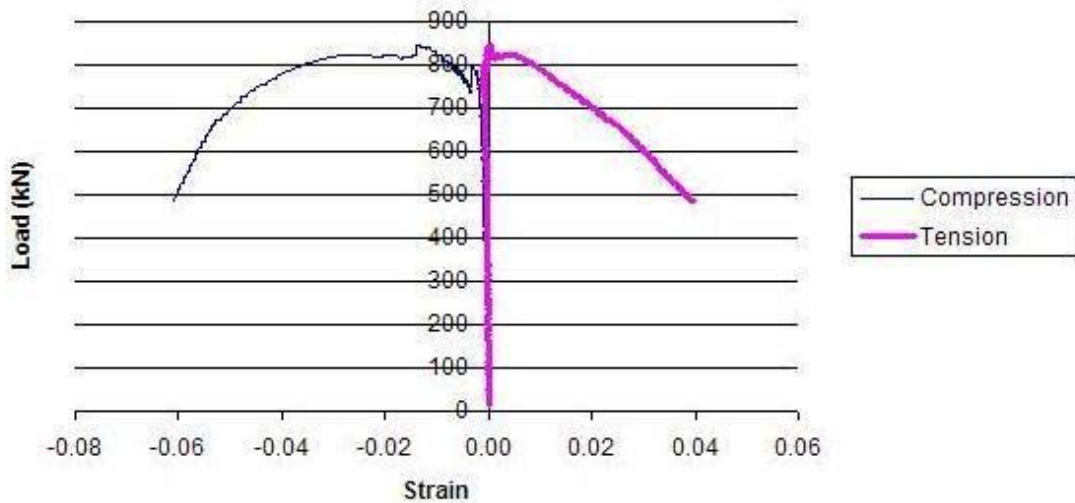


Figure 6.20. Load-Strain Graph of Specimen Type 4

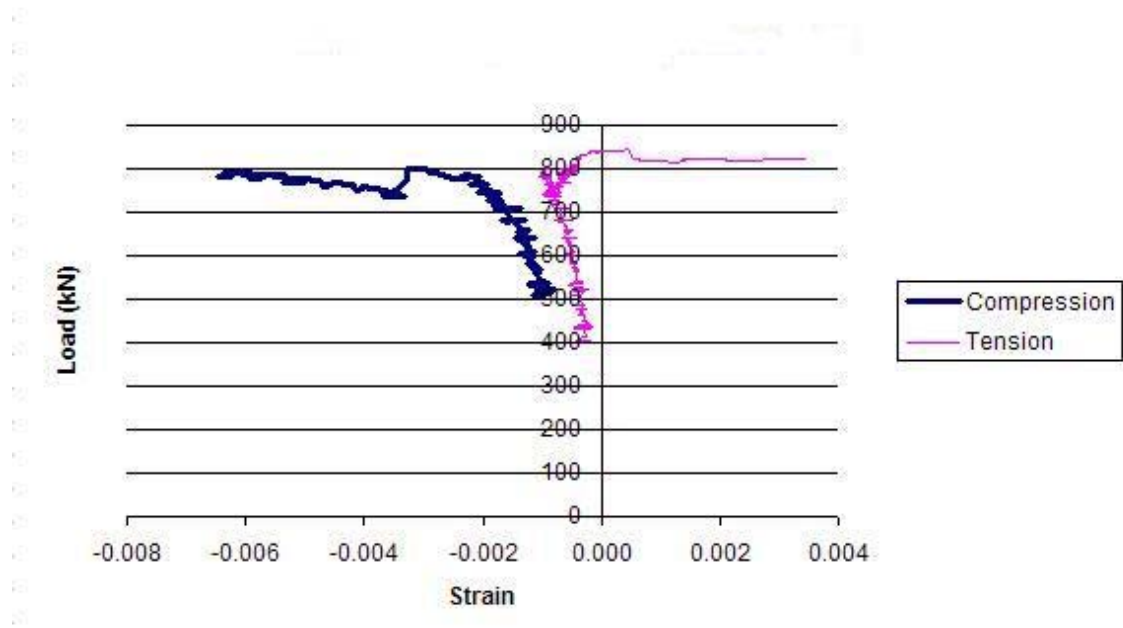


Figure 6.21. Load-Strain Graph of Specimen Type 4 (Yield Strain)

### 6.6.3.5 Axially Loaded Steel Specimen Type 5

This experiment consists of GFRP strengthened steel plate specimen. This specimen has 2 layers of GFRP with 16x30 cm dimensions. Experimental results of axially loaded GFRP strengthened steel plate including Load-Displacement and Load-Strain Graphs are shown below.

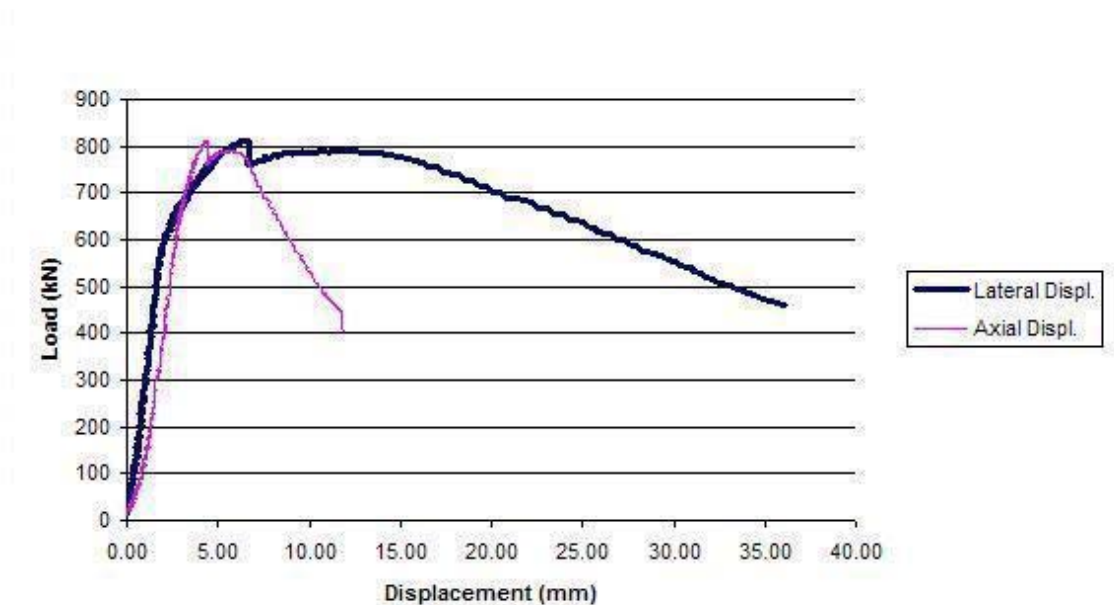


Figure 6.22. Load-Displacement Graph of Specimen Type 5

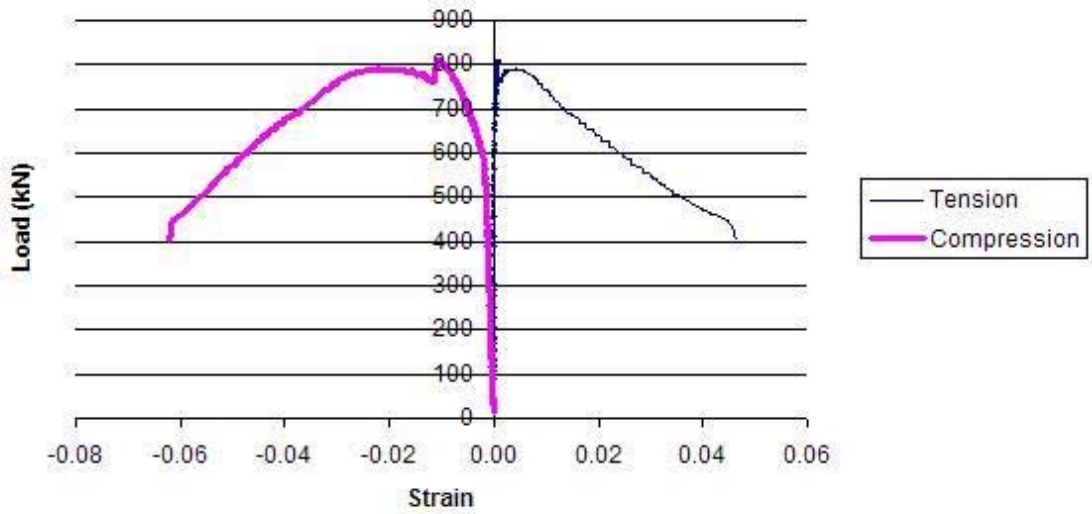


Figure 6.23. Load-Strain Graph of Specimen Type 5

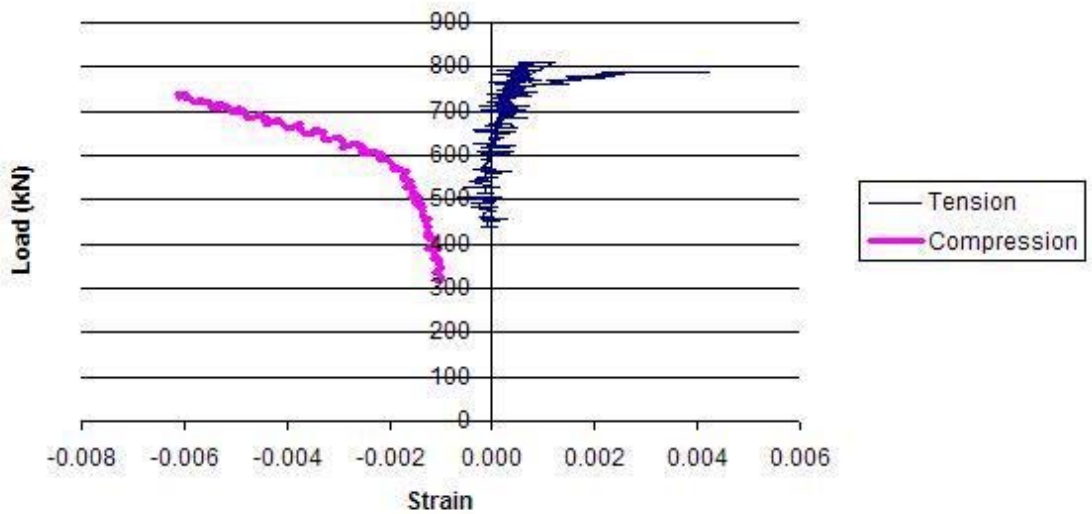


Figure 6.24. Load-Strain Graph of Specimen Type 5 (Yield Strain)

### 6.6.3.6. Axially Loaded Steel Specimen Type 6

This experiment consists of GFRP strengthened steel plate specimen. This specimen has 4 layers of GFRP with 16x30 cm dimensions. Experimental results

of axially loaded GFRP strengthened steel plate including Load-Displacement and Load-Strain Graphs are shown below.

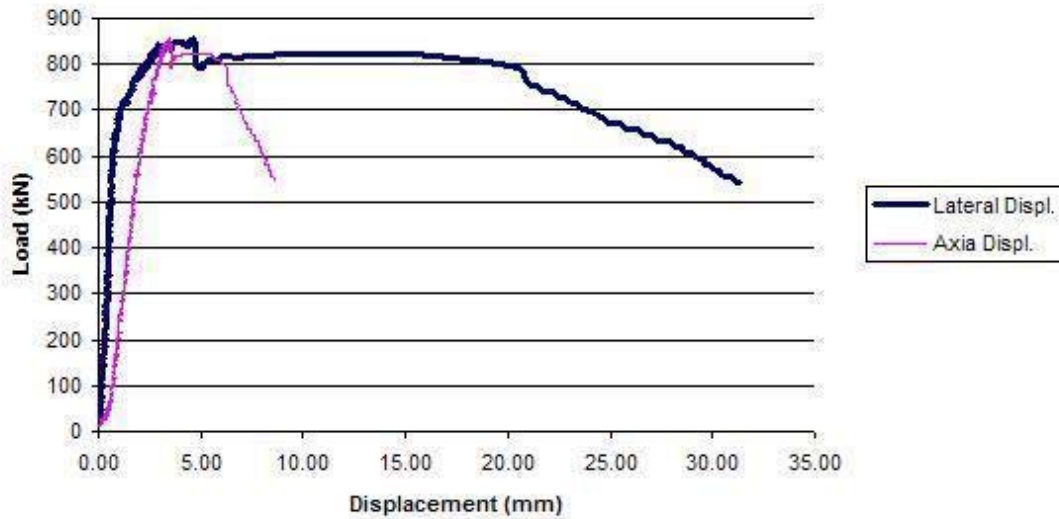


Figure 6.25. Load-Displacement Graph of Specimen Type 6

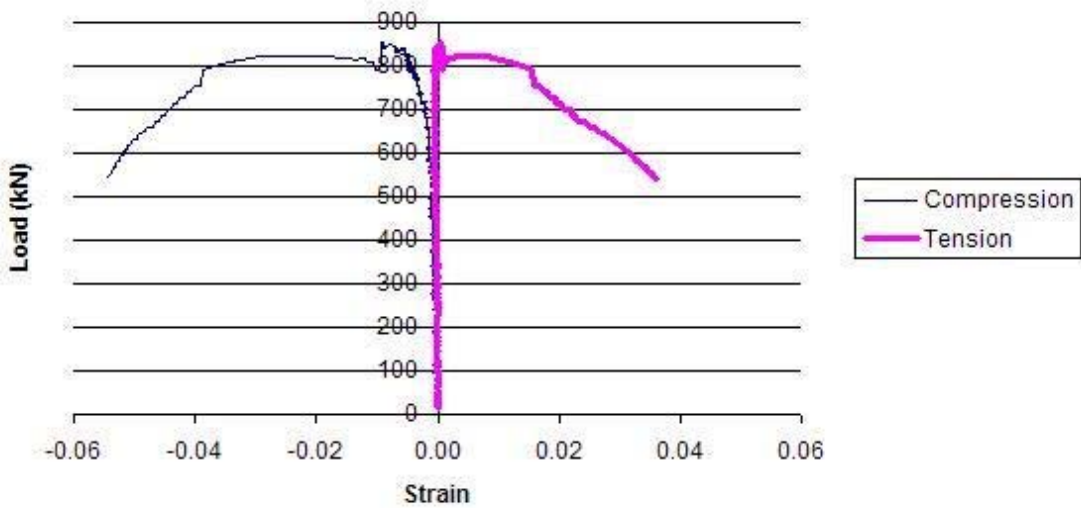


Figure 6.26. Load-Strain Graph of Specimen Type 6

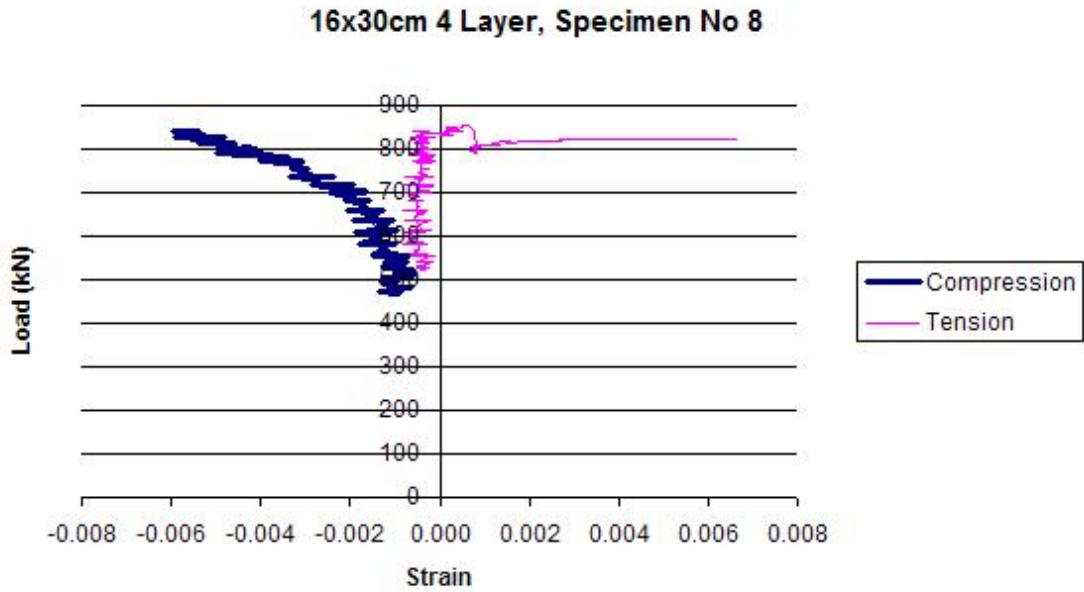


Figure 6.27. Load-Strain Graph of Specimen Type 6 (Yield Strain)

### 6.6.3.7. Axially Loaded Steel Specimen Type 7

This experiment consists of GFRP strengthened steel plate specimen. This specimen has 16 layers of GFRP with 16x30 cm dimensions. Experimental results of axially loaded GFRP strengthened steel plate including Load-Displacement and Load-Strain Graphs are shown below.

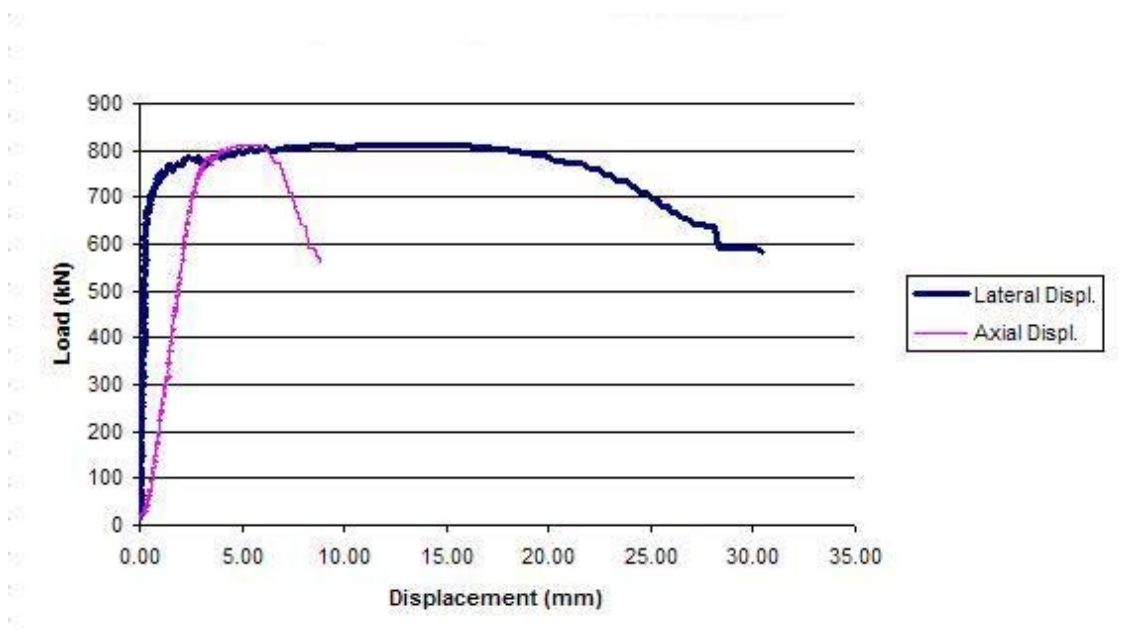


Figure 6.28. Load-Displacement Graph of Specimen Type 7

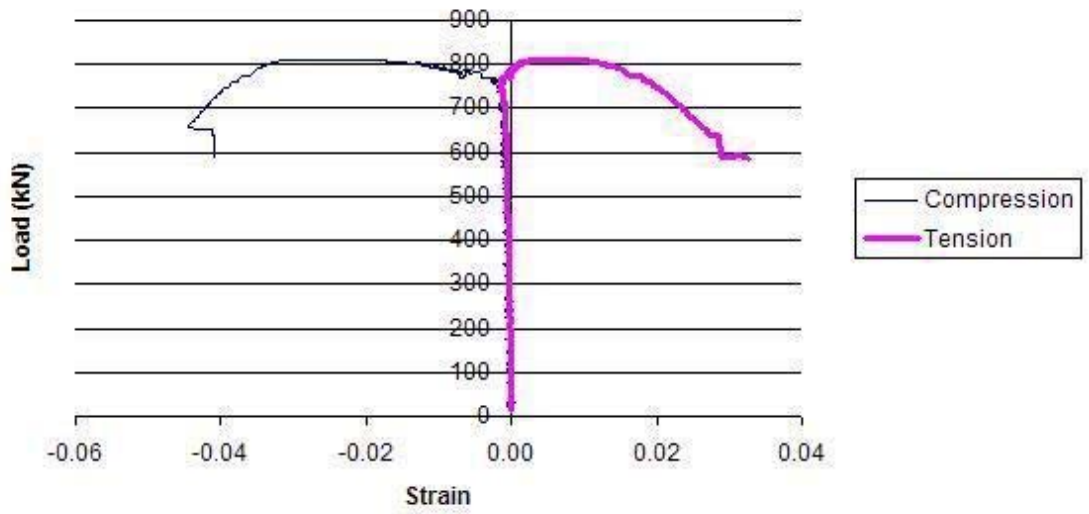


Figure 6.29. Load-Strain Graph of Specimen Type 7

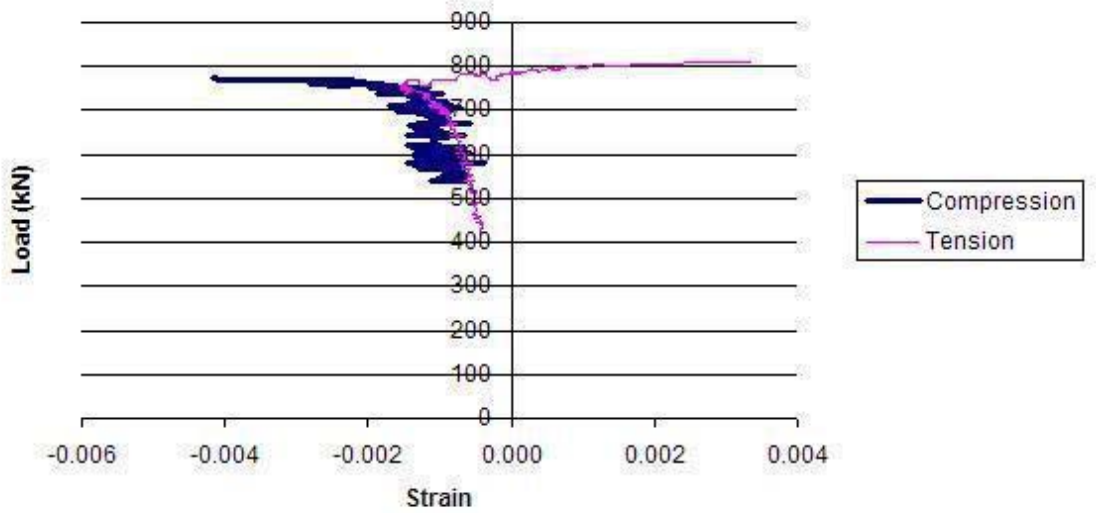


Figure 6.30. Load-Strain Graph of Specimen Type 7 (Yield Strain)

## CHAPTER 7

### CONCLUSIONS AND RECOMMENDATIONS FOR FUTURE STUDY

#### 7.1 Conclusions

Prior to GFRP strengthened steel plate tests, small scale standard tests were conducted to determine the tension, compression and shear properties of GFRP; as well as lap shear tests to determine the shear tests to determine the shear behavior of the interface between steel and GFRP.

Tensile and compressive tests were conducted with both  $0^\circ/45^\circ/90^\circ/-45^\circ$  and  $0^\circ/90^\circ$  fiber orientations with same fiber density of  $1250 \text{ gr/m}^2$ . The tests showed that GFRPs with  $0^\circ/90^\circ$  fiber orientation had better tensile strength, as fiber density in the tension direction was more. On the other hand, the compressive strength of GFRPs with either fiber orientation were very close to each. Since local buckling of steel plates on flanges and webs is an instability that occurs under compression forces, the compressive properties of GFRPs become more important in choosing which GFRP orientation to use. In steel plate tests GFRP with  $0^\circ/45^\circ/90^\circ/-45^\circ$  fiber orientation was used. However, GFRP with  $0^\circ/90^\circ$  orientation could also have been used.

In lap-shear tests the following parameters were investigated: Epoxy ( Duratek, Resoltech), surface treatment ( sand papered, sand blasted, no treatment), surface preparation primers (Duratek, Silan) and GFRP production method (Direct wet lay-up, Preformed wet lay-up). The following conclusions were drawn from lap-shear tests;

- Surface treatment methods increase the interfacial interaction between GFRP and Steel. Sand papered and sand blasted metal surfaces give nearly the same results. They both increased the surface interaction if the results are compared with specimens without any surface treatment.
- Surface preparation primers also showed improvement in interfacial interaction between GFRP and Steel. Best results were obtained by Silan surface preparation

primer which is a chemical compound. However, taking into account the in-situ application of composite material, the experimental program was continued with Duratek surface preparation primer. This implies that, interaction between steel-GFRP may be much higher with the enhancement of the commercial surface preparation primers.

- 2 epoxies (Duratek, Resoltech) , 2 fiber orientations ( $0^\circ/45^\circ/90^\circ/-45^\circ$ ,  $0^\circ/90^\circ$ ) , 2 wet lay-up composite manufacturing methods (Direct Wet Lay-up, Pre-prepared Wet Lay-up) showed no difference in interfacial strength of lap-shear specimens.

Experimental program was continued with V-Notched Beam Method Test to investigate the interlaminar shear strength of GFRP material. These tests revealed;

- The weakest interlaminar shear strength plane of GFRP material is the ZX=ZY plane, that had no reinforcing fiber in the direction of shear.
- Two different wet lay-up manufacturing for XZ and YZ planes showed no difference in interlaminar shear tests, proving the quality of GFRP manufacturing process in laboratory conditions.

The axially loaded GFRP strengthened steel plate experiments revealed the following important facts about GFRP-steel interaction and the behavior of GFRP effect on steel plate for stabilization:

- The GFRP stabilization to steel plates showed up to 11% improvement in axial loading capacity of steel plates,
- The increase of GFRP laminates and dimensions showed improvement in lateral buckling
- The stabilization effect of GFRP material on steel plates continue until the debonding of the composite material from the surface of steel material.
- The strain-gauge measurements on composite material shows that, the strain values do not exceed the materials strain capacity of GFRP material on outer surface of material, if it was not manufactured less than 4 layers.



## **7.2. Recommendations**

- This pilot study to investigate the stabilization affect of GFRP material on axially loaded steel plates revealed improvement on plastic buckling behavior of GFRP strengthened steel plate specimens. Thence, this study may lead to a further study based on investigation of plastic buckling on full scaled steel members strengthened with GFRP materials.
- Strengthening effect of GFRP material is directly related with the GFRP material's bonding capability on steel surface. This duration may be improved by increasing the interaction between steel and GFRP material. For this purpose, different epoxies, primers and surface treatment methods can also be tested to provide higher interfacial shear stress values. Continuous improvements on mechanical properties of FRP materials will increase the ductility enhancements of steel members.

## REFERENCES

- Accord, N. B., and Earls, C. J. 2006. *Use of Fiber Reinforced Polymer Composite Elements to Enhance Structural Steel Member Ductility*. Journal of Composites for Construction ASCE 10.4:337-344.
- ASTM. 2001. Standard test method for lap shear adhesion for fiber reinforced plastic (FRP) bonding (Metric), *American Society for Testing and Materials* . Designation. 15.06 D 5868M
- ASTM. 2002. Standard test method for compressive properties of rigid plastics, *American Society for Testing and Materials* . Designation. 08.01: D 695M.
- ASTM. 2003b. Standard test method for tension testing of metallic materials (Metric), *American Society for Testing and Materials* . Designation. 03 . 01: E 8M.
- ASTM. 2005. Standard test method for shear properties of composite materials by the V-notched beam method, *American Society for Testing and Materials* , Designation: 15.03. D 5379M.
- ASTM. 2008. Standard test method for tensile properties of polymer matrix composite materials, *American Society for Testing and Materials* . Designation. 15.03: D 3039M.
- Bakis, C.E. Bank, L.C. Brown, V.L. Cosenza, E. Davalos, J.F. Lesko, J.J. Machida, A. Rizkalla, S.H. Triantafillou, T.C. 2002 *Fiber-Reinforced Polymer Composites for Construction—State-of-the-Art Review 10.1061 / (ASCE) 6.2:73*
- Buyukozturk, O., Gunes, O., and Karaca, E. 2004. *Progress on Understanding Debonding Problems in Reinforced Concrete and Steel Members Strengthened Using FRP Composites*. Construction and Building Materials 18:9-19

- Cadei J. M. C., Stratford T., J., Hollaway L., C., Duckett W.G. 2004. *Strengthening Metallic Structures Using Externally Bonded Fiber-Reinforced Polymers*. Construction Industry Research and Information Association (CIRIA) – 234
- Chiew,S.P. Lie,S.T. Lee,C.K. Yu,Y. 2005 *Debonding Failure Model for FRP Retrofitted Steel Beams* . Advances in Steel Structures .1 :579 -586
- Dooley, K.M. 2009. Polymer Rheology. <http://www.che.lsu.edu> (accessed March 9,2009 )
- El Damatty, A.A. and Abushagur, M. 2003. *Testing and modeling of shear and peel behavior for bonded steel/FRP connections*. Thin-Walled Structures. 41: 987-1003.
- El Damatty, A.A. Abushagur, M., and Youssef, M.A. 2005. *Rehabilitation of composite steel bridges using GFRP plates*. Applied Composite Materials. 12 : 309 – 325
- Gibson, R. F. 1994. *Principles of Composite Material Mechanics*. McGrawHill.
- Harris,A.F. Beevers,A. 1998 *The effects of grit-blasting on surface properties for adhesion* . International Journal of Adhesion & Adhesives 19:445-452
- Hollaway, L. and Cadei, J. 2002. *Progress in the technique of upgrading metallic Structures with advanced polymer composites*. Prog. Structural Engineering Materials. 4:131-148
- Hull, D., Clyne, T. W. 2000. *An Introduction to Composite Materials*. Cambridge University Press, Cambridge, 2nd Edition.
- Hyer, M. 1998. *Stress Analysis of Fiber-Reinforced Composite Materials* McGraw-Hill

- Jang,B . 1994. *Advanced Polymer Composites: Principles and Applications*. Materials Park, OH : ASM International
- Jina,J. El-Tawil,S. 2004 *Seismic performance of steel frames with reduced beam section connections*. Journal of Constructional Steel Research. 61: 453–471
- Jones,S.L. Fry,G.L. Engelhardt,M.D. 2002 *Experimental Evaluation of Cyclically Loaded Reduced Beam Section Moment Connections*.ASCE. 128:4(441)
- Keller,T. Schollmayer,M. 2009 *Through -thickness performance of adhesive joints between FRP bridge decks and steel girders*. Composite Structures. 87:232-241
- Kim,H. Hwang,Y. Park, K. Lee, Kim,S. 2004 *Fiber reinforced plastic deck profile for girder bridges* Composite Structures 67:411-416
- Labview 8.0 .2007. National Instruments DAQ Software
- Lee, C. Jung,J. Oh,M. Koo,E. 2003. *Cyclic seismic testing of steel moment connections reinforced with welded straight haunch*. Engineering Structures. 25:1743–1753
- Matsuzaki,R. Shibata,M. Todoroki,A. 2008 *Reinforcing an aluminum/GFRP co-cured single lap joint using*. Composites Part A 39:786-795
- Melograna,J. Grenestedt,J. 2002 *Improving joints between composites and steel using perforations*. Composites Part A 33:1253-1261
- Molitor, P., Barron, V., and Young, T. 2001. *Surface treatment of titanium for adhesive bonding to polymer composites: a review*. International Journal of Adhesion and Adhesives. 1:129-136.
- Nakashima, M., Suita, K., and Morisako, K. 1998. *Tests of welded beam-column subassemblies I: global behavior*. Journal of Structural Engineering, ASCE. 124:11:1236-1244

- Park, K. Hwang, Y. Lee, Y. Kim, S. 2007. *Performance verification of a new pultruded GFRP bridge*. Composite Structures. 81:114-124
- Peck, A.J. 2007. *Investigation of FRP stabilization of plastic buckling behavior of slender steel sections*. Master of Science Thesis, University of Pittsburgh, December, Pittsburgh, PA, USA.
- Pendhari, S. Kant, T. Desai, Y. 2008 *Application of polymer composites in civil Construction : A general review*. Composite Structures. 84: 114 - 124
- Photiou, N. K., Hollaway, L. C., Chryssanthopoulos, M. K. 2006. *Strengthening of an Artificially Degraded Steel Beam Utilizing a Carbon/Glass Composite System*. Construction and Building Materials. 20:11-21
- Possart, W., Bockenheimer, C., and Valeske, B. 2002. *Network structure in epoxy aluminum bonds after mechanical treatment*. International Journal of Adhesion & Adhesives. 22:349-356.
- Resin Infusion -VARTM <http://www.resininfusion.org> (accessed January 2, 2009)
- Sayed-Ahmet, E. Y. 2004. *Strengthening of Thin-Walled Steel I-Section Beams using CFRP Strips*. Proceedings of the 4<sup>th</sup> Advanced Composites for Bridges and Structures Conference, Calgary, Canada
- Schnerch, D. Stanford, K. Sumner, E. Rizkalla, S. 2005. *Bond Behavior of CFRP strengthened Steel Bridges and Structures*. Proceedings of International Symposium on Bond Behaviour of FRP in Structures (BBFS 2005)
- Schwartz, M. M. 2002 *Composite Materials*. Prentice Hall.
- Sen, R. Liby, L. Mullins, G. 2001 *Strengthening Steel Bridge Sections Using CFRP Laminates*. Composites Part B. 32: 309-322

- Shalin R.E. 1995 *Polymer matrix composites* London;New York: Chapman-Hall.
- Shin,K. Lee,J. And Lee,D. 2000 *A study on the lap shear strength of a co-cured single lap joint*. J. Adhesion Sci. Technol. 14:123–139
- Strong, B. 1989. *Fundamentals of Composites Manufacturing : Materials, Methods and Applications*. Michigan. Society of Manufacturing Engineers.
- Tavakkolizadeh, M. and Saadatmanesh H. 2003. *Strengthening of Steel - Concrete Composite Girders Using Carbon Fiber Reinforced Polymers Sheets*. Journal Of Structural Engineering, ASCE. 129: 30-40.
- Timothy, G. Gutowski. 1997. *Advanced Composites Manufacturing* . Wiley-Interscience
- Tremblay, R. Timler, P. Bruneau, M. and Filiatrault,A. 1995 *.Performance of steel structures during 1994 Northridge Earthquake*. Can. J. Civ. Eng. 22: 338-360
- Turner, M. Harries,K. Petrou,M. Rizos,D. 2004. *In situ structural evaluation of a GFRP bridge deck system* .Composite Structures 65: 157-165
- Varadi,K. Nader,Z. Friedrich,K. Flöck,J. 2001. *The real contact area between composite and steel surfaces in sliding contact*. Composite Science and Technology 61:1853-1862
- Vasililiev,V 1993. *Mechanics of Composite Structures*. Taylor&Francis
- Yulismana,.W. 2005. *Experimental Study of the Behavior of Fiber Reinforced Polymer Deck System*. Ph.D. Thesis. University of Pittsburgh